

NACA RM E57D23

W J Smith

544

Copy

NACA RM E57D23

CLASSIFICATION CHANGED  
**UNCLASSIFIED**

**NACA**

By Authority of TP 71-614 90 SEP 1971.

# RESEARCH MEMORANDUM

Declassified by authority of NSA  
Classification Change Notices No. 215  
Dated \*\* 81 DEC 1977

**HYDROGEN FOR TURBOJET AND RAMJET POWERED FLIGHT**

By Lewis Laboratory Staff

Lewis Flight Propulsion Laboratory  
Cleveland, Ohio



**NATIONAL ADVISORY COMMITTEE  
FOR AERONAUTICS**

WASHINGTON  
April 26, 1957  
Reclassified May 29, 1959

**LIBRARY COPY**  
JUN 15 1965  
SAMUEL REXHAUSEN CENTER  
LIBRARY NACA  
HAMPTON, VIRGINIA





## TABLE OF CONTENTS

	Page
I - COMBUSTION CHARACTERISTICS OF HYDROGEN by Andrew E. Potter, Frank E. Belles, and Isadore L. Drell . . . . .	1
II - COMBUSTION IN RAMJETS AND AFTERBURNERS by Roland Breitwieser and H. George Krull . . . . .	13
III - COMBUSTION IN TURBOJET ENGINES by E. William Conrad and Lester C. Corrington . . . . .	29
IV - FUELING PROBLEMS WITH LIQUID HYDROGEN by Glen Hennings, William H. Rowe, and Harold H. Christenson . . . . .	45
V - AIRPLANE TANKAGE PROBLEMS WITH LIQUID HYDROGEN by Solomon Weiss, Thaine W. Reynolds, and Loren W. Acker . . . . .	59
VI - AIRCRAFT FUEL SYSTEM FOR LIQUID HYDROGEN by Paul M. Ordín, David B. Fenn, and Edward W. Otto . . . . .	71
VII - FLIGHT EXPERIENCE WITH LIQUID HYDROGEN by Donald R. Mulholland, Joseph S. Algranti, and William V. Gough, Jr. . . . .	85



CONFIDENTIAL

CONFIDENTIAL

1 - COMBUSTION CHARACTERISTICS OF HYDROGEN

Andrew E. Potter, Frank E. Belles, and Isadore L. Drell



## NATIONAL ADVISORY COMMITTEE FOR AERONAUTICS

RESEARCH MEMORANDUM

## 1. COMBUSTION CHARACTERISTICS OF HYDROGEN

By Andrew E. Potter, Frank E. Belles, and Isadore L. Drell

## Introduction

The chemistry of the hydrogen flame is comparatively well understood. Much more is known about the reaction between hydrogen and oxygen than the reactions between hydrocarbons and oxygen. However, the science of combustion has not advanced far enough to make possible prediction of the combustion properties of hydrogen from this knowledge. The combustion properties must be measured. Fortunately, the hydrogen flame has received considerable attention from experimenters, and much is known about it. From the wealth of information available, just a few items of practical interest are discussed here. Reference 1 gives an extensive review of the combustion properties of hydrogen, and it is recommended that the reader see reference 1 for a detailed discussion.

The material discussed here is divided into three parts: (1) "transient" combustion properties, which have to do with starting and stopping the flame, for example, ignition and blowoff; (2) the steady flame, in particular, the burning velocity; (3) the possibility of shortening combustors designed for hydrogen fuel.

"Transient" Combustion Properties

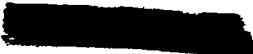
Flammability range. - The range of fuel concentrations which will support a flame (refs. 1 and 2) is shown in figure 1. For comparison, the flammable range for JP-4 fuel is also shown. The striking feature of hydrogen that is demonstrated is the wide range of fuel concentration that will support a flame. The limits of flammability are substantially independent of pressure, provided the apparatus used for the measurement is not so small as to quench the flame at low pressures. If a hydrogen flame is allowed to propagate for some distance inside a tube, the flame will turn into a detonation. Detonations in hydrogen-air mixtures can also be initiated by shock waves from explosions. The concentration range for detonation is from 18.2 to 58.9 percent hydrogen by volume (ref. 1).



Spark ignition energy. - Figure 2 shows the minimum amount of energy a spark must have in order to ignite a combustible mixture which has the composition indicated on the abscissa in terms of equivalence ratio (ref. 3, pp. 412 and 414). (The equivalence ratio is the fuel-air ratio divided by the stoichiometric fuel-air ratio.) Data at 1 atmosphere for hydrogen and a typical petroleum hydrocarbon fuel (propane) are shown in this figure. The principal point of interest is the fact that a spark needs only one-tenth the energy to ignite a hydrogen-air mixture that it needs to ignite a hydrocarbon-air mixture. Because so little spark energy is required to ignite hydrogen, precautions for avoiding static electrical sparks by grounding equipment must be strictly observed when handling hydrogen.

Spontaneous ignition temperature. - The spontaneous ignition temperature depends largely on the experimental technique used to measure it. This is true for all fuels. For hydrogen it is possible to specify a maximum safe temperature at atmospheric pressure of about 950° F. This is considerably higher than that for most hydrocarbons, which have spontaneous ignition temperatures ranging from 400° to 600° F. As pressure decreases, the ignition temperature for most hydrocarbons increases. Hydrogen behaves in the opposite manner; as pressure decreases, the ignition temperature decreases. At very low pressures ignition may occur at temperatures approaching 700° F. Figure 3 shows the temperature to which a 1/4-inch-diameter rod must be heated to cause ignition plotted against flow velocity for a typical hydrocarbon and for hydrogen (ref. 4). The ignition temperature for hydrogen is less than that for the hydrocarbon. Furthermore, the ignition temperature of hydrogen is not affected much by the velocity of flow. In view of these effects of pressure and flow velocity on ignition temperature, it is not surprising that hydrogen ignites spontaneously in the afterburner.

Quenching distance. - A flame can be extinguished by forcing it to propagate near cold solid walls which withdraw heat from it. A measure of the flame's resistance to being extinguished by cooling is the quenching distance. Figure 4 shows quenching distances at a pressure of 1 atmosphere for a typical hydrocarbon and hydrogen (ref. 3). The quenching distance is the distance between two parallel walls which will just allow a flame to pass between them. The smaller the quenching distance, the greater the resistance of the flame to being extinguished by cooling. The quenching distance for hydrogen is a little less than one-third the quenching distance for the hydrocarbon (fig. 4), which shows that the hydrogen flame is more resistant to heat loss than the hydrocarbon flame. This is true in spite of the high thermal conductivity of hydrogen-air mixtures, because of the high rate and low activation energy of the chemical reaction between hydrogen and oxygen.



Blowoff. - The way of extinguishing a flame that is of primary interest to the combustor and afterburner designer is the blowoff of a flame stabilized behind a flameholder. Figure 5 shows a sketch of a flame stabilized behind a flameholder.

Many theories have been proposed for the mechanism of stabilization of flames by flameholders. One of the simplest, and for that reason perhaps the best, is that of Zukoski and Marble. According to them, the cool unburned gases are continuously ignited as they flow past the hot combustion products recirculating behind the flameholder. The time of contact between the hot burned gas and the cold unburned gas is inversely proportional to the flow velocity. When the velocity increases, this contact time decreases. When the velocity becomes too high, the contact time is too short to permit ignition, and the flame blows out. Very little is known about the contact time required for ignition. In a qualitative sense, it seems that there should be some connection between this time and the ignition delay, which is the time required for ignition to take place after a combustible mixture has been heated. Ignition delays for a typical hydrocarbon (isooctane) and for hydrogen (refs. 5 and 6) are compared in figure 6. The results shown are ignition delays in the presence of a flame; the equivalence ratio is unknown. The ignition delay for hydrogen is much less than the ignition delay for the hydrocarbon. Then, on the basis of Zukoski and Marble's mechanism, the blowoff velocity for hydrogen should be much greater than for a hydrocarbon. This is the case, as is shown in figure 7; the blowoff velocity for hydrogen flames is about an order of magnitude greater than for the hydrocarbon flame (ref. 7). The difference is especially impressive at very low pressures. Thus, hydrogen flames can be stabilized in combustors and afterburners at very severe flow conditions.

#### The Steady Flame

The most important property of the steady flame is the burning velocity. Burning velocities for hydrogen and a typical hydrocarbon (propane) at 1 atmosphere (refs. 1 and 2) are compared in figure 8. There are two noteworthy features in this figure. First, the burning velocity for hydrogen is very high compared to that for the hydrocarbon. Second, the maximum burning velocity for hydrogen does not occur near the stoichiometric mixture ratio, but rather in a fuel-rich mixture, at an equivalence ratio near 1.8.

The effect of pressure on burning velocity (ref. 8) is shown in figure 9. As before, hydrogen is compared with propane. Pressure affects the burning velocity of hydrogen in the opposite way that it does most hydrocarbons. The burning velocity decreases with pressure for hydrogen, while that of the hydrocarbon increases as pressure is lowered. However, even at low pressures, the burning velocity for hydrogen is much larger than that for the hydrocarbon.

There are two reasons for the comparatively large burning velocity of hydrogen. First, because of the high mass diffusivity and thermal conductivity of hydrogen, active particles and heat are conducted ahead of the burning zone to ignite fresh mixture faster for hydrogen-air mixtures than for hydrocarbon-air mixtures. Second, hydrogen and oxygen react chemically to produce heat faster than hydrocarbons and oxygen. The high reactivity of hydrogen is reflected in ease of spark ignition and in difficulty in extinguishing the flame either by quenching or blowoff. The reactivity of hydrogen has important consequences in combustor design, as can be seen from the following discussion.

#### Minimum Volume Required for Combustion

Reduction of the length of the combustor in a jet engine is very desirable because of the saving in weight which results. For a given heat output, reduction of combustor length requires that the combustion process be completed in a smaller space. A convenient measure of the use of space is the space heating rate, the rate of heat release per unit volume. Combustor volume is inversely proportional to the space heating rate; hence, increased space heating rate permits decreased combustor length. The space heating rate may be defined as follows:

$$\text{Space heating rate} = \frac{(\text{Heating value})(\text{Combustion efficiency})}{\text{Combustion time}}$$

The heating value is defined here as the heat obtained from the combustion of a unit volume (at inlet conditions) of fuel-air mixture. Combustion efficiency has its usual meaning. The combustion time is the time required to complete the combustion process to the extent specified by the combustion efficiency. Once the fuel and inlet conditions are fixed, the heating value is fixed. The combustion efficiency is always made as large as possible. The remaining factor is the time necessary for combustion. This time must be reduced in order to increase space heating rate, and thereby shorten the combustor.

Two factors, one physical, the other chemical, control combustion time. The physical factor is the time used for various physical processes, such as mixing of fuel and air, mixing of flame and burned gas with fresh unburned gas, and evaporation of fuel droplets. The chemical factor is the time used for the chemical reaction between fuel and oxygen to produce the heat of combustion. If mixing in the combustor is very intense, the time required to complete the various physical processes can be reduced. Theoretically, this time can be made to approach zero by sufficiently vigorous mixing. However, this does not affect the time needed for the chemical reaction, which is controlled by type and concentration of fuel, inlet temperature and pressure, and combustion efficiency. Fixing these variables fixes chemical time. With negligible physical time, the chemical time sets a minimum on the time required for combustion, and therefore a maximum on the space heating rate and a minimum on the combustor size.

Y

REPRODUCED

The maximum space heating rate determined by the chemical time is called the chemical limit. There have been some efforts to measure and to calculate this chemical limit on the space heating rate for various fuels, and some results for JP-4 fuel and hydrogen are shown in figure 10, where space heating rate is plotted against pressure. The chemical limits for the space heating rates shown are for 95-percent combustion efficiency to make them comparable with engine combustor performance. The inlet temperature is 25° C, and the fuel concentration is stoichiometric. The line shown for JP-4 fuel was calculated from experimental results of reference 9 for isooctane. The line shown for hydrogen was estimated by multiplying the isooctane data by the ratio of hydrogen to isooctane space heating rates calculated from burning velocities and quenching distances of reference 10. For comparison, a band is shown in which fall space heating rates for many jet and ramjet combustors. The volume used for this latter calculation was the actual combustor volume rather than the true volume occupied by the flame.

The chemical limit on the space heating rate is much larger for hydrogen than for JP-4 fuel. This is partly due to the higher heat of combustion of hydrogen, but mostly due to the high reactivity of hydrogen, that is, the high rate of heat production by the chemical reaction. The purpose of figure 10 is to show that the possibility exists of getting high space heating rates, therefore small combustors, by using hydrogen as fuel. Considerations of pressure loss and outlet temperature make it unlikely that the theoretically possible reduction in combustor size is feasible, or even desirable. Nevertheless, a significant reduction in combustor size should be possible, and in fact, is possible through the use of hydrogen fuel.

#### Summary

Hydrogen can be burned over a wider range of fuel concentration than any hydrocarbon. Even though hydrogen has a high ignition temperature, it is about ten times easier to ignite with a spark than a hydrocarbon, and the flame is about ten times harder to blow out once it is lit. Hydrogen has a higher burning velocity than any hydrocarbon, partly as a result of the greater rate of heat production in the flame. The practical result of this is that, when hydrogen is substituted for a hydrocarbon in a conventional combustor, performance of the combustor improves. More important, combustors and afterburners designed especially for hydrogen can be made very short and thus reduce engine weight.

## References

1. Drell, Isadore, and Belles, Frank E.: Survey of Hydrogen Combustion Properties. NACA RM E57D24, 1957.
2. Fuels and Combustion Research Division: Adaptation of Combustion Principles to Aircraft Propulsion. Vol. I. Basic Considerations in the Combustion of Hydrocarbon Fuels with Air. NACA RM E54I07, 1955.
3. Lewis, Bernard, and von Elbe, Guenther: Combustion, Flames and Explosions of Gases. Academic Press, Inc., 1951, pp. 412; 414.
4. Mullen, James W., II, Fenn, John B., and Irby, Moreland R.: The Ignition of High Velocity Streams of Combustible Gases by Heated Cylindrical Rods. Third Symposium on Combustion and Flame and Explosion Phenomena, The Williams & Wilkins Co. (Baltimore), 1949, pp. 317-329.
5. Mullins, B. P.: Studies of the Spontaneous Ignition of Fuels Injected into a Hot Air Stream. V - Ignition Delay Measurements on Hydrocarbons. Fuel, vol. XXXII, no. 3, July 1953, pp. 363-379.
6. Mullins, B. P.: Studies of the Spontaneous Ignition of Fuels Injected into a Hot Air Stream. IV - Ignition Delay Measurements on Some Gaseous Fuels at Atmospheric and Reduced Static Pressures. Fuel, vol. XXXII, no. 3, July 1953, pp. 343-362.
7. Friedman, J., Bennet, W. J., and Zwick, E. G.: The Engineering Application of Combustion Research to Ramjet Engines. Fourth Symposium (International) on Combustion, The Williams & Wilkins Co. (Baltimore), 1953, pp. 756-764; discussion by E. A. DeZubay, p. 764.
8. Fine, Burton: Stability Limits and Burning Velocities of Laminar Hydrogen-Air Flames at Reduced Pressures. NACA TN 3833, 1956.
9. Longwell, John P., and Weiss, Malcolm A.: High Temperature Reaction Rates in Hydrocarbon Combustion. Ind. and Eng. Chem., vol. 47, no. 8, Aug. 1955, pp. 1634-1643.
10. Potter, A. E., Jr., and Berlad, A. L.: A Relation Between Burning Velocity and Quenching Distance. NACA TN 3882, 1956.

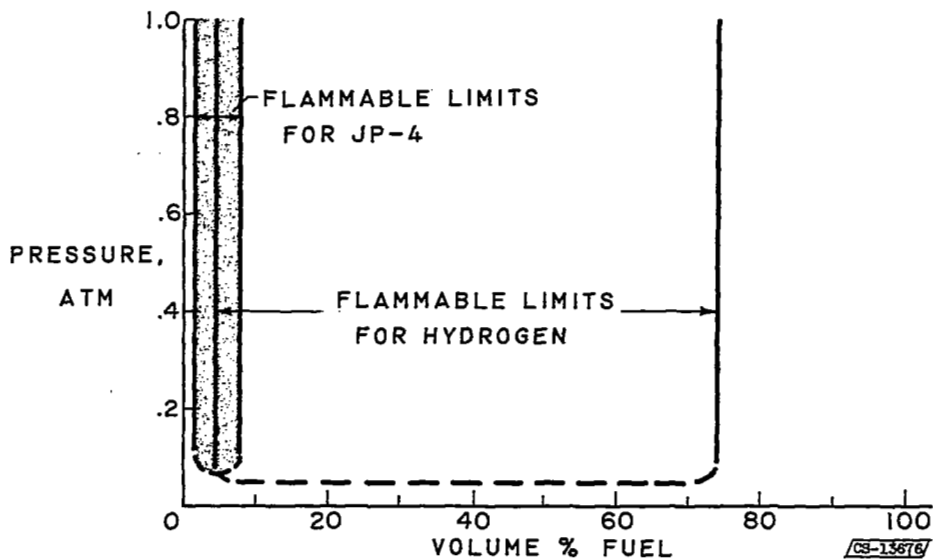


Figure 1. - Flammable range of hydrogen and JP-4 fuel.

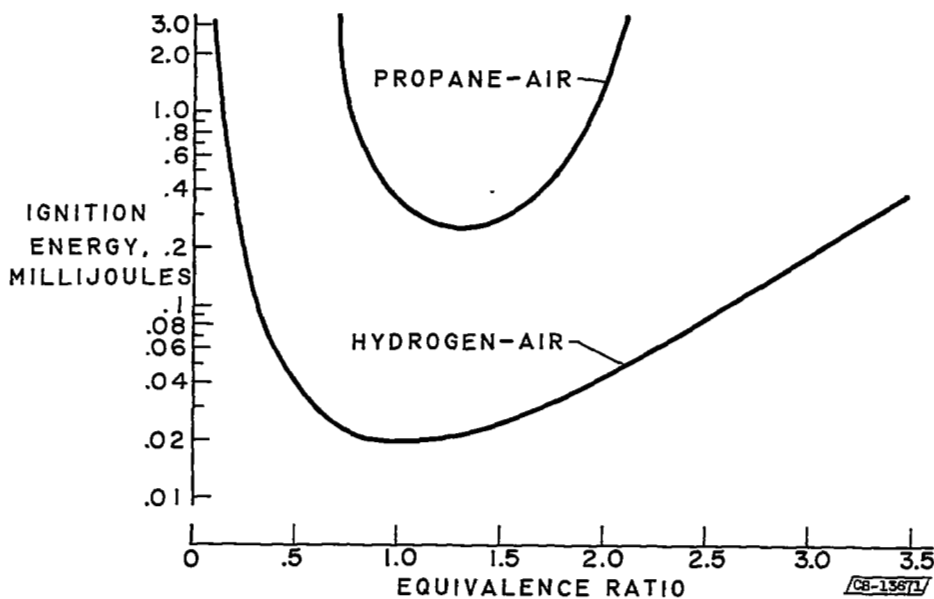
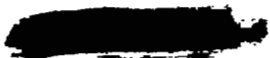


Figure 2. - Minimum spark ignition energies for hydrogen-air and propane-air mixtures (data from ref. 3).



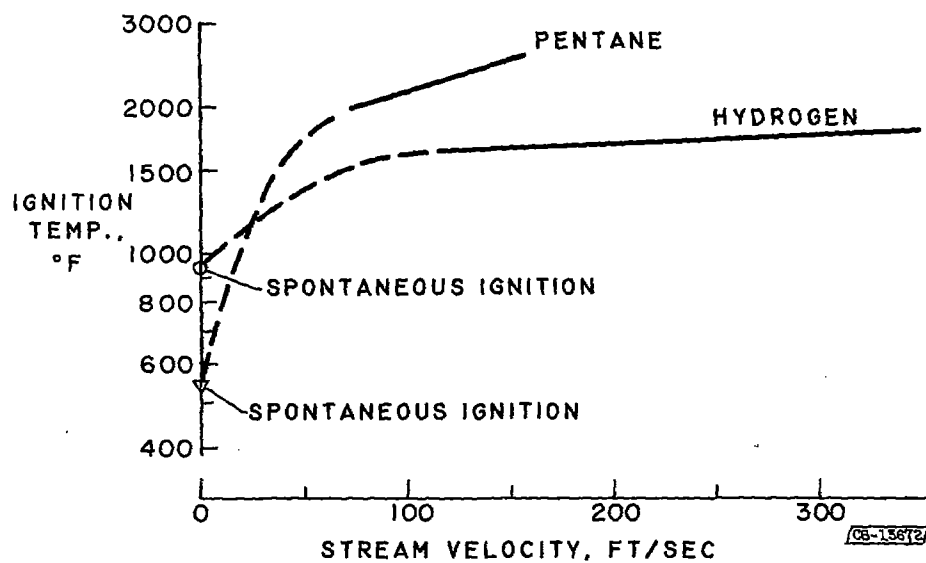


Figure 3. - Ignition of flowing mixtures by heated 1/4-inch-diameter rod. Equivalence ratio, 1 (data from ref. 4).

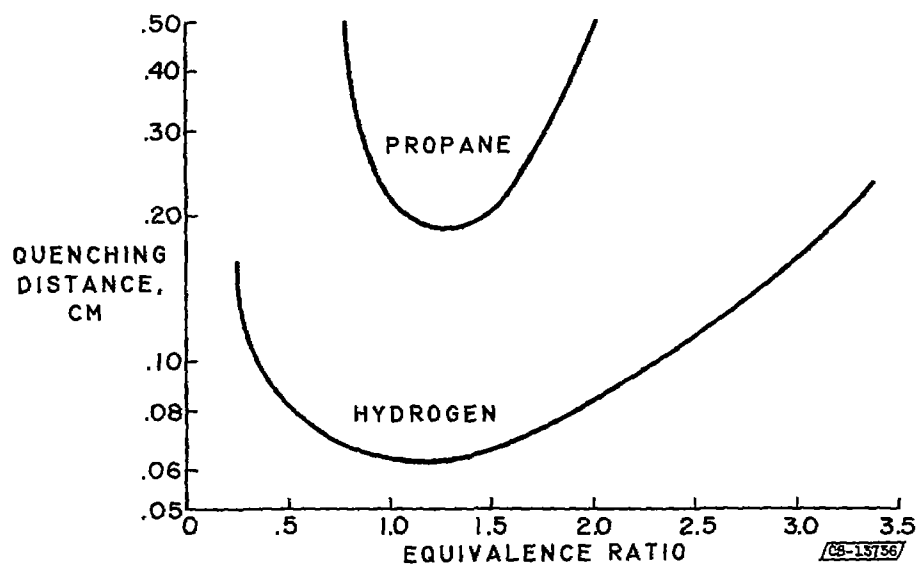


Figure 4. - Quenching distances for hydrogen and propane flames. Pressure, 1 atmosphere (data from ref. 3).

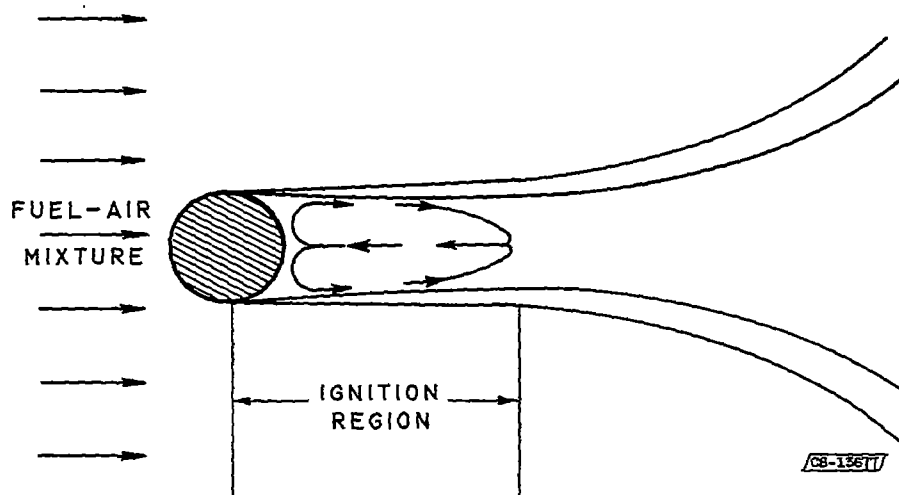


Figure 5. - Flame stabilization by bluff body.

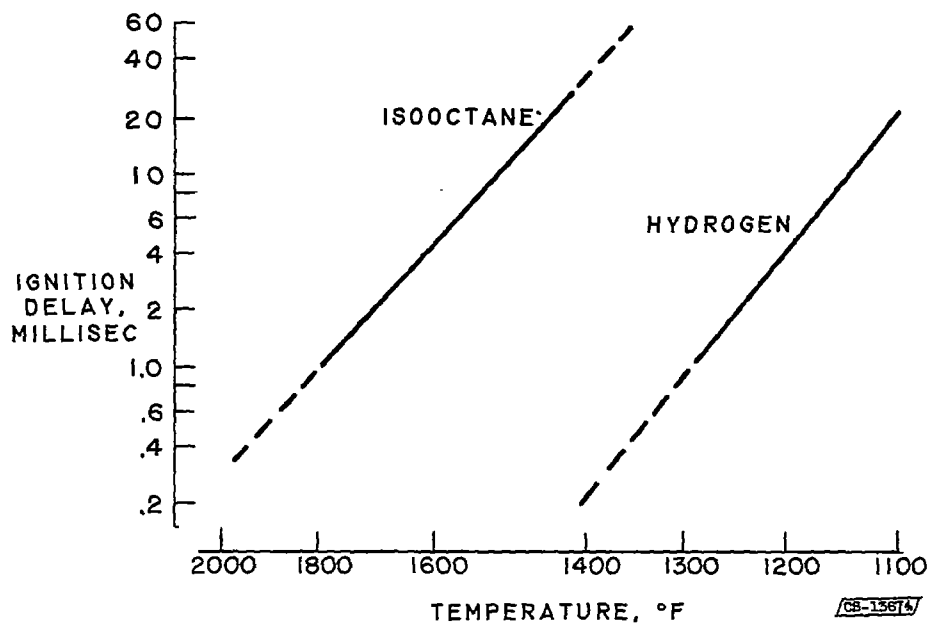


Figure 6. - Ignition delays for hydrogen and isooctane (data from refs. 5 and 6).

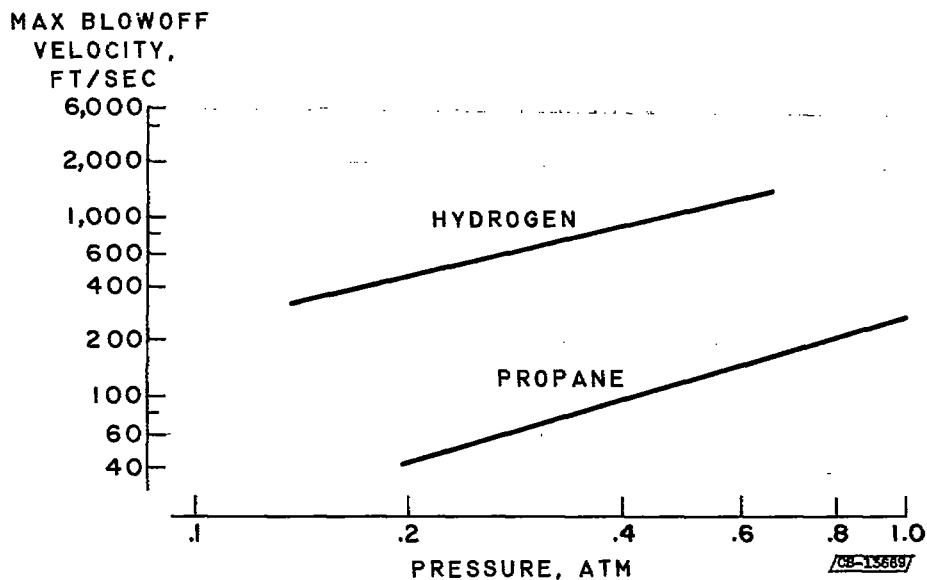


Figure 7. - Blowoff velocities for hydrogen and propane flames. 1/4-Inch disk flameholder (data from ref. 7).

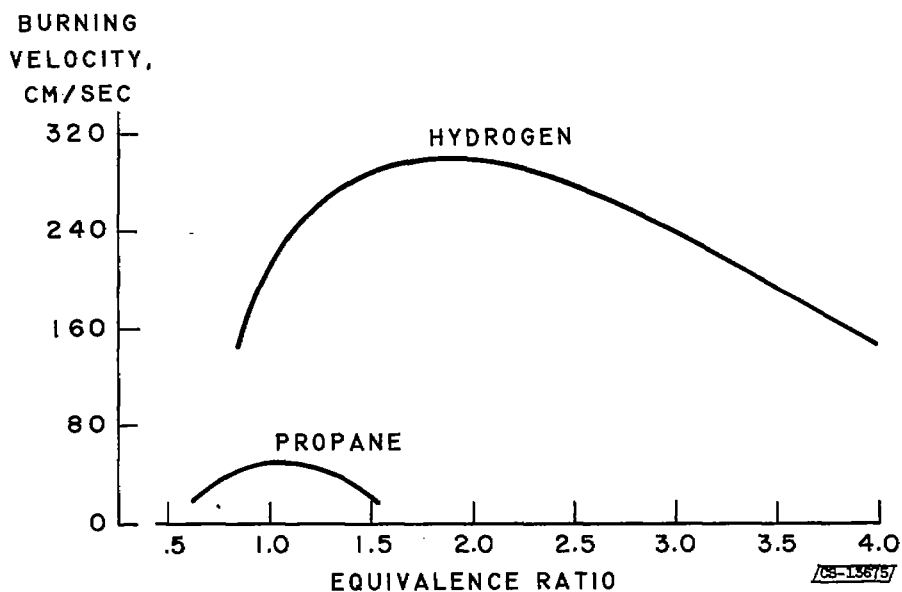


Figure 8. - Burning velocities for hydrogen and propane (data from refs. 1 and 2).

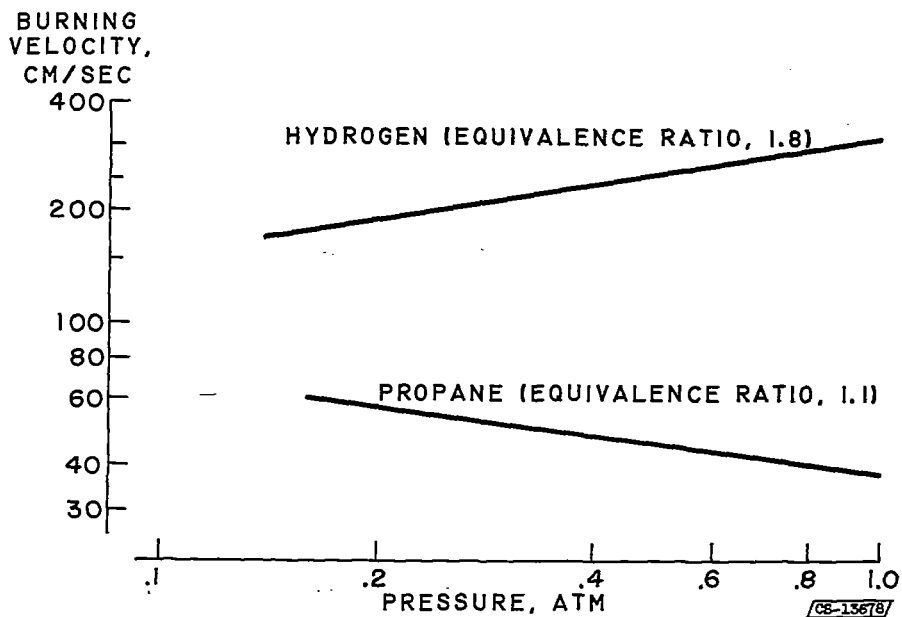


Figure 9. - Maximum burning velocity at reduced pressures for hydrogen and propane (data from ref. 8).

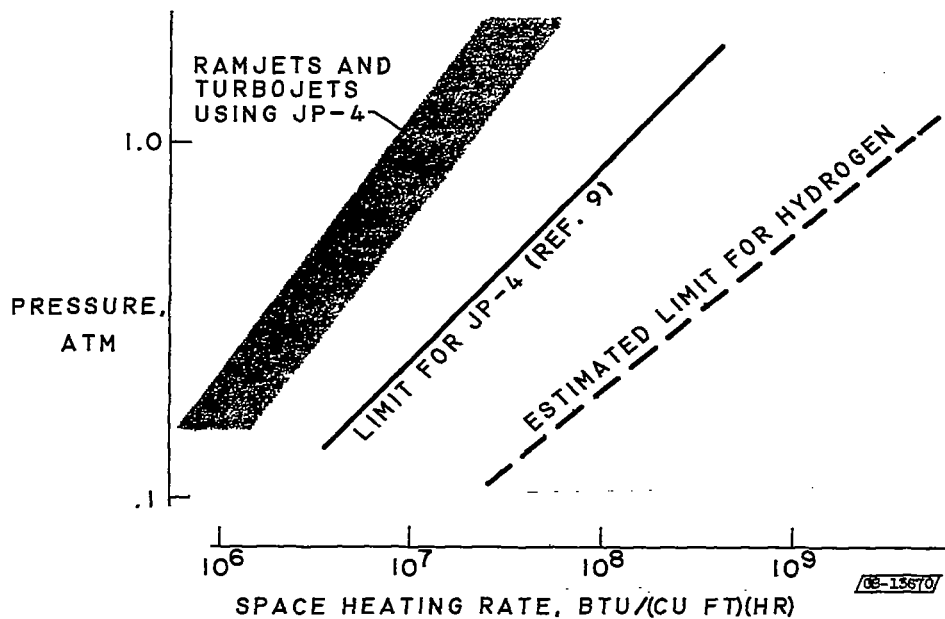


Figure 10. - Space heating rates for JP-4 fuel and hydrogen. Combustion efficiency, 95 percent.



2 - COMBUSTION IN RAMJETS AND AFTERBURNERS

Roland Breitwieser  
H. George Krull





## 2. COMBUSTION IN RAMJETS AND AFTERBURNERS

By Roland Breitwieser and H. George Krull

Recent combustion investigations in ramjet and turbojet afterburner combustors are discussed herein. The two areas of research are treated collectively since the inlet pressure, the temperature, the velocity, and the general configuration of these combustors are quite similar. The data are from small-scale investigations, some recent work on full-scale engines tested in the altitude test chambers, and a few results on a ramjet engine tested in a supersonic wind tunnel. For the most part the data are from the reports listed in the BIBLIOGRAPHY.

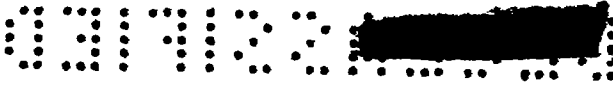
Analysis shows that, in order to use hydrogen fuel efficiently, flight systems must be operated at high altitudes. For this reason the emphasis on combustion work at the NACA Lewis laboratory has been on simple lightweight combustors that will operate efficiently at low pressures. The usual method of reducing combustor weight is shortening the combustor length.

Before presenting the combustor data, the steps and processes that are necessary to achieve complete combustion will be reviewed. The first step is that of injecting the fuel, either through fuel nozzles or spray bars. The fuel must then be mixed with air, preferably to a local fuel-air mixture near stoichiometric. After the proper mixture is produced, the flame must be stabilized at some point in the combustor and then propagated through the duct in order to complete the combustion.

An estimate of the combustion rates of hydrogen compared with those of hydrocarbons can be made by using very a very simple combustion model. First assume that both fuels have homogeneous fuel-air mixtures entering the combustor. Since the flow in the combustor systems is generally much higher than that of the flame speed, it is necessary to anchor the flame at some point by using a flameholder such as a V-gutter or a rod. After the flame is anchored, it will propagate into the fuel-air mixture.

In the development of a short combustor for hydrogen fuel, figure 1 shows that a large number of injection points will reduce the combustor length. Also, if the flame spreading rate is high, the length can be shortened still further. Hydrogen fuel has the advantage in that for a





given blockage area more flame stabilization points can be used, since very small flameholders can be used to stabilize the flame, as indicated in the preceding paper. Another advantage of hydrogen fuel compared with a hydrocarbon fuel is that the laminar flame speed of hydrogen is much higher. With the approximation that the flame propagates out as a function of the laminar flame speed, a combustor using hydrogen fuel would be much shorter than one using a hydrocarbon fuel, since hydrogen fuel has a laminar flame speed of 5 to 10 times that of a hydrocarbon fuel. A very simple example of this is illustrated in the bottom of figure 1. Ten 1/2-inch flameholders were assumed across a 1-foot duct; therefore, the flame must propagate 5/100 of a foot. At an inlet-air velocity of 200 feet per second and a laminar flame speed of 10 feet per second, the distance required to completely burn the fuel-air mixture is only 1 foot. In actual practice there will be a certain amount of turbulence in the system which will "wrinkle" the flame front and cause a still further reduction in over-all length. This model indicates that very short combustors with a hydrogen-air mixture are realizable.

The pattern of events in fuel-air mixture preparation is much the same as that of flame stabilization and spreading. The fuel is introduced from a series of fuel injectors, mixes with the air, and spreads across the duct. The rate of mixing can be increased by increasing the number of injectors or by increasing the spreading rate.

The number of fuel injection points that are feasible to use with a fuel such as hydrogen compared with JP-4 and propane fuels can be determined by the following estimates. A fixed orifice size, which is usually limited only by the mechanical problem of drilling a hole, was assumed. A constant temperature rise across the combustor and a fuel manifold pressure equal to 1 atmosphere were also assumed for this comparison. If fuel is injected at a constant velocity, the number of injection points for propane would be 400 times that for JP-4 fuel; the number of injection points for hydrogen fuel, because of its very low density, would be 3200 times that for JP-4 fuel.

The assumption of a constant injection velocity may be criticized; perhaps the assumption of critical flow through these injection orifices is more realistic. If propane and hydrogen fuels are injected at sonic velocity, and JP-4 fuel is injected with a comparable pressure drop across the system, the number of fuel injectors again can be compared. Twenty-eight times as many injection points can be used with propane fuel and 37 times as many injection points with hydrogen fuel as with JP-4 fuel. Thus, the use of hydrogen fuel enables faster fuel preparation because a larger number of fuel injectors can be used.

In order to compare the mixing rates, the steps in the mixing process will be considered. Mixing occurs by turbulent mixing and molecular diffusion. For the gaseous fuels the rate of turbulent mixing should be





essentially the same. However, there is a large change in the rate of molecular diffusion for the various fuels. For example, the molecular diffusion rate of hydrogen fuel is 10 times that of gaseous octane fuel. The large number of injection points permissible with hydrogen fuel and its high molecular diffusion rate suggest that a nearly homogeneous mixture may be obtained by relying solely on a large number of injection points and molecular diffusion alone. This is illustrated in figure 2, where the ordinant reflects the degree of mixing. The minimum fuel-air ratio is compared with the maximum fuel-air ratio at a plane 1 foot downstream of the injection points. The minimum fuel-air ratio is the lowest fuel-air ratio that is found in this plane downstream of the fuel injectors, and it is compared with the maximum fuel-air ratio at this same plane. The comparison of the degree of mixing is shown for an inlet-air velocity of 400 feet per second, a pressure of  $1/4$  atmosphere, and an inlet-air temperature of  $920^{\circ}$  F. Approximately 1800 points of injection per square foot are required to give a value of 0.9. This value corresponds to a deviation in fuel-air ratio of  $\pm 5$  percent from the mean value. Eighteen hundred points of injection is not too far from what is being used in actual combustor practice. Some of the combustor systems developed at the Lewis laboratory have as many as 900 injection points per square foot.

Greater advantage may be taken of the injection points by directing them normal to the airstream. An illustration of this is shown in the sketch in figure 2, where a manifold spacing of 1 inch was selected. The fuel sprays normal to the stream, and the point sources are arranged so that they form a series of line sources. From the line source the number of points of injection that will be required to get a near-homogeneous fuel-air mixture can be calculated. The dotted lines show that a near-homogeneous fuel-air mixture can be obtained with something on the order of from 300 to 400 injection points per square foot. Hydrogen, therefore, can be mixed quite rapidly with a realistic number of injectors by molecular diffusion alone.

Normally, this rate of mixing would be expected to increase with the use of turbulence in the airstream, which would shorten the preparation time of the fuel-air mixture still further. However, some turbulence and flow distortions can actually delay and interfere with the mixing processes, as developed in the following examples.

Assume that a stoichiometric fuel-air ratio is required and that the system has uniform fuel injection. In actual combustors distorted profiles often exist, as shown in figure 3, which, in turn, will give a fuel-air-ratio distortion. The obvious solution would be to match the fuel flow to the airflow distortion, but, unfortunately, this airflow distortion often changes with operating conditions. Variations in flow caused by acoustic resonance are also often encountered which would give time-varying fuel-air ratios. In an analogous manner the use of large



turbulence promoters upstream of the fuel injector could produce time-varying airflow at the fuel injectors. This would lead, then, to non-uniform fuel-air mixtures in a time sense. If the scale of the disturbances is large, the variations in fuel-air ratio will have insufficient time to even out in the combustor. This is a serious problem in hydrogen combustors, because generally these combustor systems are quite short. The criterion that should be used for the tolerable scale of disturbances in the system is that the flow distortions should be small with respect to the length of the combustor.

The models that have been discussed so far are fairly well idealized. They are idealized in the sense that they separated the various processes in the combustor, that is, the fuel preparation was separated from the combustion. In actual practice with hydrogen fuel, both occur simultaneously, as illustrated in figure 4. Since the fuel has a wide flammability limit, high flame speeds for a wide range of fuel-air ratios, and high blowout velocities, the flame will tend to seat at the point of fuel injection. It cannot be premixed, as is often done with hydrocarbon fuels. Therefore, the fuel injector must also serve as a flame stabilizer. In one sense this is desirable because now the mixing processes and combustion processes are occurring simultaneously, thereby decreasing the length requirements for the system. However, because the stabilization process is occurring a very short distance downstream of these very small fuel injectors, a combustible mixture must be generated in extremely short times. If adequate mixing is not obtained, the flame will no longer satisfactorily anchor itself at the point of fuel injection. Current experiences with this kind of combustor show that at conservative conditions of moderate velocities, pressures, and inlet temperatures the flame will seat on simple spray bars; but it will tend to blow away as the inlet conditions become more severe.

Another factor that tends to anchor the flame at the point of fuel injection is the approach to the spontaneous ignition temperature of the fuel at many operating conditions. For example, the combustor-inlet temperature is close to  $1200^{\circ}$  F for a ramjet flying at a Mach number of 4. In an afterburner, the spontaneous ignition temperature of hydrogen fuel is usually exceeded by the turbine-outlet temperature.

Figure 5 shows some of the spontaneous ignition temperatures of a 16-inch afterburner. The velocity was 200 to 800 feet per second, based on the maximum cross-sectional area of the combustor. The length from the fuel injector to the water spray bar used to quench the reaction was  $14\frac{1}{2}$  to  $16\frac{1}{2}$  inches. Inlet temperature is plotted against pressure. Bench-scale studies by Dixon (ref. 1) predicted ignition at the inlet temperature shown by the solid line. Dixon's data were obtained in a small coaxial tube experiment. The full-scale data are similar. No consistent effect of velocity (residence time) was found. Normally, in ignition

experiments, lower ignition temperatures would be expected as the residence time was increased. The independence of the data to velocity suggests that ignition occurred in the recirculation zone downstream of the fuel spray bars or in a separated region on the centerbody.

Good combustor performance would be expected in a system in which the fuel spontaneously ignited. Also, the futility of using the usual flameholder at some distance down of the spray bar was indicated, since it would generally be immersed in the flame under most conditions of operation. This simple configuration was investigated over the range of conditions shown in figure 6. High efficiencies were obtained at intermediate equivalence ratios.

In an attempt to get a still shorter combustor, the diffuser centerbody was shortened. The performance with a short blunt centerbody is shown in figure 7. The combustion efficiency was again near 100 percent at the intermediate equivalence ratios and dropped off slightly at the extremes of both the lean and rich zones.

On the basis of the moderately good combustion efficiency, the simplicity of the device, and the low pressure drop, this configuration was tested in a full-scale engine located in an altitude test facility. Instead of using concentric spray bars, as in the 16-inch-diameter afterburner, radial injectors were used; the number of fuel orifices per square foot was 300. The combustion-chamber length was 39 inches. The data were taken at an inlet velocity ranging from 560 to 630 feet per second and an inlet temperature of 1240° F. Combustion efficiency is plotted against equivalence ratio in figure 8. At the pressure range of 0.35 to 0.45 atmosphere, the combustion efficiency was about 100 to 90 percent at lean equivalence ratios. At the lower pressure of 0.19 to 0.24 atmosphere, much the same characteristic was observed. Only at the very lean fuel-air ratios was the combustor performance high.

Before the shape of these curves is discussed, the performance with hydrogen fuel will be compared with that with JP fuel at similar conditions. The performance with JP-4 fuel is presented at pressures of 0.42 and 0.35 atmosphere (fig. 8). The configuration used for the data with the JP-4 fuel was a combustor of considerably greater length but similar diameter. It used a flameholder similar to the better ones in use in existing engines and had comparable inlet velocity and inlet temperature. Even with this more elaborate combustor system, the data with JP-4 fuel were considerably lower than those with hydrogen fuel. The peaks of the two curves, hydrogen and JP-4 fuels, occurred at different equivalence ratios. This is believed to be due, in part, to the type fuel-air-ratio distribution in the region of flame stabilization and in the main combustor region for the particular configuration used with the fuels. Apparently a more elaborate combustor system than was used in these tests is needed to obtain high performance for hydrogen fuels at richer

equivalence ratios. A method of improving fuel-injector and flame-stabilizer designs will be illustrated in the discussion on ramjet performance.

The performance of the simple radial fuel-bar injector and flameholder in the ramjet combustor is shown in figure 9. The same kind of combustor was used in the afterburner work. Two configurations were chosen in order to show the effect of blockage and orifice density. In order to bring out the differences between these configurations, severe operating conditions were chosen since both configurations had high performance with long combustors (44 in.) and high burner pressures (1 atm and above). The burner pressure was quite low, ranging from 0.2 to 0.35 atmosphere, and the burner length was 18 inches. The burner length was measured from the point of fuel injection to the throat of the exhaust nozzle. The diffuser centerbody extended to the inlet of the exhaust nozzle. One of the configurations had a fuel orifice density of 450 orifices per square foot and a blockage of 20 percent, while the other had approximately twice the orifice density and twice the blockage.

The performance of the radial spray-bar system that had only 450 orifices per square foot and 20 percent blockage was quite poor. The combustion efficiency level was about 50 percent, and blowout occurred at equivalence ratios leaner than 0.80. Increasing the blockage from 20 to 45 percent and increasing the orifice density from 450 to 900 orifices per square foot improved the efficiency considerably. The combustion efficiency was on the order of about 80 percent. The reason for this improvement was believed to be due to several causes. First, the increased orifice density improved the local fuel-air ratio at the point of flame stabilization since the fuel spray bars also served as flame stabilizers. The higher orifice density also improved the over-all mixing rate. The higher blockage gave a larger stability zone since the blockage was achieved by increasing the size of the radial spray bars. The higher blockage also improved the rate of mixing. The total pressure drop of this configuration was low, on the order of 5 to 6 percent.

Since this configuration was simple, its performance at less-severe operating conditions was recorded, even though its performance was low at severe conditions. An example of the type of data obtained is shown in figure 10. Combustion efficiency is shown plotted against burner length for various burner-inlet pressures at a constant equivalence ratio of 0.6. At a pressure on the order of  $1/3$  atmosphere, the efficiency did not increase much beyond 80 percent, even with long burner lengths; but at pressures above  $1/2$  atmosphere, the efficiency was quite good, even with burner lengths as short as 25 inches. At the higher pressures (0.835 atm and above), very short combustors could be used with good performance. Note the burner length was measured from the point of fuel injection to the exhaust-nozzle throat.

If the combustor is operated at conditions of lower pressures or at conditions of low fuel-air ratio, certain techniques can be employed to improve the performance, as illustrated in figure 11. In this figure combustion efficiency is plotted against equivalence ratio. The data for a simple injector and a shrouded injector are shown. The tests were bench-scale tests taken in sectors of complete engines. The pressure, velocity, and temperature conditions are shown in the figure.

The simple injector system consisted of a spray bar with fuel issuing out normal to the airstream. The efficiency of the simple injector was poor and fell off very rapidly at the lean equivalence ratios; however, it improved to nearly 100 percent with the addition of a fuel-controlling shroud around the spray bar. The proper fuel-air mixture was generated within the shroud, since the penetration of the fuel jet was controlled. The size of the air openings allowed the proper amount of air to enter. The fuel mixture was usually richer than stoichiometric, which is desirable for hydrogen fuel. The mixture was at a lower velocity than previously so that the flame could stabilize more securely. Small tabs were sometimes put on the end of the shrouds to improve the mixing processes.

The use of these shrouds on a full-scale engine was investigated in the Lewis 10- by 10-foot supersonic wind tunnel at a simulated Mach number of 3 and an altitude of 71,000 feet. The stagnation temperature was not simulated for this flight condition, since the facility was limited to an inlet temperature of 665° R, which is considerably lower than actual flight operation. The engine was 16 inches in diameter and had a fixed-area inlet and exhaust. The combustor length from the point of fuel injection to the exhaust-nozzle throat was 3 feet. Hydrogen fuel was used in the engine, which was started by a spark located at the trailing edge of the centerbody. During ignition of the combustor, supersonic flow existed in parts of the flameholder. As the fuel flow was increased, after ignition, the combustor pressure increased and the terminal shocks moved forward, decreasing in strength until the flow in the diffuser was subsonic past the throat; at this point the diffuser was operating critically. This point is the design point of this fixed-area system.

The performance of this engine with both a shrouded and an unshrouded injector is shown in figure 12, where combustion efficiency is plotted against equivalence ratio. The efficiencies were low for the unshrouded injector and did not exceed 80 percent, even at the design point. Lean blowout occurred at a equivalence ratio of 0.25. Putting a shroud around the injector, similar to the one shown in figure 11, controlled the penetration of the fuel and generated a more desirable combustion environment downstream of this flameholder injector. In the actual engine, the shrouds were tabbed to increase mixing. The injector details shown in figure 12 are highly schematic. The use of the shroud gave

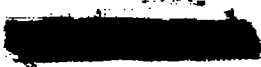


much more stable operation over the entire equivalence-ratio band. No serious flame instability was observed. At critical flow conditions, the design point for the engine, combustion efficiency was near 95 percent. The low combustion efficiency in the leaner regions was not too serious, since this engine is designed to operate only over the range of equivalence ratio from about 0.3 to 0.5.

So far the application of hydrogen fuel to fairly conventional engine and combustors systems has been discussed. The high reactivity of the hydrogen fuel (and therefore its ability to burn in short combustors) also provides the opportunity to try more novel ideas. If the engine length is to be reduced, the diffuser, the combustor, and the exhaust nozzle must be shortened. This shortening can be done by building small engines and then increasing the thrust by merely stacking these independent engines. Because of the small scale of each independent unit, the diffuser and the exhaust nozzle will be short. The idea is not particularly original, but hydrogen fuel makes it practical as it can burn in small spaces. Also, it can be used to cool the inner passages that are necessarily introduced in scaling by multiplicity. The advantages of the system are short length, the ability to scale by multiplicity, the flexibility of the engine design, and the flexibility of installation. Also, since simple testing facilities can be used because of the small size of these units, the development time may be reduced. Figure 13 illustrates several of these stacked units.

Some combustion performance has already been obtained on these units. One of the single elements was run in a small connected-pipe facility, and the results are shown in figure 14. A combustion efficiency of about 90 percent was obtained at a pressure of  $1/2$  atmosphere, an inlet velocity of 220 feet per second, and an inlet temperature of  $80^{\circ}$  F in a  $6\frac{1}{2}$ -inch combustion chamber. The spacing between the combustor walls of this two-dimensional unit is only 1 inch. This means that a total ramjet-engine length of  $1\frac{1}{2}$  feet is becoming more realistic. The actual final engine may not look like the sketch, but hydrogen fuel could make a similar engine design possible.

In summary, if the afterburner or ramjet is designed to operate at mild combustor conditions, a simple injector flameholder should give adequate performance. As the conditions of operation become more severe, such as shorter lengths or lower pressures, more care must be exercised in the design of the combustor. Finally, some recent work shows that because of the higher reactivity of hydrogen fuel new engine designs are becoming more feasible.

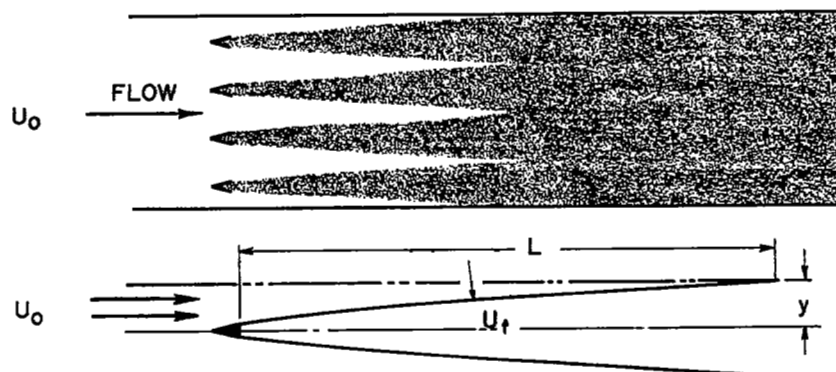




## REFERENCE

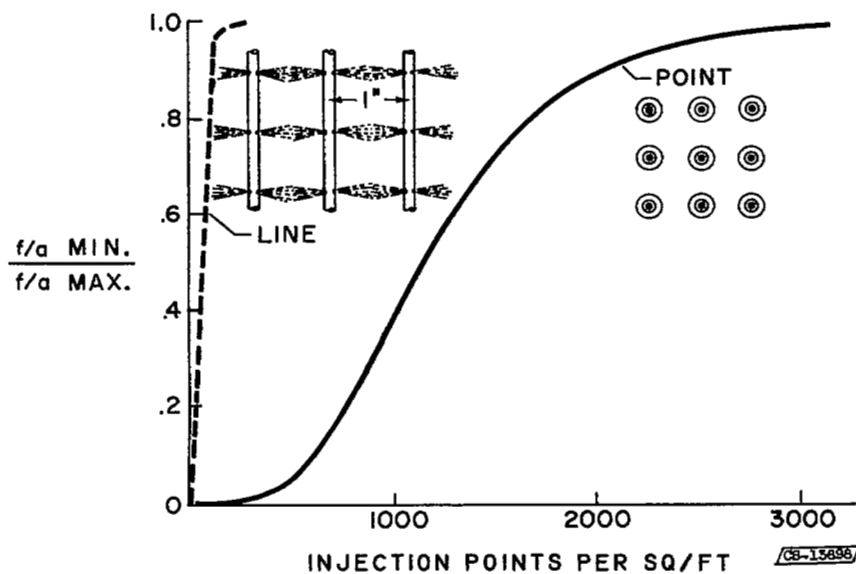
1. Coward, H. F.: Ignition Temperatures of Gases. "Concentric Tube" Experiments of (the late) Harold Daily Dixon. Jour. Chem. Soc. (London), pt. II, July-Dec. 1934, pp. 1382-1406.





CS-15700

Figure 1. - Simplified model of flame spreading.  $\rho_0 A_0 U_0 = \rho_0 A_f U_f$ ;  
 $y U_0 \approx L U_f$ ;  $L = 1$  foot for  $Y = 0.05$  ft;  $U_0$ , 200 feet per second;  
 $U_f$ , 10 feet per second.



CS-15686

Figure 2. - Fuel-air mixing by molecular diffusion. Velocity; 400 feet per second;  $L$ , 1 foot; temperature,  $920^\circ$  F; pressure,  $1/4$  atmosphere.

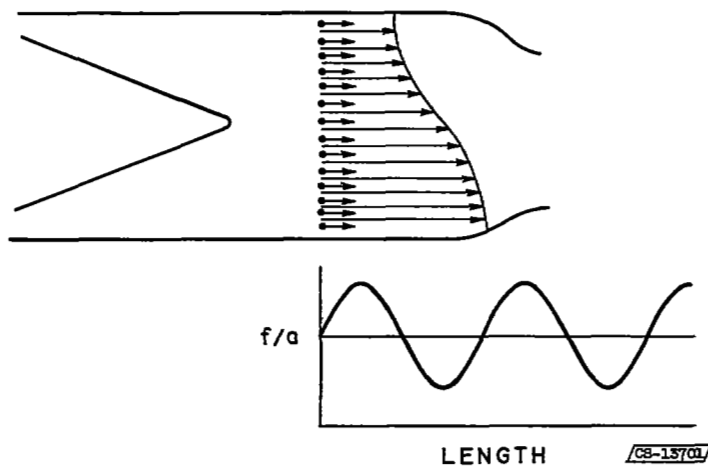
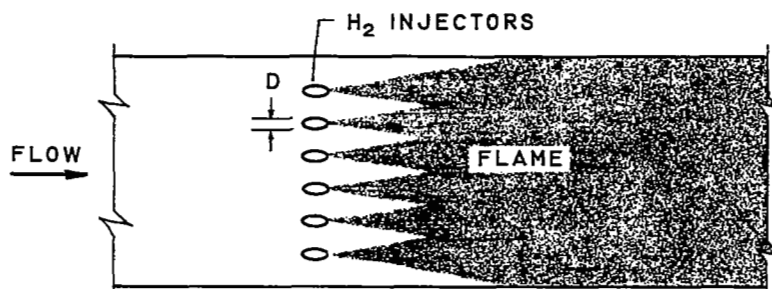


Figure 3. - Effect of large-scale disturbances.



- 1 WIDE FLAMMABILITY
- 2 HIGH FLAME SPEED FOR WIDE F/A RANGE
- 3 HIGH  $V_{B,0}$  (800 FPS AT  $P = 1/2$  ATMOS,  $D = 1/4$  IN.,  $T = 80^\circ$  F)
- 4 SPONTANEOUS IGNITION TEMP ( $\sim 1100^\circ$  F)

CB-13696

Figure 4. - Typical combustion with hydrogen.



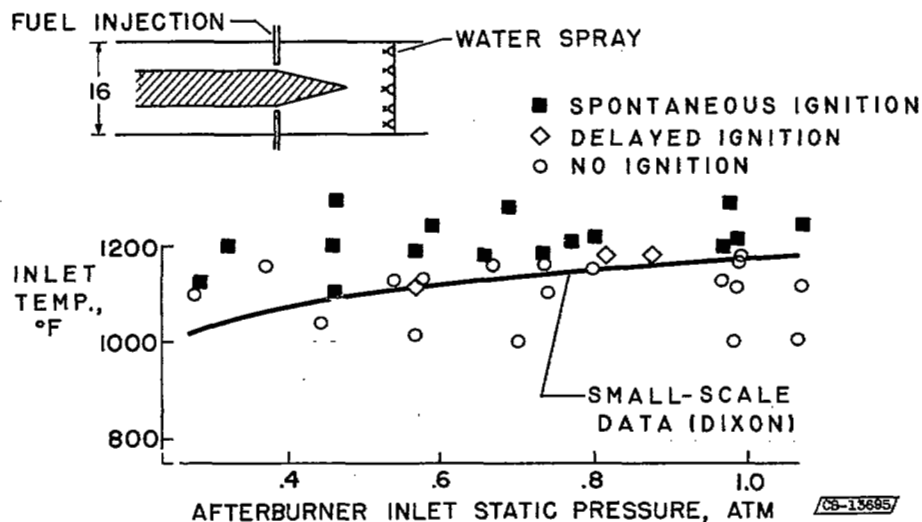


Figure 5. - Spontaneous ignition temperature of hydrogen. Afterburner length,  $14\frac{1}{2}$  to  $16\frac{1}{2}$  inches; velocity, 200 to 800 feet per second.

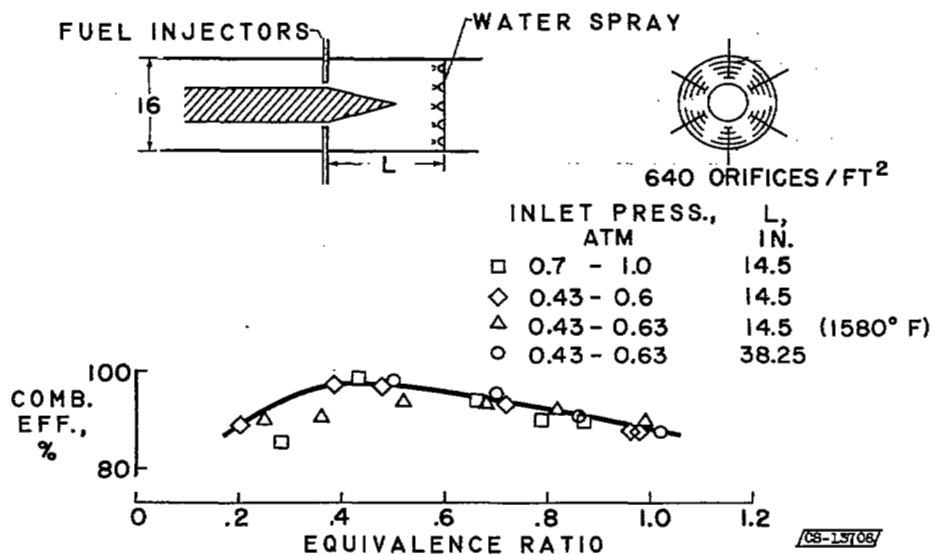


Figure 6. - Performance of 16-inch afterburner. Fuel, hydrogen; inlet temperature,  $1230^{\circ}$  F.

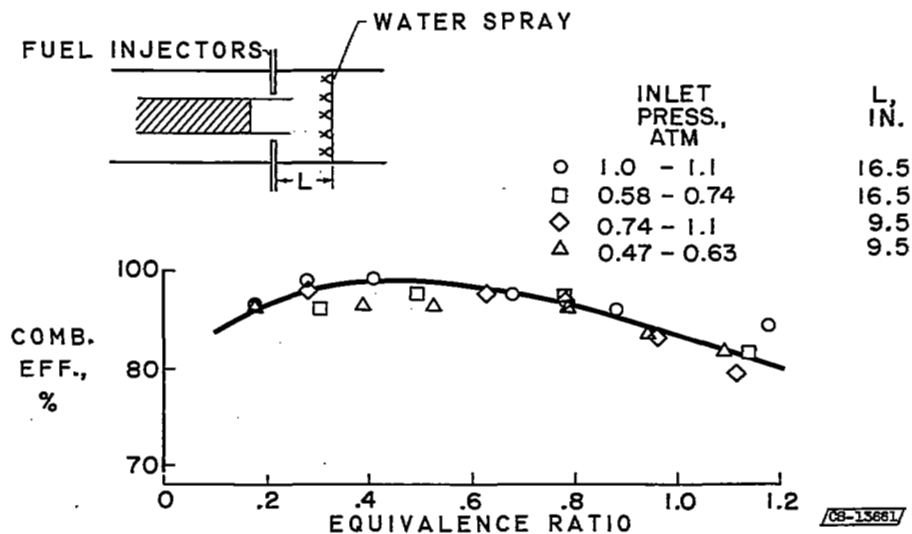


Figure 7. - Effect of blunt centerbody on afterburner performance. Fuel, hydrogen; inlet temperature, 1220° to 1520° F.

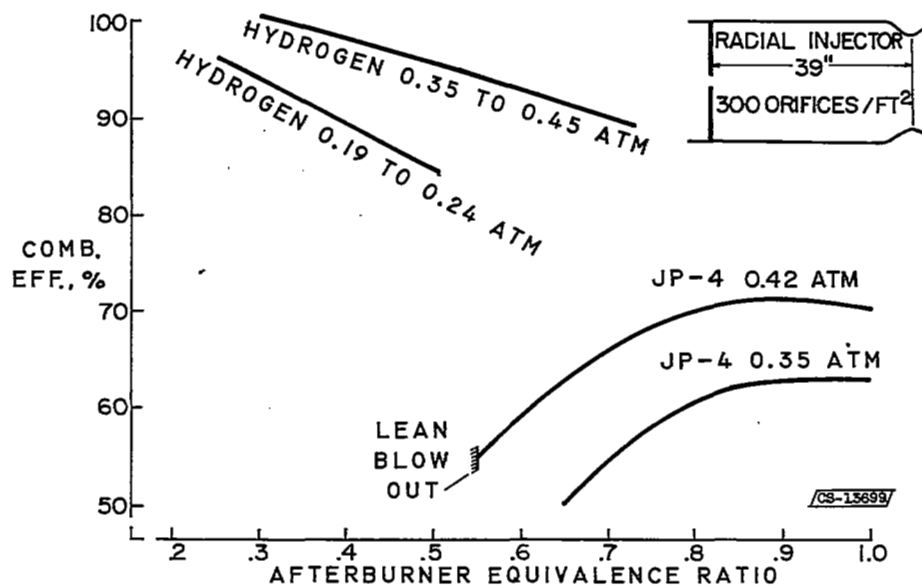
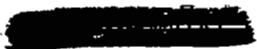


Figure 8. - Full-scale afterburner. Inlet velocity, 560 to 630 feet per second; inlet temperature, 1240° F.



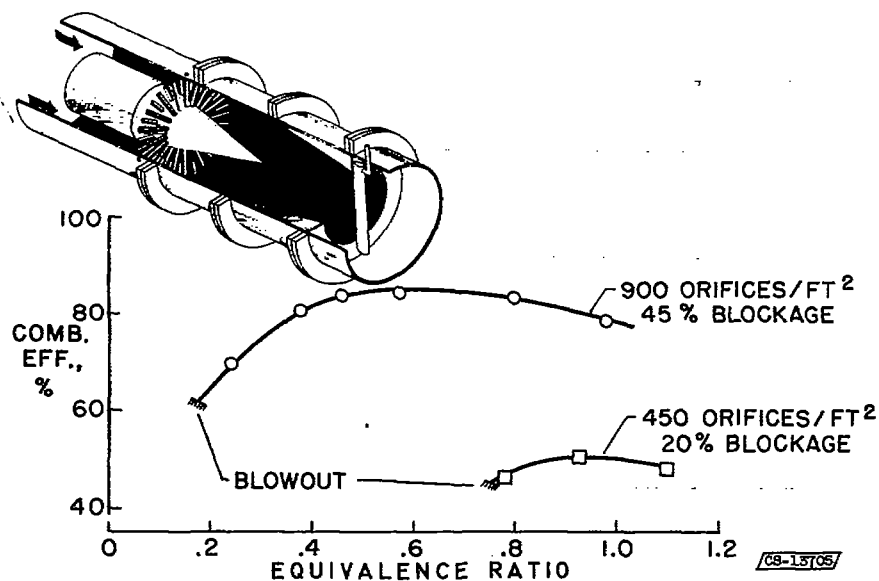


Figure 9. - Comparison of two ramjet configurations with different injector diameters and orifice densities. Burner length, 18 inches; inlet temperature, 640° F; inlet velocity, 250 to 400 feet per second; inlet pressure, 0.2 to 0.35 atmosphere.

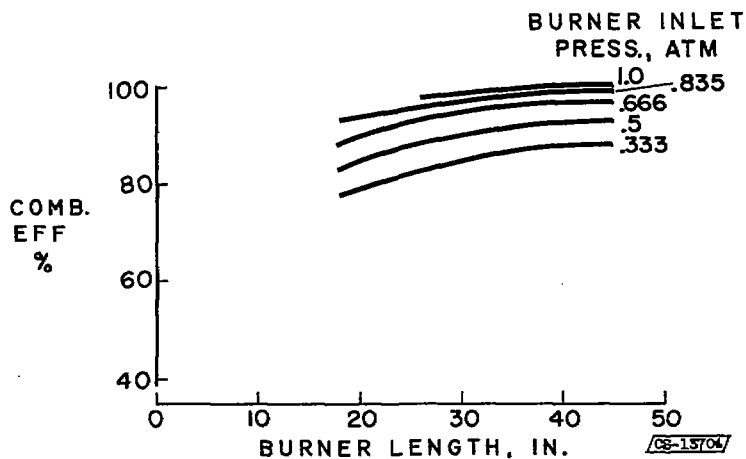


Figure 10. - Effect of burner pressure and length on performance of 16-inch ramjet. Equivalence ratio, 0.6.

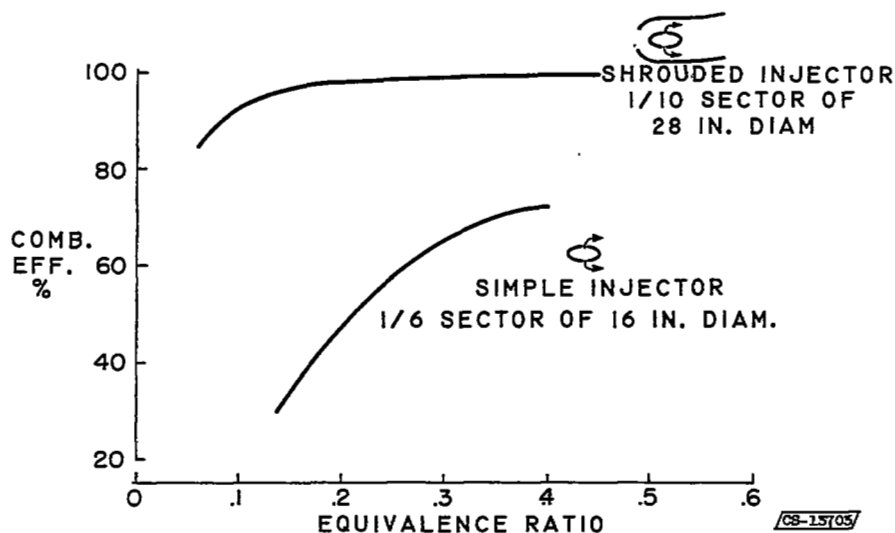


Figure 11. - Effect of fuel shrouds. Pressure, 0.24 to 0.4 atmosphere; velocity, 140 to 240 feet per second; temperature, 240° F.

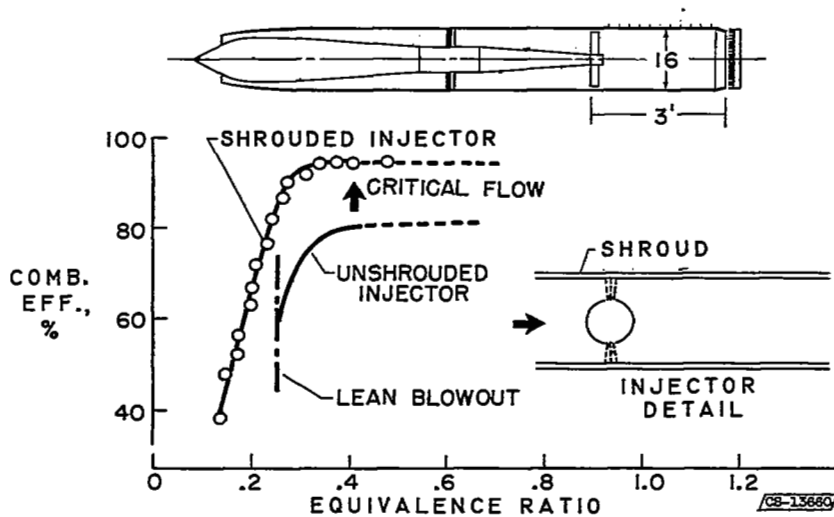


Figure 12. - Performance of ramjet engine in 10- by 10-foot supersonic wind tunnel. Fuel, hydrogen; altitude, 71,000 feet; temperature, 665° R.



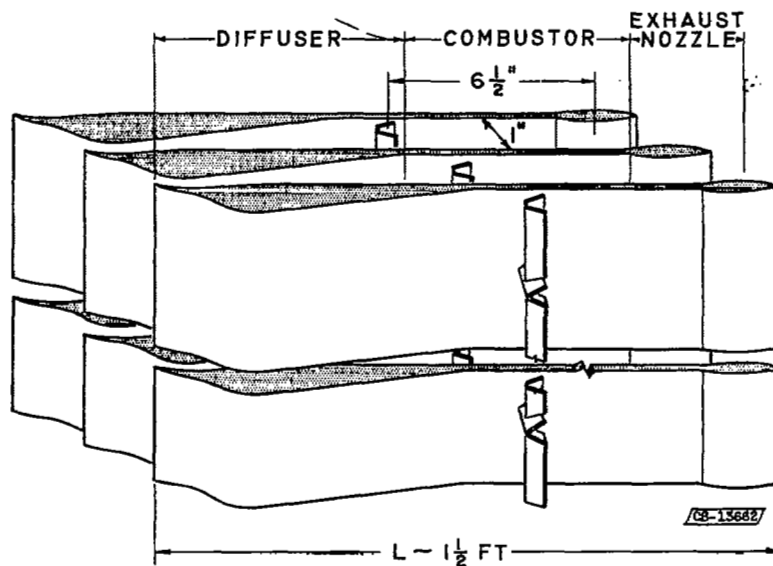


Figure 13. - Cascaded ramjet.

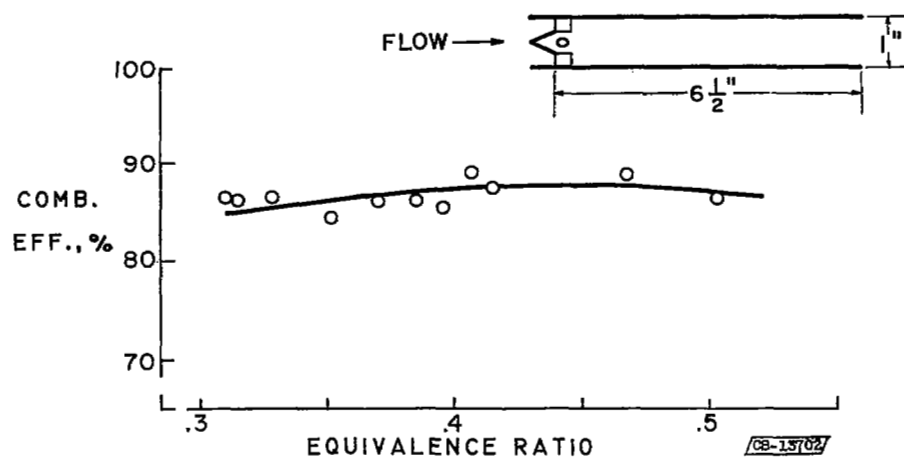


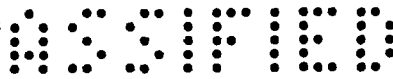
Figure 14. - Single-element test of cascaded combustor. Pressure, 1/2 atmosphere; inlet velocity, 220 feet per second; inlet temperature, 80° F.



3 - COMBUSTION IN TURBOJET ENGINES

E. William Conrad  
Lester C. Corrington





### 3. COMBUSTION IN TURBOJET ENGINES

By E. William Conrad and Lester C. Corrington

#### Introduction

A number of experimental investigations have been conducted at the Lewis laboratory in which hydrogen has been burned in primary combustors of turbojet engines. The first objective was to determine immediately what performance gains and operating problems would occur when this fuel was substituted for conventional turbojet fuels in production turbojet engines. A second objective was to learn how to exploit the superior combustion properties of hydrogen in order to make the combustors shorter and thus reduce engine weight. Most of the research in connection with shorter combustors was done in combustion rigs; however, the results are presented only for the few most promising configurations which were evaluated in current turbojet engines under altitude operating conditions.

This paper presents the results obtained from experimental work toward both objectives. Turbojet engines with the production or special combustors were operated with hydrogen fuel in altitude test chambers. Altitude was increased until either an engine limitation or a facility limitation was reached. For comparison purposes the engines with the production combustors were also operated with JP-4 fuel.

#### Performance of Production Combustors in Engines

In determining the performance gains and operating problems associated with production turbojet engines, no modifications were made to the production engines other than changes in the fuel injectors and the external fuel systems. However, in one case a cooled turbine was used. In all cases the hydrogen fuel used was gaseous at about room temperature and was injected at low pressure.

Engine A. - Figure 1 shows some of the combustion results obtained with engine A, an engine in the 10,000-pound-thrust class with cannular combustors and a compressor pressure ratio of about 8.5. In this engine, the fuel injectors were removed and replaced by open tubes that injected the hydrogen in a downstream axial direction. The combustion efficiency appears rather low, but it should be noted that the operating conditions



were rather severe, corresponding to altitudes from 78,000 to 89,000 feet at a flight Mach number of 0.8. No combustor blowouts were experienced at the lowest combustor pressures available with the test facility, approximately 500 pounds per square foot. Additional information on tests with hydrogen in this engine is presented in reference 1.

Engine B. - Combustion efficiency data for engine B, an engine in the 7500-pound-thrust class with an annular vaporizing combustor and a compressor pressure ratio of about 7, are presented in figure 2. During operation with conventional fuels, the fuel enters the vaporization tubes through open fuel tubes. A small amount of air passes through the vaporization tubes and mixes with the vaporizing fuel as it flows toward the combustion chamber. This fuel-air mixture is normally too rich to burn until it is mixed with additional air in the combustion chamber. However, because of the extremely wide flammability limits of hydrogen-air mixtures, it was felt that operation with hydrogen might result in combustion within the vaporization tubes and possible damage due to overheating. Consequently, for initial operation with hydrogen, the inlet ends of the vaporization tubes were sealed to prevent air flow. The hydrogen fuel was injected through the normal fuel tubes without alteration.

The combustion efficiency of this configuration using hydrogen is indicated in figure 2 by the closed-vaporization-tube curve. At very low combustor-inlet pressures the combustion efficiency using hydrogen was considerably better than that with JP-4 fuel (normal configuration), and at pressures above about 1000 pounds per square foot the combustion efficiency was about the same. Blowout occurred with JP-4 fuel at a combustor-inlet pressure of 700 pounds per square foot.

Subsequent experience with this engine indicated that the vaporization tubes could be left open during operation with hydrogen fuel without damage due to combustion within the tubes. The combustor performance for this configuration is indicated by the open-vaporization-tube curve in figure 2. An appreciable improvement resulted over most of the pressure range investigated. Again, combustion blowout was not experienced with hydrogen even at the minimum attainable combustor pressure of 400 pounds per square foot. Additional information on hydrogen tests in this engine is contained in references 1 and 2.

Engine C. - Figure 3 presents the performance of the combustor for engine C. This engine is in the 6000-pound-thrust class with can-type combustors and a compressor pressure ratio of about 5.3. A cooled turbine was installed in this engine, and liquid-hydrogen fuel was used as a heat sink to refrigerate the turbine cooling air (refs. 3 to 5). This permitted turbine-inlet gas temperatures up to 2500° F. In order to operate this engine with hydrogen, the fuel injectors were removed and replaced by tubes having the ends closed and the walls near the ends slotted.

This engine was not operated over a range of altitudes but instead was operated over a range of turbine-inlet gas temperatures at a fixed altitude. For this reason the data are presented with combustion efficiency as a function of combustion temperature rise. The values of temperature rise shown are considerably higher than those of current engines and correspond to turbine-inlet temperatures up to 2500° F. The combustion efficiency is affected only a small amount over the entire range. The combustion efficiency of hydrogen at 60,000 feet is about the same as that of JP-4 fuel at 50,000 feet.

#### Altitude Limits of Production Engines

Engine A. - Because the use of hydrogen fuel permits turbojet-engine operation at much higher altitudes than has been otherwise possible, it is important to investigate other factors which may limit the operation of engines at these high altitudes. Figure 4 shows the altitude operational limits of engine A. For reasons of simplification, the flight Mach number is constant at 0.8 for all altitudes shown.

The minimum engine speed at high altitude is defined by the intersection of the steady-state operating line with the compressor stall line. As altitude is increased, the stall limit line is lowered because of Reynolds number effects, and, consequently, the intersection occurs at progressively higher speeds. The stall limit line shown in figure 4 indicates the limits imposed by these steady-state intersections. The engine cannot be operated at lower speeds than indicated by this stall limit line without encountering compressor stall. This line is substantially independent of the fuel used.

With a variable-area jet nozzle no high-speed limit other than rated mechanical speed was encountered up to the altitude limits imposed by the facility. However, these data represent operation under ICAO (International Civil Aviation Organization) standard altitude conditions, and it is possible that a high corrected-speed stall limit might be encountered under very low inlet air temperature conditions.

If the engine had a fixed-area jet nozzle sized for limiting temperature at low altitude, a high-speed limit would be imposed by the limiting turbine-outlet temperature. As the altitude increased, the engine speed would have to be reduced as indicated by the temperature limit lines in figure 4 in order to avoid excessive turbine temperatures. The thrust would drop correspondingly. The engine speed limitation using the same size nozzle is less severe with hydrogen fuel. This is primarily due to the change in the thermodynamic properties of the products of combustion when hydrogen is used. The specific heat of the turbine working fluid is higher with hydrogen fuel, resulting in a lower turbine temperature ratio. The turbine pressure ratio is therefore lower, and



the turbine-outlet pressure is higher. This higher pressure in the tail-pipe can force more mass flow through a fixed-size exhaust nozzle, and therefore engine speed can be increased. Several other considerations also enter into this shift in the temperature limit curve when hydrogen is used instead of JP-4 fuel, but their effects are minor.

The shaded area of figure 4 indicates a region of marginal burning with JP-4 fuel. Operation in this region required careful throttle manipulation, and random blowouts occurred despite the care used. The JP-4 fuel combustion limit line indicates altitudes above which combustion was never sustained. In view of this area of marginal operation, the maximum practical operating altitude for this engine with JP-4 fuel is considered to be about 62,000 feet. In contrast, the combustion of hydrogen was stable up to the facility-limited altitude of 89,000 feet, and blowouts did not occur even during compressor surge.

Engine B. - A similar altitude-limit picture for engine B is presented in figure 5. These data are presented primarily to show the typical variation which may be expected from one engine to another. The limits in this case are slightly more restricted than those for engine A. The stall-limited speed is appreciably higher, the temperature-limited speed is appreciably lower, and the JP-4 fuel combustion limit is slightly lower. Here, again, the combustion of hydrogen was always stable, and severe transients such as compressor surge did not cause combustor blowout.

Even if the facility had not limited the maximum altitude to about 89,000 feet, a turbine limitation would have appeared at slightly higher altitude. This limitation is illustrated for engine B in figure 6, in which the turbine-outlet axial Mach number is shown as a function of altitude. The limiting-loading line is indicative of the maximum work per pound of working fluid that the turbine can produce. This condition occurs when the axial component of the velocity of the gas leaving the last stage rotor blade passages reaches a Mach number of 1. For the geometry of this particular engine the axial Mach number in the annulus just downstream of the turbine is about 0.77 when this condition occurs, and in figure 6 the limiting-loading line is shown at this Mach number. When this Mach number is reached, further increases in the turbine pressure ratio produce no increase in turbine work per pound of working fluid.

For operation at rated speed and temperature with JP-4 fuel, the turbine-outlet Mach number increases with altitude because of reduction in compressor and turbine efficiency. Limiting-loading was not reached because combustor blowout occurred at about 77,000 feet. Had combustion continued, it appears probable that limiting-loading would have been reached at about 79,000 feet.



When hydrogen is used instead of JP-4 fuel, the turbine-outlet Mach number at a given altitude is lower. This is principally due to the change in thermodynamic properties of the turbine working fluid when the fuels are changed. For operation at a given altitude, the turbine work and, hence, the gas velocity in the turbine are common for operation with both fuels if the difference in fuel weight is ignored. Because the gas constant and, hence, the sonic velocity are higher for the products of combustion of hydrogen, the Mach number level is reduced. An extrapolation of the curve for hydrogen indicates that limiting-loading would probably occur at an altitude of about 89,000 feet.

The data thus far presented show that the substitution of hydrogen for JP-4 fuel in production turbojet engines allows operation at considerably higher altitudes. The operating limits of two current engines operating on hydrogen are shown. The thrust, specific fuel consumption, and an analysis of component performance losses at extreme altitude are given in references 1 and 2.

#### Performance of Short Combustors in Engines

Because of the high reactivity of hydrogen, it appeared that engine combustors could be made much shorter for a given application, and thereby a significant weight saving could be made with no sacrifice in combustor performance. The first approach in this direction is illustrated in figure 7. This configuration was first made up in the form of a one-quarter segment of an annular combustor for duct tests (ref. 6). Because of the high reactivity of hydrogen and the short wall-quenching distance, the primary combustion zone was made considerably smaller than that for conventional combustors. The use of channeled walls ensured maximum rate penetration of the secondary air without adverse effects on stability and allowed a shorter secondary zone or mixing length. The fuel was injected under choked-flow conditions into an enclosed V-gutter from two circumferential manifolds having a large number of drilled orifices. It then entered the primary combustion zone from the trailing edges of this gutter.

Duct tests with this one-quarter segment combustor indicated sufficient promise that a complete annular combustor was constructed and evaluated in a turbojet engine. The configuration in the engine and some of the test results are shown in figure 8. The dashed line indicates the outline of the production combustor liner, and the solid line is the outline of the channeled-wall short combustor. This hydrogen combustor is about 40 percent shorter than the production combustor, and the combustor volume is about 50 percent smaller. Ignition was obtained by a single spark plug downstream of the fuel-injection gutter.

The results of altitude chamber tests with this combustor in an engine (fig. 8) indicate that the combustion efficiency was almost identical with the best results obtained with production combustors. In addition, the stability was good in that blowout was never encountered even during compressor surge at the lowest combustor pressures. Complete information on engine tests with this combustor is contained in reference 7.

"Flower-pot" combustor. - Because of the encouraging results obtained with the channeled-wall short combustor, more drastic measures were taken to capitalize further on the excellent reactivity characteristics of hydrogen fuel. The method used is illustrated in figure 9. In the conventional combustor (upper part, fig. 9), the primary combustion zone is in the form of a single large volume. With this large column of hot gas leaving the primary zone, considerable length is required for the secondary air to penetrate to the center and to mix adequately.

Relying heavily on the high reactivity and short wall-quenching distances of hydrogen, the size of the primary zone was greatly reduced, and a multiplicity of primary zones was employed. With the smaller primary zones (lower part, fig. 9), less radial penetration is required behind a given element; hence, it should be possible for the secondary length to be considerably shorter.

Work was done in a small duct setup to evolve suitable geometry for small combustor elements, and one of the most promising configurations is illustrated in figure 10. For obvious reasons this configuration was called the flower-pot combustor. The fuel is injected at sonic velocity near the wall almost tangentially but aimed slightly upstream. Primary air enters through an orifice in the upstream end. The vortex path of the fuel provides a high shear area between the fuel and air and also results in a high residence time for the fuel and air to mix and react within the primary zone. Small V-gutters attached to the downstream end of the flower pot promote spreading of the hot gases and mixing with the secondary air.

Duct tests were conducted with an array of 10 flower pots in a one-quarter segment of an annulus. With a combustor length of 12 inches, an inlet reference air velocity of 115 feet per second, and a pressure of 420 pounds per square foot, the combustion efficiency was 93 percent. Because this performance was appreciably better than that of any of the previous combustors that had been tested in engines, a full assembly was fabricated and installed in an engine (fig. 11). The over-all length of this combustor from the upstream end of the flower pots to the turbine stator was about  $9\frac{1}{2}$  inches. Three rows of flower pots were used, with three different sizes to keep the secondary air spaces between them of a more or less uniform size. After a preliminary run, upstream screens and a single annular V-gutter near the outer wall were added to improve

the turbine temperature profiles. In the inner two rows of flower pots, the fuel was injected tangentially from one orifice, while in the outer row, two orifices on opposite sides of the flower pots were used. Ignition was obtained from a single spark plug.

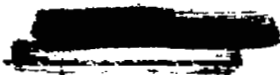
The performance of this configuration is indicated by the data points in figure 12. Data were obtained at only one pressure level for reasons that will be discussed later. At this pressure level the combustion efficiency compares favorably with the best previous results with hydrogen, and was about 5 percent better than that with JP-4 fuel in the production combustor (see fig. 2). The combustor total-pressure drop was about 2 percent, less than half that of the production combustor. In addition, the weight of this combustor was less than half that of the production combustor liner for this engine.

Although the efficiency of this very short combustor appeared satisfactory, the turbine-inlet temperature profiles were poor, and, consequently, the performance evaluation was restricted to the data points shown. Figure 13 shows typical profiles obtained. Radial profiles are shown at five different circumferential positions. Although the average radial temperature profile shown by the broken curve is satisfactory for safe operation of the turbine rotor, local gradients of several hundred degrees per inch are not considered suitable for the stators. Additional work is required to achieve more uniform temperature patterns. This additional work will be done with a complete full-scale assembly in a combustion duct. The approach will be to use more and smaller flower pots spaced more closely together. The V-gutters will be eliminated because of the close spacing of the flower pots.

For many reasons it is desirable that a combustor developed especially to operate on hydrogen also be capable of satisfactory operation on hydrocarbon fuels, particularly at low altitude. The performance of the array of 10 flower-pot elements was investigated in a combustion duct using propane fuel to simulate vaporized hydrocarbon fuels (fig. 14). The combustion efficiency was very satisfactory at the pressure level of 2100 pounds per square foot (about 55,000 ft altitude at Mach number 0.8) and was only a small amount lower than that for JP-4 fuel in the production combustor at the pressure level of 1050 pounds per square foot (about 70,000 ft altitude at Mach number 0.8).

#### Concluding Remarks

The use of hydrogen in production engines has allowed operation at considerably higher altitudes than were possible with JP-4 fuel. At the maximum altitude possible with the facility, 89,000 feet at a Mach number of 0.8, no combustion limit was reached. Minimum engine speed was restricted by compressor stall, and maximum speed was restricted by



turbine temperature in the case of fixed-jet-nozzle-area engines and only by rated mechanical speed in the case of variable-area-nozzle engines.

Turbine temperature profiles with production engines using hydrogen were almost identical to those obtained using JP-4 fuel. Altitude starting limits were not determined with hydrogen; however, many air starts were made at altitudes between 45,000 and 55,000 feet, and all were exceptionally smooth and cool. Combustor blowout was not encountered with hydrogen, even during compressor surge at an altitude of 80,000 feet.

The superior combustion properties of hydrogen have been exploited to achieve a completely satisfactory combustor 40 percent shorter than the production unit. Further shortening to an over-all length of about  $9\frac{1}{2}$  inches has been also satisfactory with respect to combustion, but work is still required to obtain satisfactory turbine-inlet temperature distribution.

#### References

1. Fleming, W. A., Kaufman, H. R., Harp, J. L., Jr., and Chelko, L. J.: Turbojet Performance and Operation at High Altitudes with Hydrogen and JP-4 Fuels. NACA RM E56E14, 1956.
2. Kaufman, Harold R.: High-Altitude Performance Investigation of J65-B-3 Turbojet Engine with Both JP-4 and Gaseous Hydrogen Fuels. NACA RM E57A11, 1957.
3. Corrington, Lester C., Thornbury, Kenneth L., and Hennings, Glen: Some Design and Operational Considerations of a Liquid-Hydrogen Fuel and Heat-Sink System for Turbojet Engine Tests. NACA RM E56J18a, 1956.
4. Slone, Henry O., Cochran, Reeves P., and Dengler, Robert P.: Experimental Investigation of Air-Cooled Turbine Rotor Blade Temperatures in a Turbojet Engine Operating at Turbine-Inlet Temperatures up to 2580° R and Altitudes of 50,000 and 60,000 Feet. NACA RM E56C26, 1956.
5. Cochran, Reeves P., Dengler, Robert P., and Esgar, Jack B.: Operation of an Experimental Air-Cooled Turbojet Engine at Turbine-Inlet Temperatures from 2200° to 2935° R. NACA RM E56D24a, 1956.
6. Friedman, Robert, Norgren, Carl T., and Jones, Robert E.: Performance of a Short Turbojet Engine Combustor with Hydrogen Fuel in a Quarter-Annular Duct and Comparison with Performance in Full-Scale Engine. NACA RM E56D16, 1956.
7. Sivo, Joseph N., and Fenn, David B.: Performance of a Short Combustor at High Altitudes Using Hydrogen Fuel. NACA RM E56D24, 1956.

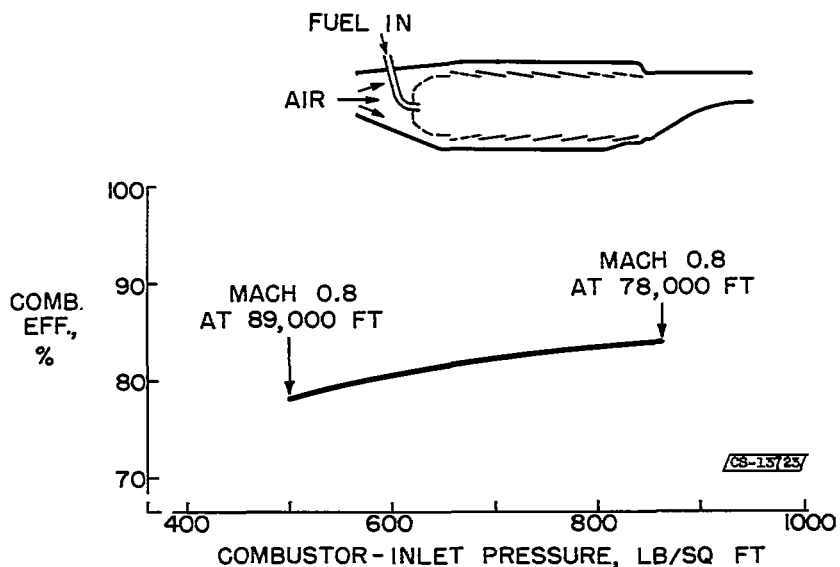


Figure 1. - Performance of production cannular combustors with hydrogen fuel.

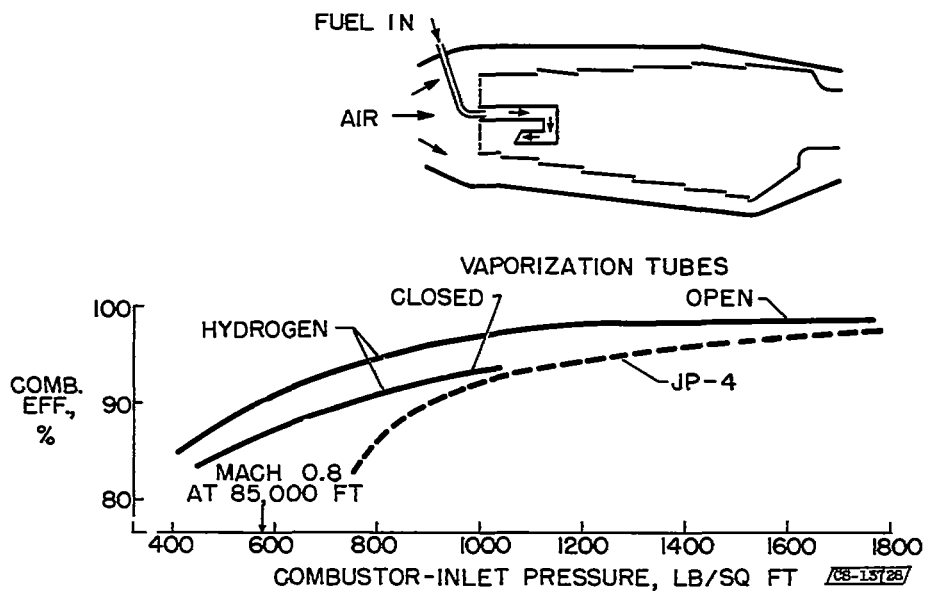


Figure 2. - Performance of production annular combustor with hydrogen and JP-4 fuels.

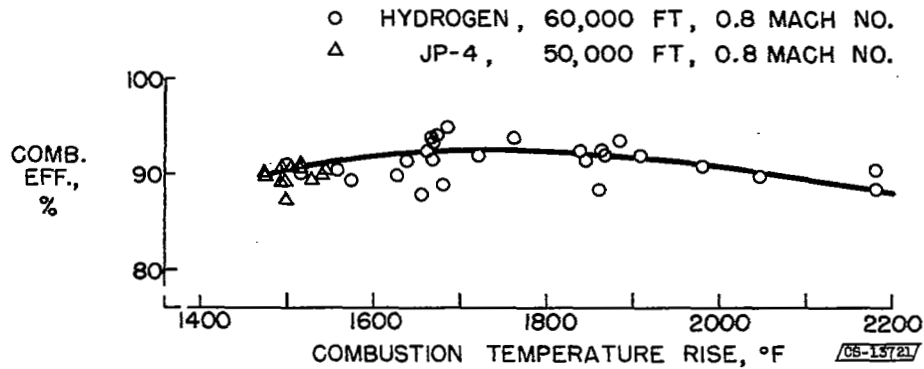


Figure 3. - Performance of production can-type combustors with hydrogen and JP-4 fuels.

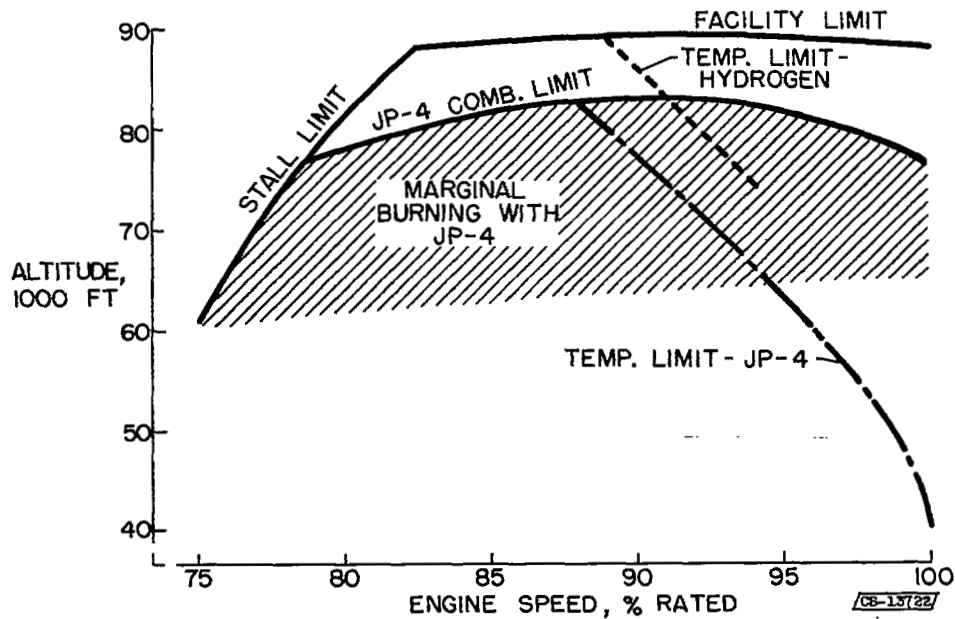


Figure 4. - Effect of fuels on engine performance limits with engine A at high altitude.

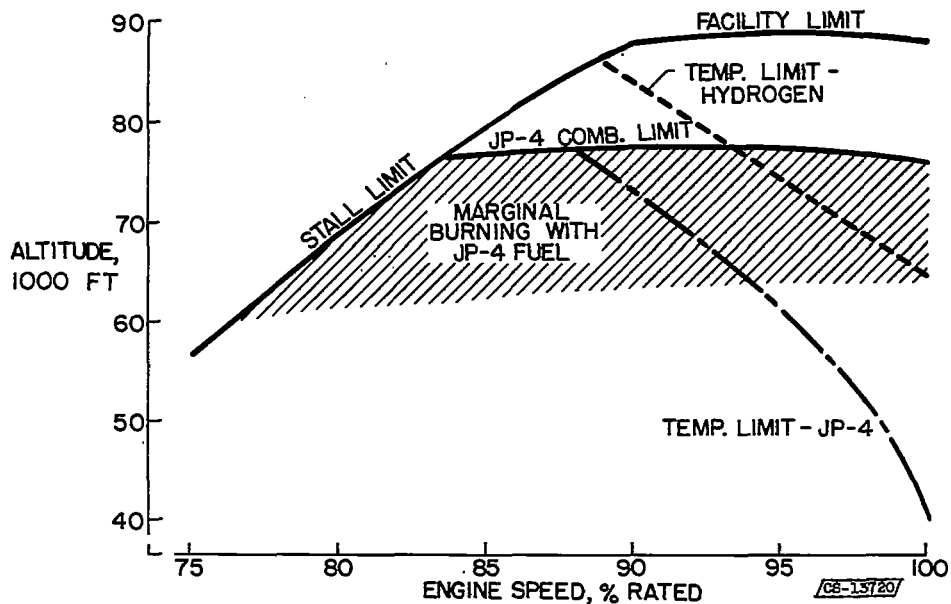


Figure 5. - Effect of fuels on engine performance limits with engine B at high altitude.

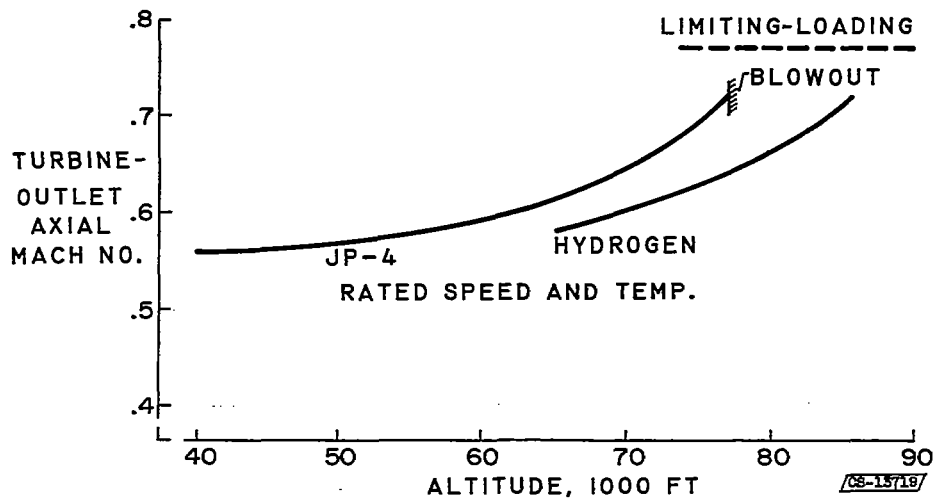


Figure 6. - Effect of fuels on turbine loading at high altitude.

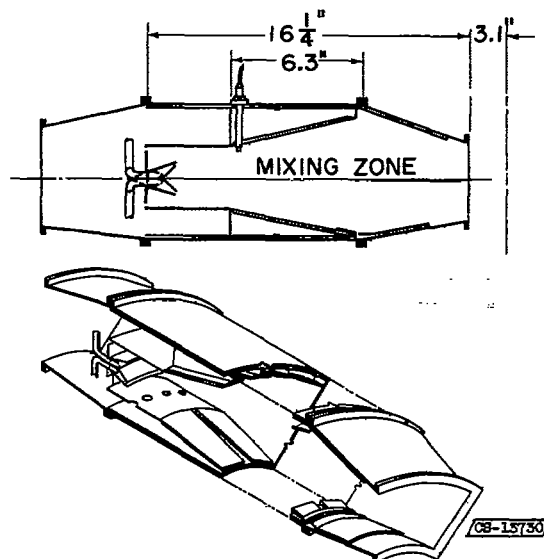


Figure 7. - Experimental hydrogen turbojet combustor (channeled-wall design).

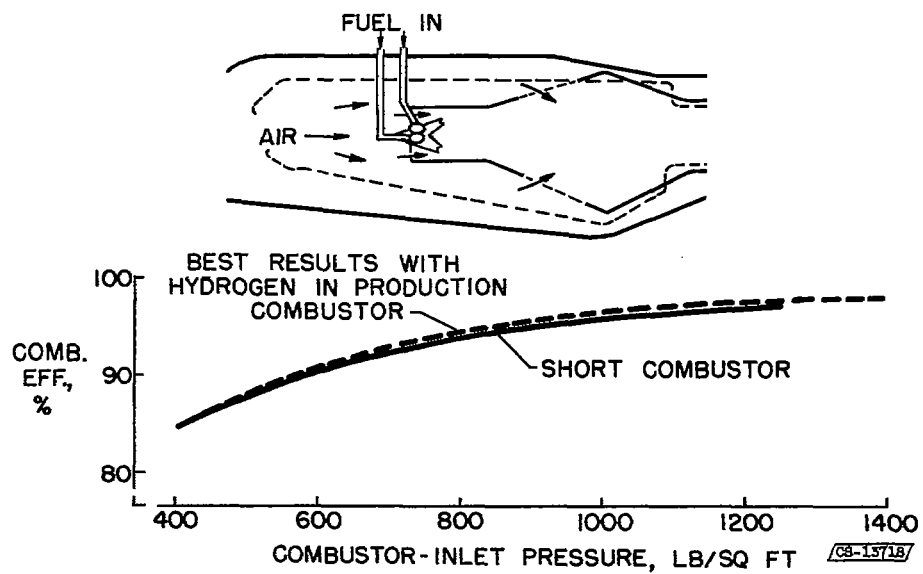


Figure 8. - Comparison of performance of short annular combustor with production combustor.

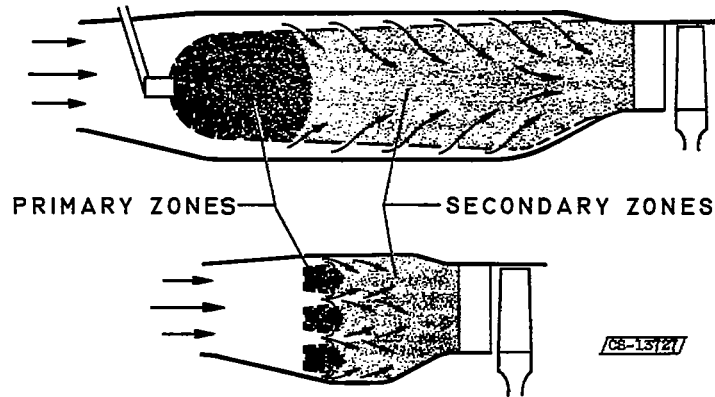


Figure 9. - Comparison of conventional combustor with small-element combustor.

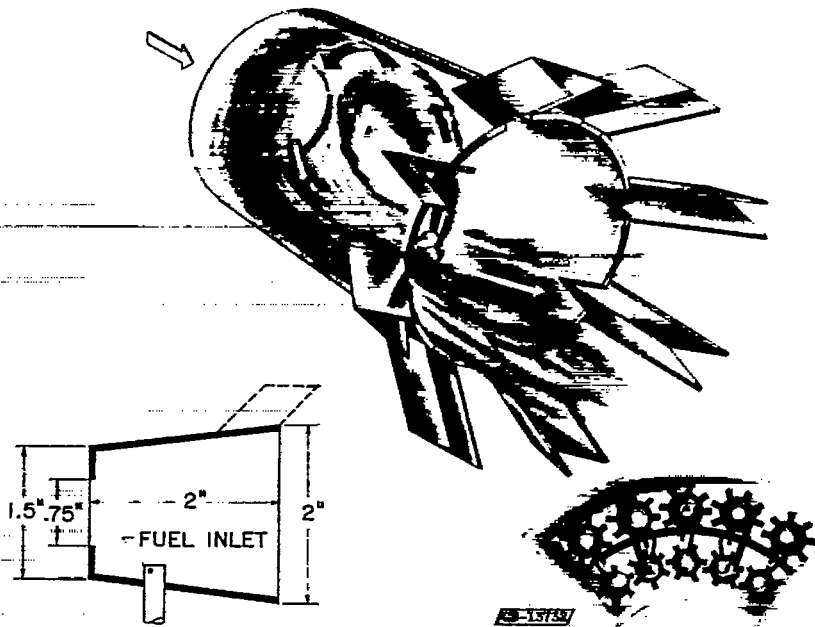


Figure 10. - Flower-pot combustor element.

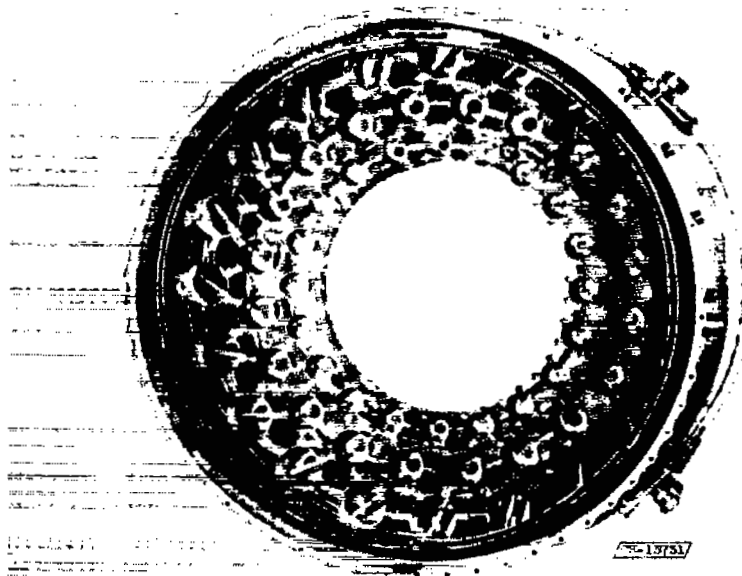


Figure 11. - View looking upstream of flower-pot combustor for turbojet engine.

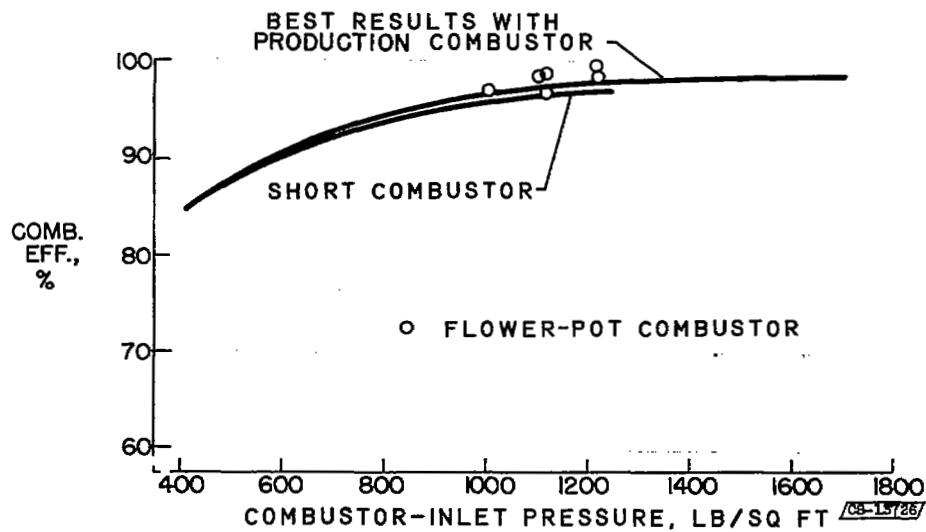


Figure 12. - Comparison of performance of flower-pot combustor with other combustors. Hydrogen fuel.

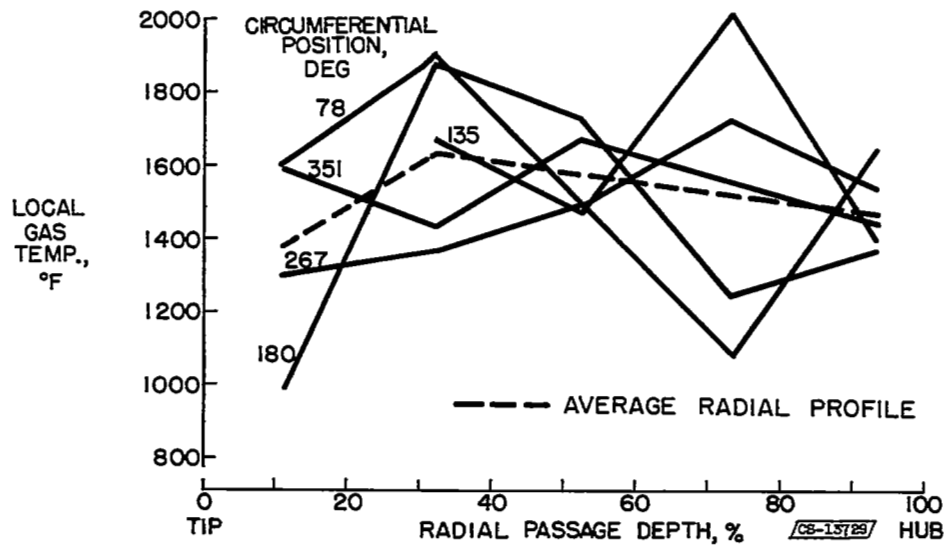


Figure 13. - Temperature distribution at turbine inlet with flower-pot combustor.

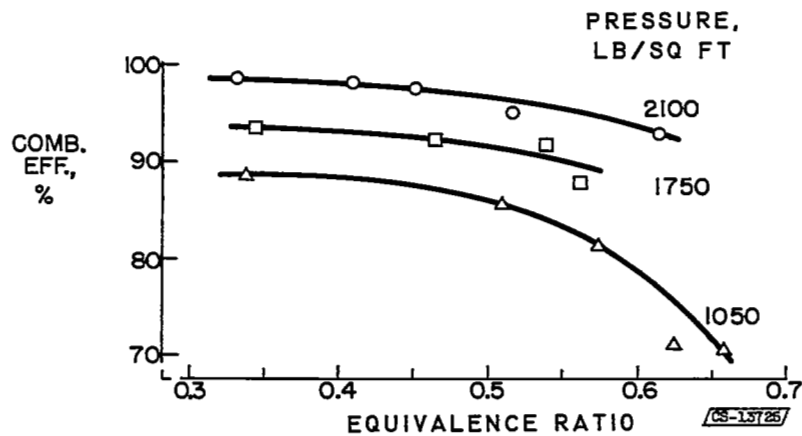
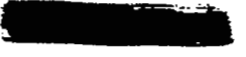


Figure 14. - Performance of an array of flower-pot combustors with propane fuel.





DECLASSIFIED

4 - FUELING PROBLEMS WITH LIQUID HYDROGEN

Glen Hennings  
William H. Rowe  
Harold H. Christenson



#### 4. FUELING PROBLEMS WITH LIQUID HYDROGEN

By Glen Hennings, William H. Rowe, and Harold H. Christenson

##### Introduction

Hydrogen is not a newcomer to aviation. Its light weight and high flammability have both plagued and tantalized the industry from the beginning. People concerned with lighter-than-air craft are interested in it because of its light weight but are precluded from using it because of its flammability. Those concerned with combustion engines are interested in it because of its high flammability but have been deterred from using it because of its low density. A partial solution to the density problem has come about through the use of modern low-temperature technology. Liquefying hydrogen increases its density by a factor of about 900; and by present-day processes large quantities of hydrogen can be liquefied. The NACA Lewis laboratory has used liquid hydrogen as a fuel for full-scale turbojet engines for the past year and a half; over 20 tons have been produced for these programs.

This paper is primarily concerned with the ground-handling problems associated with the use of liquid hydrogen as an aircraft fuel. The discussion is divided into four parts: (1) the significance of the physical and thermodynamic properties of hydrogen, (2) materials and methods of construction for liquid-hydrogen equipment, (3) safety, and (4) aircraft fueling procedures.

##### Physical and Thermodynamic Properties

Some of the problems associated with the handling of liquid hydrogen can be attributed to the unique physical properties of the fluid listed in the following table:

Property	Hydrogen	Other
Boiling point, °R	37	O <sub>2</sub> , 163
Liquid density, lb/cu ft	4.42	JP-4, 48.7
Liquid head (for 10 psi), ft	325	JP-4, 29.5
Viscosity, centipoise	Liquid, 0.0139 at 37° R	JP-4, 1.70 at 460° R air, 0.0165 at 460° R

The boiling point of hydrogen is 37° R, compared with 163° R for oxygen. At the boiling point of hydrogen, all other materials except helium will be solids. This means that contaminants in the liquid-hydrogen system would tend to freeze out and plug small flow passages.

The density of liquid hydrogen is 4.42 pounds per cubic foot, or about one-tenth that of JP-4. Consequently, large tanks are required to hold liquid hydrogen. Another consequence of this low density is that a 325-foot column of liquid hydrogen will produce a pressure of 10 pounds per square inch. This compares with a column of 29.5 feet for JP-4. For pumps, the discharge pressure expressed in feet of liquid head is a major parameter. Liquid-hydrogen pumps require large power inputs because the pump power is equal to the product of the discharge head and the weight-flow rate. For centrifugal pumps, very high rotational speeds or multiple staging is necessary to achieve reasonable discharge pressures.

The viscosity of hydrogen is very low. The liquid viscosity is two orders of magnitude lower than that of JP-4 and about the same as that of air. For applications in which viscosity aids in sealing (in gear pumps, e.g.), liquid hydrogen would be very difficult to seal.

Not only the physical properties but also the thermodynamic properties of hydrogen fall outside the range of common engineering experience. One of the most important thermodynamic properties of the hydrogen molecule is that it can exist in either of two energy states; namely, the ortho or para. The physical difference between the two states is illustrated by figure 1. Each molecule has two atoms, and the nuclei of atoms are represented by the spheres. For ortho hydrogen, the nuclei rotate in the same direction about the common axis; for para, the nuclei rotate in opposite directions.

The equilibrium ratio of ortho to para hydrogen is determined by the absolute temperature, as shown in figure 2, where equilibrium para content is plotted as a function of absolute temperature in °R. At room temperature the equilibrium composition is 75 percent ortho and 25 percent para. As temperature is decreased, the equilibrium composition

shifts toward higher para content and becomes substantially 100 percent para hydrogen at the boiling point. Now, when normal room-temperature hydrogen gas is liquefied, the liquefaction rate is so high that there is hardly any time for conversion from ortho to para hydrogen. The result is liquid hydrogen with an actual para content of 25 percent and an equilibrium para content of 100 percent. The way the excess ortho is converted to para hydrogen is shown by the right side of figure 2. According to this schedule, 10 days are required to change from 25 to 75 percent para, 40 days to change to 92 percent para, and a year to reach 99 percent para. Thus, equilibrium is very slow to be established.

Unfortunately, 300 Btu are released for each pound of ortho converted to para hydrogen, enough heat to vaporize 1.5 pounds of liquid. The implications of such a large heat release are obvious with respect to storing liquid hydrogen. Figure 3 shows the storage losses that would be incurred with liquid hydrogen beginning immediately after liquefaction. A perfect storage vessel (zero heat leak) vented to the atmosphere is assumed. At first the vessel is full, and the para content is 25 percent. Because of the heat released by converting from ortho to para hydrogen, after 5 days only 43 percent of the liquid remains, and the para content has increased from 25 to 62 percent.

From the storage situation just discussed, it is obvious that high para content is very desirable; but how can it be produced? Actually, this problem has been solved. Catalysts are available that can bring about almost instantaneous conversion from ortho to para hydrogen. Such catalysts can be installed in the liquefaction plant, and the liquefier will then deliver the high-percentage para hydrogen. One more consideration remains. When the hydrogen is converted at the liquefier, it still releases the large heat of conversion; therefore, the liquefier must be designed with the additional refrigeration capacity necessary to handle the large heat load.

The specific heats of hydrogen gas are also functions of the ortho and para states. Specific heat at constant pressure  $c_p$  and the ratio of specific heats  $\gamma$  are plotted in figure 4 for hydrogen gas at a pressure of 1 atmosphere. The  $c_p$  values of ortho and para hydrogen vary substantially between 80° and 700° R. For ortho hydrogen,  $c_p$  increases gradually with temperature; and for para hydrogen,  $c_p$  increases rapidly to a maximum at about 300° R and then decreases to the value for ortho hydrogen at about 700° R. Since normal hydrogen contains 75 percent ortho hydrogen by definition, its value of  $c_p$  more closely approximates that of the ortho curve. The curve at the bottom of the figure is the  $\gamma$  value for normal hydrogen gas. At room temperature,  $\gamma$  is 1.4; and at the normal boiling point, it is nearly 1.8. Typical

examples of equipment that depends on these properties of hydrogen are (1) heat exchangers, where  $c_p$  is a primary variable, and (2) orifice-type flowmeters, where  $\gamma$  is an important parameter.

The thermal conductivities of ortho and para hydrogen also differ; it is this difference in thermal conductivity upon which ortho-para analyzers are based.

The information presented shows that the thermal properties of hydrogen vary substantially between room temperature and the normal boiling point. However, these data are for a pressure of 1 atmosphere. If pressure is varied, the properties will undergo the usual changes associated with pressure, and the rate of change of the properties will become very severe in the range of the critical point. The critical pressure is 190 pounds per square inch absolute, and the critical temperature is  $60^\circ$  R.

#### Materials and Construction of Equipment

The properties of hydrogen that have been discussed affect the kind of materials and equipment with which it can be handled. Gaseous hydrogen at ambient temperature has been handled commercially for many years; and, except for its great tendency to diffuse through porous materials, it presents no unusual problems. Only the low-temperature gas and the liquid require special attention. As temperature is lowered, the strength of most materials increases, but some become so brittle at low temperature that they have no practical application.

For example, three metals are examined at low temperature. The metals chosen are a copper, an aluminum alloy, and a stainless steel. Figure 5 shows the effect of temperature on yield strength for the three metals. The yield strength of annealed copper is almost independent of temperature. For both the 2024-T3 aluminum alloy and the 347 stainless steel, the yield strength increases about 30 percent as the temperature is reduced from room temperature to liquid-hydrogen temperature. Since impact strength is a measure of brittleness, the effect of low temperature on this strength is considered. The same three materials are shown again, along with two common steels, in figure 6. The impact strength of both steels decreases rapidly with temperature, and they are not recommended for use at liquid-hydrogen temperature. The impact strength for the copper and the aluminum alloy increases slightly at the low temperature. Even though the impact strength of the stainless steel decreases slightly at the low temperature, it has far greater strength than the other materials presented.

The annealed copper, the 2024-T3 aluminum, and the 347 stainless steel are more or less representative of three classes of material. As

a general rule, copper, brass, aluminum and some of its alloys, monel, nickel, and the austenitic or 300-series stainless steels, are all satisfactory for use at low temperature. On the other hand, 400-series stainless steels and the common steels are not recommended, because they become too brittle. For applications that require low thermal conductivity, high strength, or weldability, stainless steels are suitable. For special applications in which high thermal conductivity is required (in heat exchangers, e.g.), copper and aluminum may be used.

Plastic materials may also be useful at low temperatures. Several organizations have reported plastic films that are flexible down to liquid-hydrogen temperature. Preliminary investigations conducted at the Lewis laboratory indicate that Mylar film and nylon parachute cloth are quite flexible at liquid-hydrogen temperature. Teflon has been extensively used for gaskets and valve seats at the low temperature. As temperature is decreased, Teflon shrinks to a greater extent than the adjacent metal parts; therefore, good gasket design is necessary to prevent low-temperature leaks. The compressive strength of Teflon at liquid-hydrogen temperature is about the same as that of aluminum at room temperature - about 30,000 psi.

Almost all conventional fabrication techniques have been satisfactorily used in the cryogenic field. Conventional arc-welding, heliarc-welding, silver-soldering, and soft-soldering have all been used with success; however, the quality of a solder joint is often very sensitive to solder composition. Success in fabrication of cryogenic equipment depends on a skilled fabricator, good materials, and careful attention to detail.

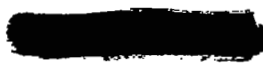
### Safety

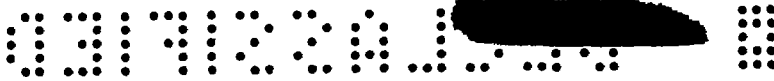
Gaseous hydrogen has been handled commercially for many years, and safe procedures are well established. Liquid hydrogen introduces two new problems: (1) the freezing out of air in the liquid and the consequent formation of a combustible mixture, and (2) the exposure of personnel to very low temperatures.

Three basic principles of safety may be stated briefly:

(1) At least two improbabilities should be placed between the man and an accident. For example, make a system that cannot leak and then put it in an area with no ignition sources. With this arrangement there is only a remote possibility that the unexpected leak will occur at the same time as the unexpected ignition source.

(2) Acts of commission and omission can best be controlled by the use of a well-planned check sheet.





- (3) There is no substitute for well-informed, alert people.

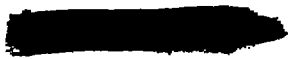
### Fueling Procedure

In ground operations with liquid hydrogen, the following equipment and procedure are necessary:

- (1) A large primary storage vessel is needed.
- (2) The fuel must be transferred from the storage area to the airport.
- (3) The fuel must be loaded into the aircraft tank.
- (4) Provision must be made for handling the aircraft on the ground in the event of a delayed takeoff.
- (5) The airplane must be cared for after each flight.

The construction of three typical types of storage tanks is shown in figure 7. The first vessel is liquid-nitrogen-shielded and vacuum-jacketed. The vacuum space virtually eliminates heat leak due to gas conduction. The liquid-nitrogen shield intercepts enough of the radiant heat so that, as to the liquid hydrogen, the outdoor temperature is  $-320^{\circ}$  F. This type of vessel is expensive and difficult to construct, but it has a very low hydrogen-loss rate. The second container has no liquid-nitrogen shield, and the radiant heat transfer is thus higher. However, for large vessels with small surface-to-volume ratios, the loss rates of this kind of tank are sufficiently low. The vacuum spaces in these two vessels can either be empty or be filled with powdered insulation. Since powders, such as silica aerogel and pearlite, are relatively opaque to thermal radiation, they act as radiation shields. The third vessel is a conventionally insulated tank. The loss rate of such a vessel is far too great for a long-term storage tank. This type of vessel can be used for short times, however. Heat leaks into such a tank are discussed in the next paper. On the basis of the points discussed and other considerations, the center tank with a powder-filled vacuum space is the most practical for large-scale long-term storage.

The next operational step is to move the liquid hydrogen from the storage area to the airplane. This can be accomplished in one of two ways, either by pipeline or by trailer truck. Design studies by the Bureau of Standards indicate that liquid hydrogen can be piped for a number of miles if the flow rate is very high and the line is in continuous service. For small-scale operations, transportation of liquid hydrogen in trailers is more feasible. Such a trailer would be similar in construction to the storage tanks.

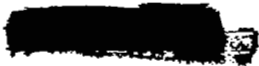


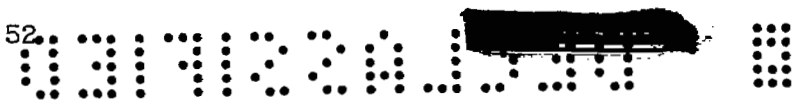
For transfer of liquid hydrogen from one vessel to another, special transfer tubing is required. This tubing is generally vacuum-insulated. Figure 8 shows a cross section through a joint for such a tube, which consists of an inner flow tube, a vacuum space, and an outer tube. A bellows is used to compensate for differential contraction. The unit can be made flexible by using bellows for the entire inner and outer tubes. The joint shown is a bayonet type and is designed for low heat leak. Thin stainless steel is used for the bayonet parts. The liquid hydrogen is prevented from circulating in the clearance space by a close radial tolerance or by a partial seal at point A. Therefore, the clearance volume is filled with stagnant gas, and heat can leak only by conduction over a long path. The positive seal is made by a conventional neoprene O-ring.

In figure 9, liquid-hydrogen fuel is about to be transferred from the fuel trailer to the aircraft wing tank. The fuel trailer is in place, and the vacuum-jacketed transfer line is assembled. The remote vent system will be connected to the tank vent. The fuel is transferred from the trailer by pressurizing the trailer tank. The hydrogen gas boiled off in the aircraft tank during filling is carried away by the vent system and discharged to the atmosphere in a remote location. Regular aircraft mechanics carry out the fuel-transfer operation. During the loading procedure the liquid hydrogen is filtered. In spite of many purification steps taken during liquefaction, crystals are found in the liquid fuel. Analysis of one batch of crystals that was collected revealed that nitrogen was the principal impurity. The total contamination is estimated to be only a few parts per million.

The handling of the aircraft after it has been fueled but before takeoff is also a problem, because, if the tanks are sealed and no fuel is being used, heat leak causes the tank pressure to build up to an excessive value. In order to prevent pressure buildup, the tanks should remain connected to the vent system until the engines are about to be started for takeoff. As soon as the engines start using fuel, tank pressure ceases to be a problem.

Finally, how should an airplane be handled after returning from a flight? One proposed method would be as follows: Because such an aircraft would land with some liquid fuel in its tanks, for economy, the remaining liquid fuel would be transferred to storage. Since the tanks would then contain very cold hydrogen gas, if they were sealed off the pressure would rise excessively as the tanks became warmer. If the tanks are connected to a gas holder instead of being sealed, the gas holder will take the excess gas and will maintain constant positive pressure in the system. No air could leak into such a system, but hydrogen could leak out and fill the aircraft structure with a combustible mixture. To protect the aircraft against such leaks, it can be force-ventilated, and the interior of the aircraft can be monitored with combustibles detectors.





### Conclusions

The following conclusions can be stated:

- (1) The many peculiar properties of hydrogen are well known and are reported in the literature.
- (2) Suitable materials and fabrication methods exist for using liquid hydrogen, and some experience has already been gained in the construction of this type of equipment.
- (3) Liquid-hydrogen fueling procedures can be carried out by competent aircraft mechanics.



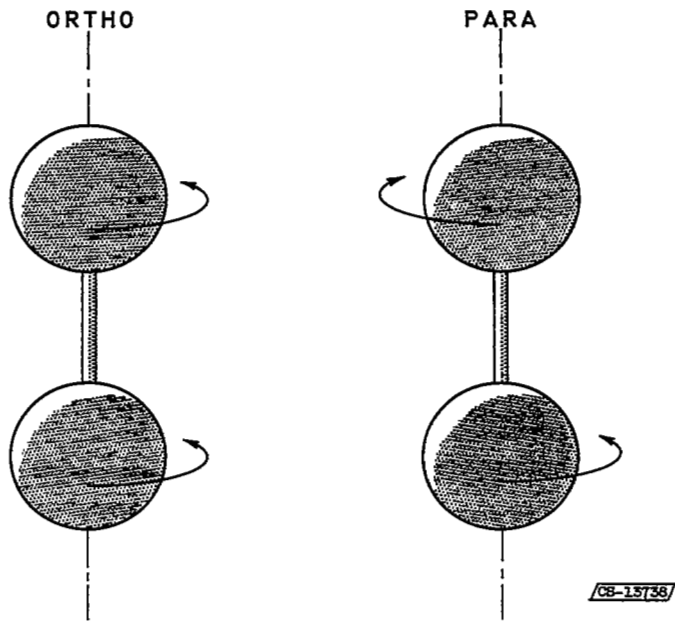


Figure 1. - Thermodynamic states of hydrogen.

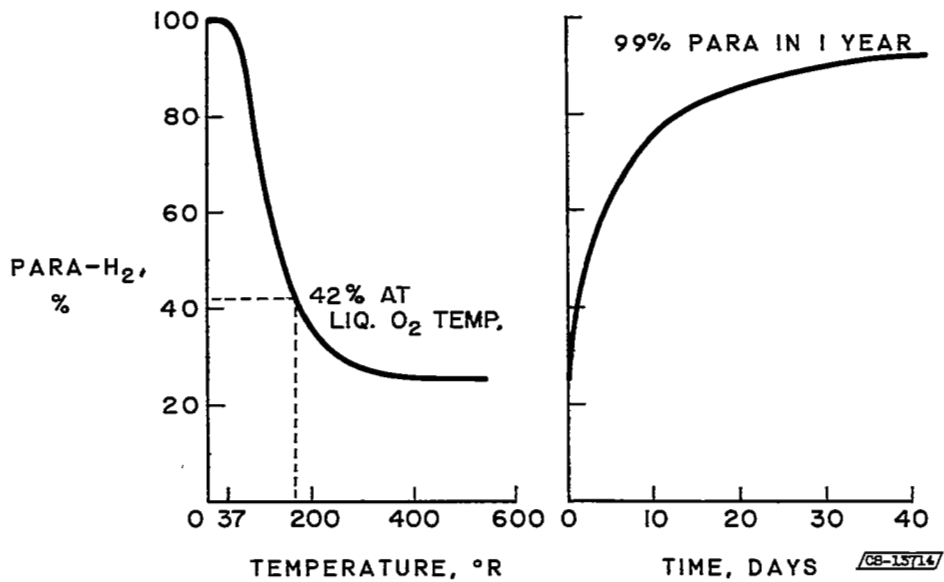


Figure 2. - Ortho-para hydrogen conversion (NBS data).

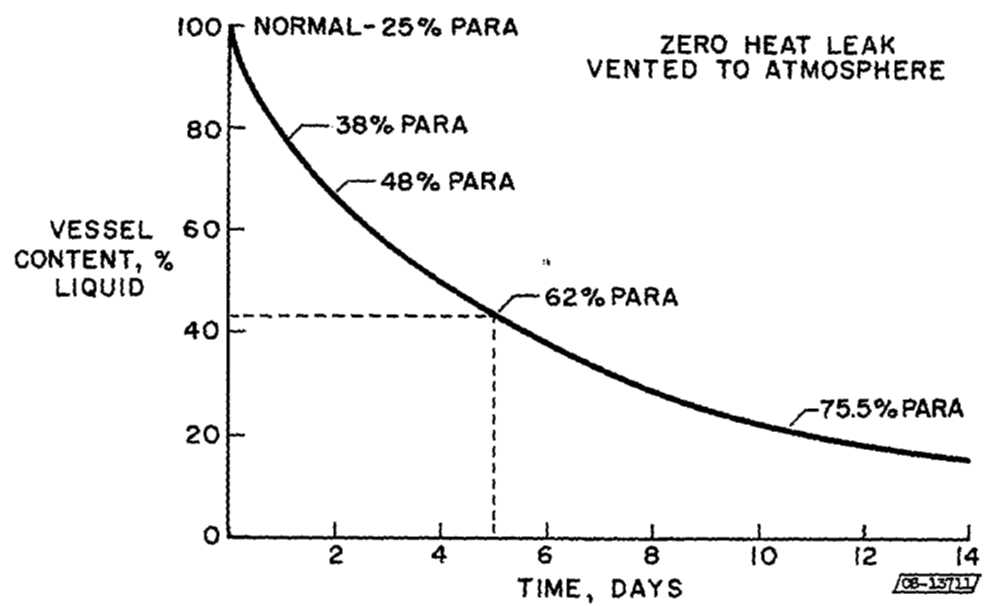


Figure 3. - Loss of hydrogen due to ortho-para conversion.

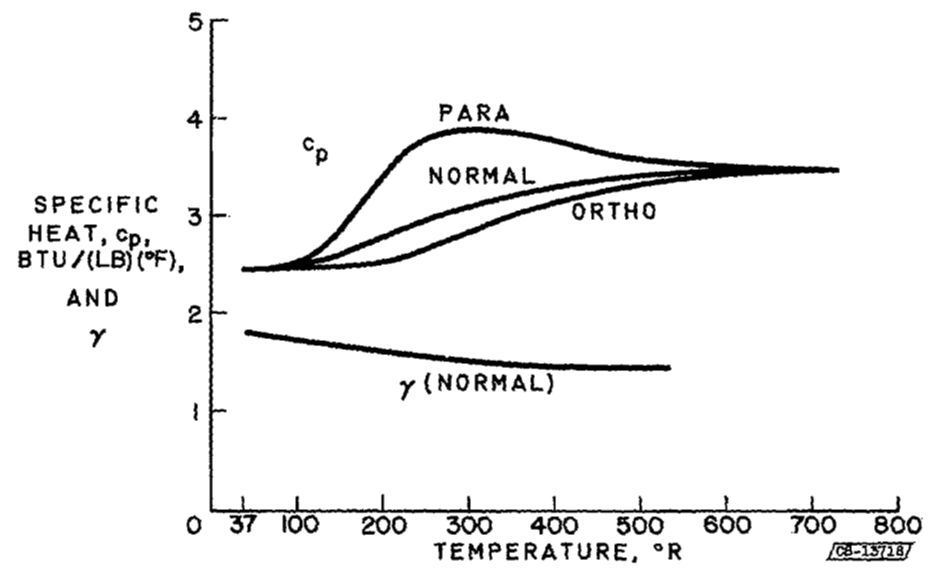


Figure 4. - Specific heat and ratio of specific heats for hydrogen gas. Pressure, 1 atmosphere (NBS. data).

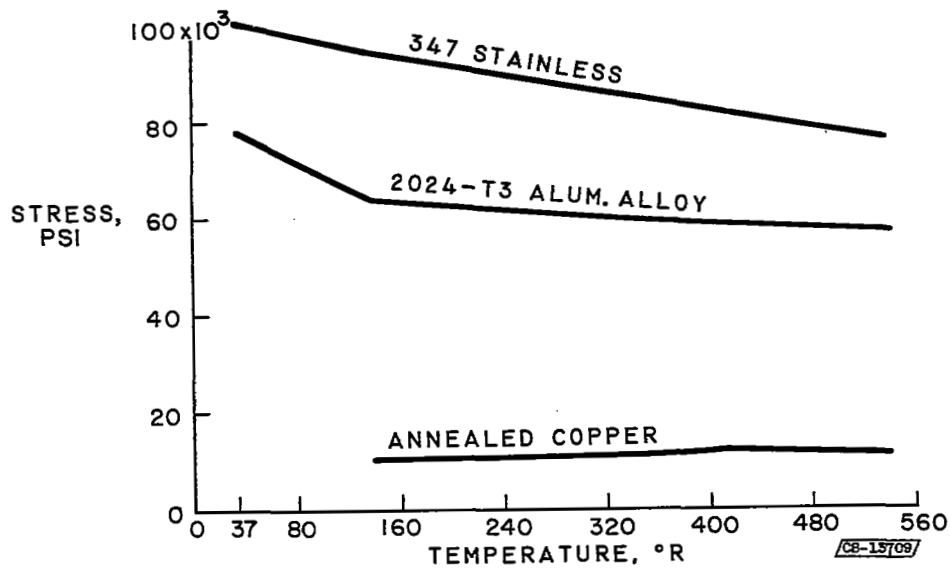


Figure 5. - Yield strength of metals (NBS data).

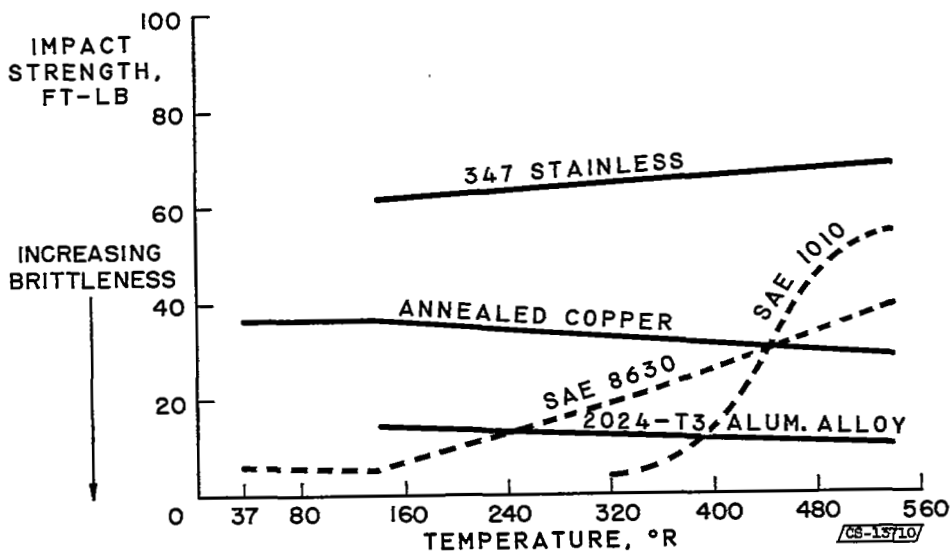


Figure 6. - Impact strength (Charpy) of metals.

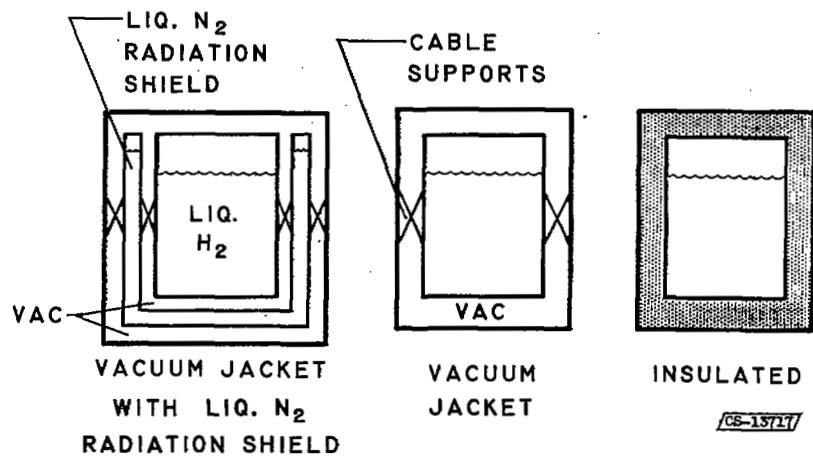


Figure 7. - Liquid-hydrogen storage vessels.

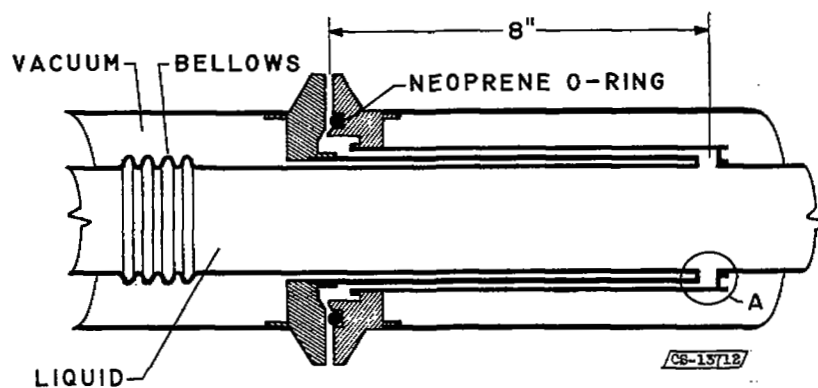


Figure 8. - Bayonet-type low-temperature joint.





CLASSIFIED

CLASSIFIED

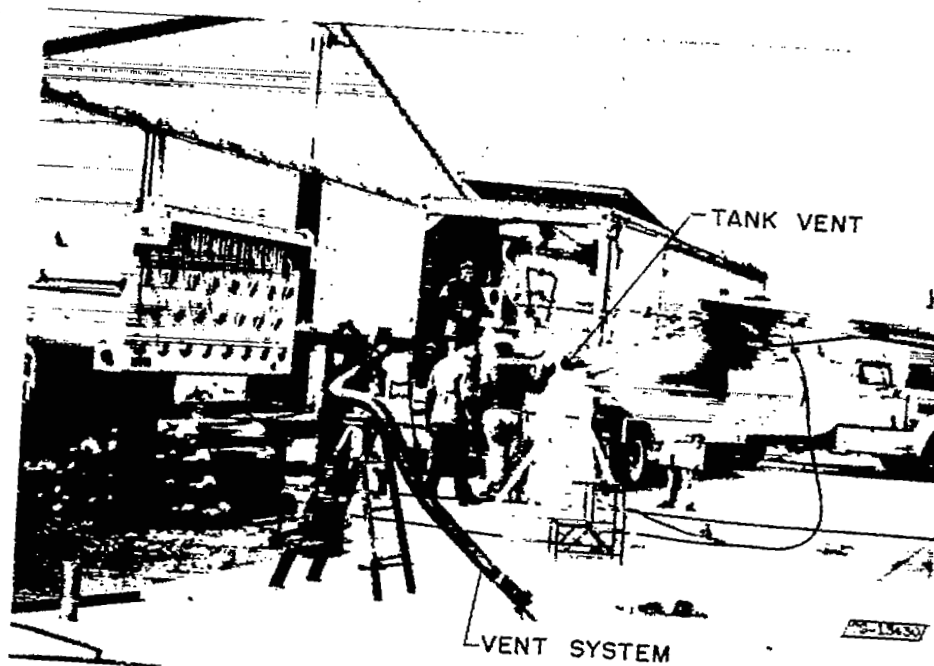
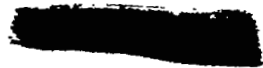


Figure 9. - Liquid-hydrogen transfer.



# [REDACTED] DECLASSIFIED

5 - AIRPLANE TANKAGE PROBLEMS WITH LIQUID HYDROGEN

Solomon Weiss  
Thaine W. Reynolds  
Loren W. Acker

[REDACTED]

## 5. AIRPLANE TANKAGE PROBLEMS WITH LIQUID HYDROGEN

By Solomon Weiss, Thaine W. Reynolds, and Loren W. Acker

Because of its low boiling temperature, liquid hydrogen must be stored in an insulated tank to prevent losses. Therefore, people concerned with prolonged ground storage of liquid hydrogen have built several types of containers employing the insulating qualities of a vacuum jacket. Although these tanks meet the requirements for extended ground storage, the method of construction produces a tank that is too heavy to be considered for aircraft use. Fortunately, the time during which the aircraft tanks require good insulating qualities is relatively short. During flight, the aircraft engine will consume hydrogen faster than it can be vaporized, even with a poorly insulated tank. However, when the airplane is on the ground and the engines are not operating, heat leak through the tank walls causes the hydrogen to vaporize; then hydrogen must be lost overboard to prevent high tank pressures.

Since the problem of storage on the aircraft involves factors different from those encountered with protracted ground storage, a tank could be designed with a relatively lightweight insulating material. Tanks of the type shown in figure 1 have been investigated experimentally at the NACA Lewis laboratory in order to gain an appreciation of some of the factors involved in the design of tanks insulated with a foamed plastic material. These tanks consist of a thin metallic inner shell covered with a lightweight, low-thermal-conductivity foamed plastic insulation and an outer covering to enclose the insulation and protect it against air erosion. The inner-shell material, the quality of the insulation, the atmosphere surrounding the tank in the insulation space, and the state of motion of the liquid hydrogen within the inner shell were studied to determine their influence on the heat-leak performance of an external wingtip tank.

Tanks of this type depend largely on the material surrounding the shell for insulation from heat conducted radially into the tank. However, as the liquid level of the tank declines, heat that is conducted through the insulation above the liquid level can be conducted down into the liquid by the metal inner liner. The importance of this conduction by the liner was one of the points investigated with the simple vessel shown in figure 2. This apparatus consists of a block of Styrofoam machined out to receive open-top cylinders of test materials. This assembly is

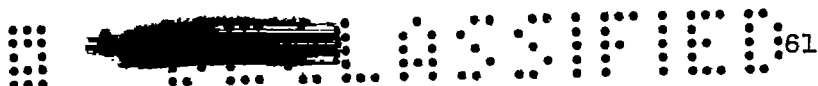
placed in a stainless-steel shell. Heat-leak rates are calculated from the gas boiloff history of the liquid nitrogen that is used in the inner liner. Liquid levels are determined from thermocouples on the liner walls or from gas-meter readings. Experiments were conducted with an aluminum liner, representing a high-thermal-conductivity material, and a stainless-steel liner, representing a low-thermal-conductivity material. Tests simulating a tank with the insulation applied on the inside were made with no liner in the Styrofoam block.

Results of boiloff experiments are shown in figure 3. At the full-tank level, there can be no conduction of heat along the walls of the inner liner, since the temperature throughout the tank is uniform. Therefore, at the full-tank condition, the thermal conductivity of the inner liner is not an important factor. At this level the total heat-leak rate into the liquid is about 128 Btu per hour for all three conditions. This rate, calculated from gas boiloff data, was predicted from the known heat-transfer properties of the surrounding insulation.

With a decline in liquid level, the thermal conductivity of the liner material influences the quantity of heat conducted into the liquid, as shown by the slopes of the curves. The heat-leak rates for the two low-thermal-conductivity materials (stainless steel and no liner) decrease in direct proportion to the decrease in liquid level or wetted area; but the heat-leak rate for the high-thermal-conductivity material (aluminum) does not decrease as rapidly with a lowering of liquid level. Because of the higher conductivity of aluminum, a larger proportion of the heat flow through the insulation above the liquid level is conducted along the aluminum walls and down into the liquid than is conducted by the lower-conductivity materials. The significance of low thermal conductivity declines as the surface-to-volume ratio decreases. For wingtip tanks, which have long, slender proportions and consequently high surface-to-volume ratios, these considerations are important.

The liner and insulation in this apparatus are covered with a metal shell that isolates the Styrofoam from the surrounding air. Because of its weight, this metal cover would not be practicable for a wingtip tank, but instead a lightweight shell capable of protecting the Styrofoam from air erosion would be employed. In tank studies at the Lewis laboratory, a lightweight shell made of resin-impregnated Fiberglas was used. Since this structure exhibits a relatively high degree of porosity, the space within the insulation chamber will "breathe" with changes in atmospheric conditions. To study characteristics of this kind of tank, the apparatus shown in figure 4 was used. The essential difference between this rig and the one shown in figure 2 is that the outer shell is made of Fiberglas instead of stainless steel.

When liquid hydrogen is put into the inner shell, the air in the insulation chamber condenses. As air condensation progresses, the pressure



in this space is reduced, and more air is drawn in through the porous outer covering. Heat released by the condensation of air causes a more rapid vaporization of the liquid hydrogen in the tank. In addition to the increase in heat leak, this phenomenon results in an additional tank weight because of the liquid air in the insulation chamber. An alternative to building the insulation space vacuum-tight so that no air can enter is to introduce into the chamber a gas that is noncondensable at these temperatures, such as helium.

Results of experiments made with an air atmosphere and with a helium atmosphere in the insulation jacket are compared in figure 5. With helium in the jacket, heat leak declines with liquid level, as in similar earlier experiments where condensation of air was not involved. With air in the jacket, the initial heat-leak rate is 28 percent higher than it is with helium in the jacket because of the condensation of air around the outside of the tank. As the layer of condensed air develops, the rate of further condensation declines and the curve of heat-leak rate approaches the helium curve. Since the thermal conductivity of helium is much higher than that of air, the over-all thermal conductivity of the insulation increases about 20 percent when helium is used. Even with this increase in conductivity, the heat-leak rate into the tank with helium in the jacket is less than that with condensing air. The matter of conversion of ortho to para hydrogen was not an important factor in these heat-leak studies because of the short durations of these experiments.

While the airplane is on the ground, the loss of hydrogen gas due to heat leak into the liquid can be avoided if the tank is built to withstand increases in pressure. It is then possible to keep the tank outlet closed until heat leak into the tank has raised the internal pressure to the design limit of the tank. At this time gaseous hydrogen must be bled off from the tank to restore the pressure to safe values. In flight, all or most of this gas is used by the engines and constitutes no waste. However, when the airplane is on the ground, this gaseous hydrogen is lost overboard, resulting in decreased airplane range. The time elapsed between tank filling and the first venting off of gaseous hydrogen is the so-called "no-loss" time for the tank. For airplane ground operations, it is obviously desirable to have this no-loss time as long as possible.

In this connection it is useful to review briefly what happens in a tank filled with liquid hydrogen in which the tank valve has been closed. A curve of the equilibrium vapor pressure and temperature for liquid hydrogen is shown in figure 6. Assume that a tank contains liquid hydrogen at a temperature of  $36.5^{\circ}$  R and, therefore, a pressure of 14.7 pounds per square inch absolute. If the tank is closed so that no gas escapes, heat leaking into the liquid through the insulation is absorbed as sensible heat by the liquid to raise its temperature and consequently its vapor pressure. The curve (fig. 6) indicates that for each temperature there is a corresponding pressure. For example, if the liquid temperature

increases from  $36.5^{\circ}$  to  $42.5^{\circ}$  R, the vapor pressure of the liquid should increase from 14.7 to about 35 pounds per square inch absolute. With this information and the measured heat leak into the tank, it is possible to calculate a pressure-time history for the tank.

The pressure rise in a wingtip aircraft tank filled with liquid hydrogen was studied under conditions simulating an airplane waiting to take off. The results (fig. 7) show a wide departure from the calculated pressure rise. In order to determine the reason for this discrepancy, liquid-hydrogen temperatures were measured at various levels within a tank. One temperature profile is shown in the lower part of figure 8. The tank was filled to approximately the 7.5-inch level, and the vent valve was closed. Heat leaking into the liquid caused its temperature to rise. The corresponding rise in pressure is shown in the upper part of figure 8. According to calculations based on heat-transfer properties, the pressure should have risen as indicated by the calculated curve. However, the actual pressure rise was much more rapid.

The temperature profile at the maximum pressure of 39 pounds per square inch absolute is shown by the solid curve in the lower part of figure 8. The temperature close to the interface between liquid and gas corresponds to an equilibrium vapor pressure of 39 pounds per square inch absolute (fig. 6), but near the bottom of the tank the temperature of the liquid corresponds to an equilibrium vapor pressure of only 23.5 pounds per square inch absolute. This temperature stratification accounts for the discrepancy between the predicted and experimental pressure-time curves.

This undesirable rapid pressure rise can be avoided if temperature stratification is prevented. One way to prevent stratification is to keep the fluid mixed. When the fluid was mixed by agitating the liquid, the pressure dropped from 39 pounds per square inch absolute to about the calculated pressure; and the resulting temperature profile is nearly uniform, as shown by the circles in the lower part of figure 8. Then the temperature of the entire liquid mass corresponds to a vapor pressure in the tank according to the pressure-temperature equilibrium curve.

Even though the wingtip fuel tank that was built for liquid-hydrogen use in the NACA flight program incorporated the results of these studies, a weight compromise was still necessary for a useful tank. The previous paper indicates that the strength of stainless steel increases with declining temperature. However, experiments show that wall temperatures in the gas space above the liquid may be as much as  $200^{\circ}$  R higher than the temperature of the liquid. Therefore, the design stress of the inner metal liner must be based on the highest tank temperature anticipated. In order to provide a margin of safety, room-temperature strength was chosen for the inner metal liner of the wingtip tank. Furthermore, because tanks of this type must be rigid and because proper fuel-system operation

requires a tank pressure 50 pounds per square inch above atmospheric, an inner-shell thickness of 0.050 inch was necessary. This heavy-gage material results in a ratio of tank weight to fuel weight of about 1.0, which is undesirable for flight. However, since this weight did not handicap flight efforts and did provide a large margin of safety, the weight compromise was accepted.

The wingtip tank, shown in figure 9, is about 23 feet long and 30 inches in diameter and has a 430-gallon capacity. The inner shell is made of stainless steel. It is covered with a 2-inch-thick insulation of low-thermal-conductivity lightweight Styrofoam to provide a reasonable heat-leak rate while the airplane is on the ground. This insulation is applied in two 1-inch layers. Since the contraction rate of Styrofoam is considerably greater than that of stainless steel, the steel shell and the insulation are not bonded. Joints made necessary by the sectional application of the insulation are tongued and lapped to allow for movement during contraction. In order to lengthen heat-leak paths, the second layer of Styrofoam is applied so that its joints do not coincide with the joints of the inner layer. Four layers of resin-impregnated Fiberglas compose the outer shell. A thin sheet of aluminum foil is installed between the insulation and the Fiberglas to preclude the disintegrating effects of the resin on the Styrofoam. To prevent air condensation, arrangements are made to maintain helium at positive pressure in the insulation space during filling and flight operations. The wingtip tank in figure 9 is not complicated with an agitation mechanism to stir the liquid, since desired no-loss time can be achieved even though temperature stratification is permitted.

In order to compare experimental operation of this tank with predicted heat-leak values, a heat-leak test was made with liquid hydrogen in the tank. The results are shown in figure 10. When the tank is full, the maximum heat-leak rate is 5400 Btu per hour, which is consistent with the calculated heat leak based on the heat-transfer properties of the tank materials. The instantaneous rate of fuel loss corresponding to the heat-leak rate is also shown in figure 10. At the highest heat-leak rate, the fuel-loss rate is approximately 27 pounds per hour. This is equivalent to a 3-minute loss of flying time at the cruise altitude of 50,000 feet for each hour the airplane tank is vented on the ground.

In summary, these experiments indicate the following:

- (1) Heat-leak rates for tanks insulated with foamed-plastic materials can be predicted from known heat-transfer properties. Purging the insulation space with helium gas prevents air condensation but results in an increase in the effective thermal conductivity of the insulation.



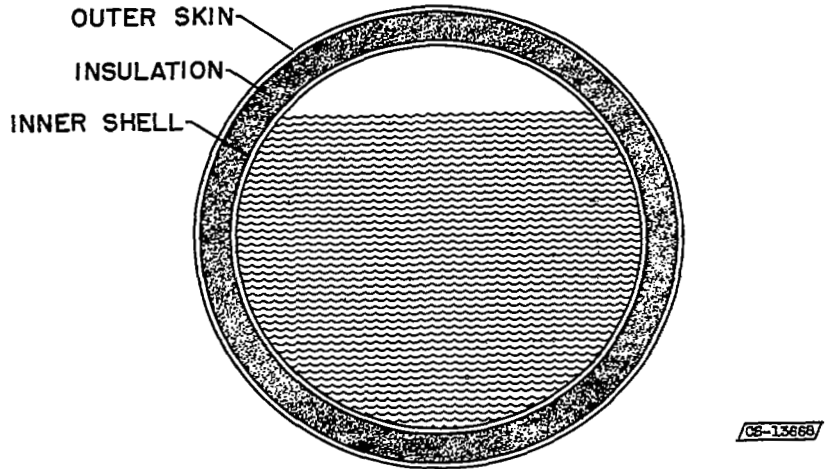


Figure 1. - Cross section of typical insulated tank.

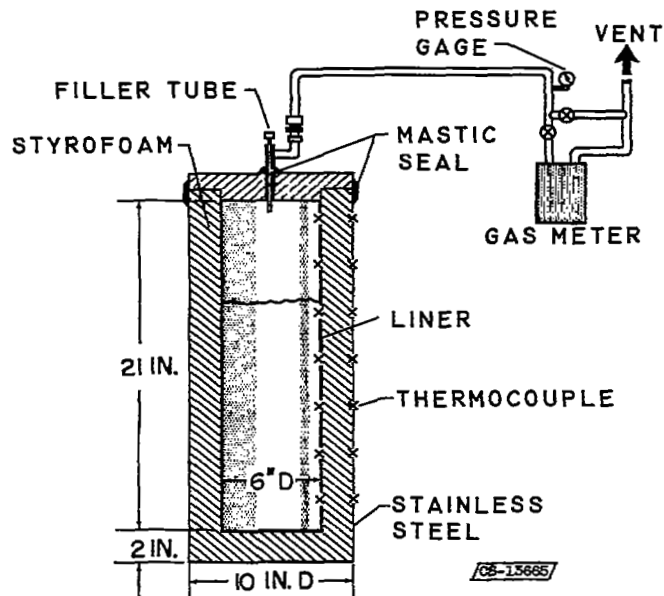


Figure 2. - Steel-jacketed heat-leak apparatus.

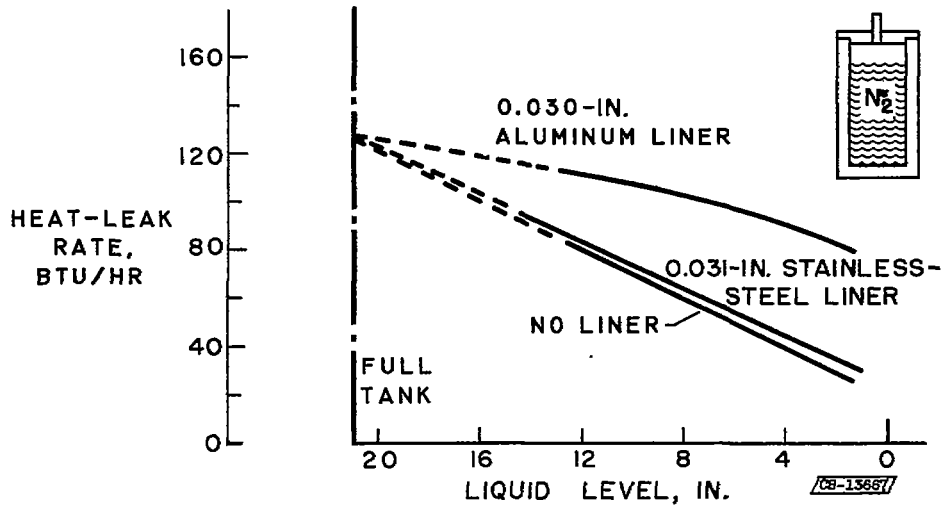


Figure 3. - Effect of liner material on vaporization.

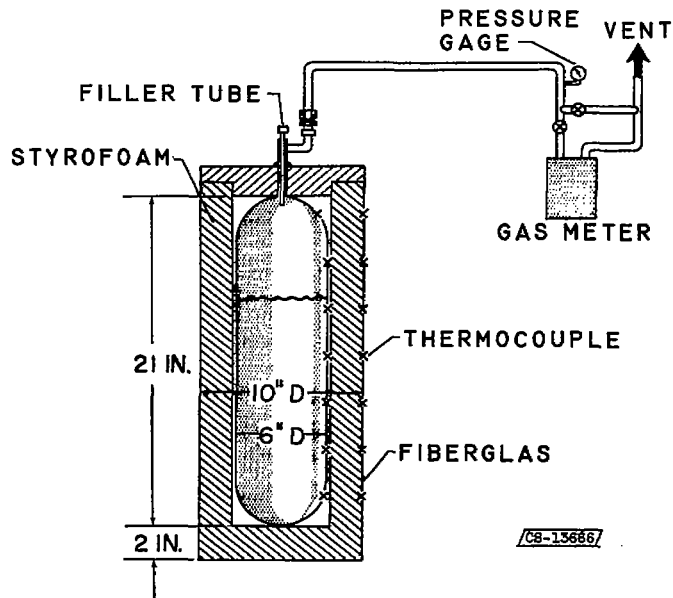


Figure 4. - Heat-leak apparatus.

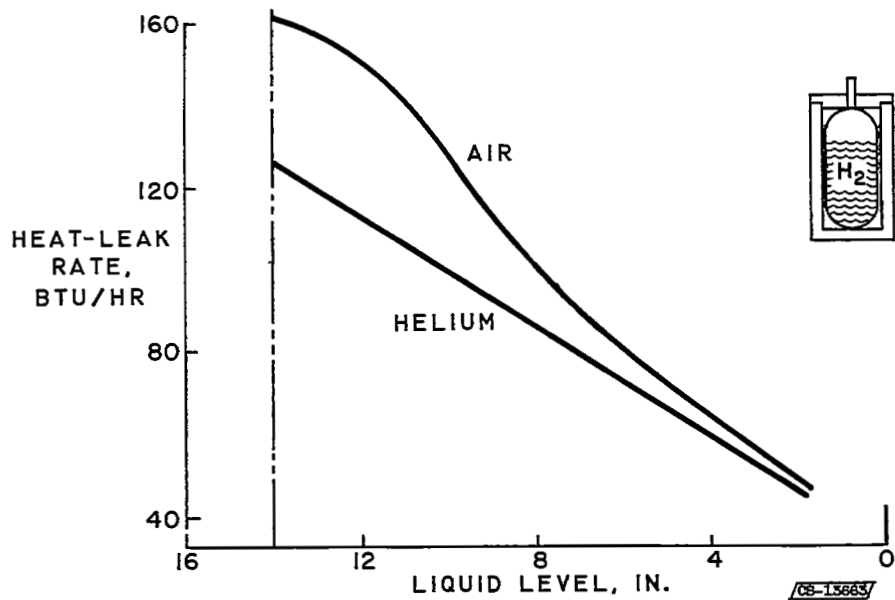


Figure 5. - Effect of atmosphere surrounding insulation on heat-leak rate.

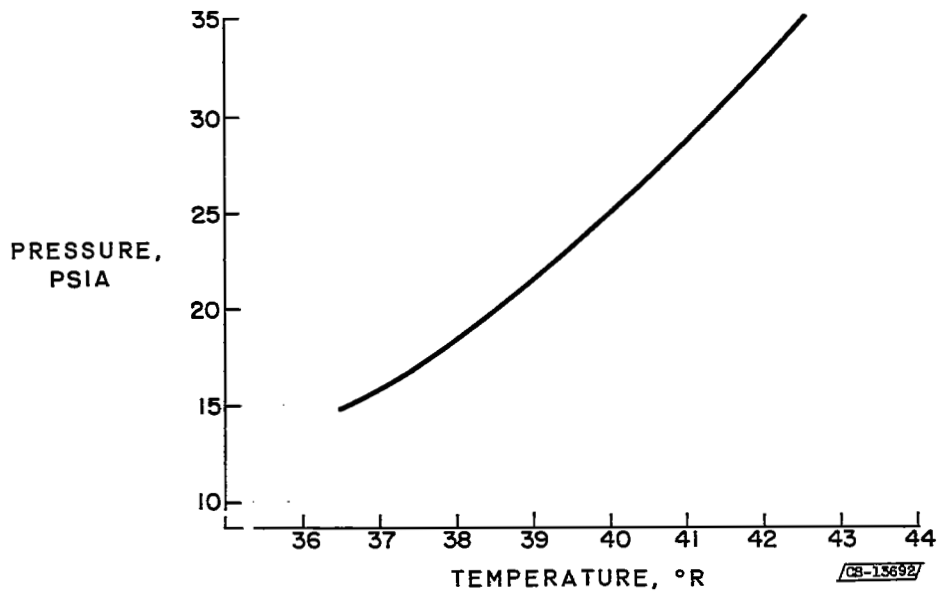
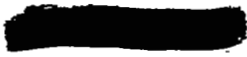


Figure 6. - Hydrogen vapor pressure - temperature equilibrium curve.



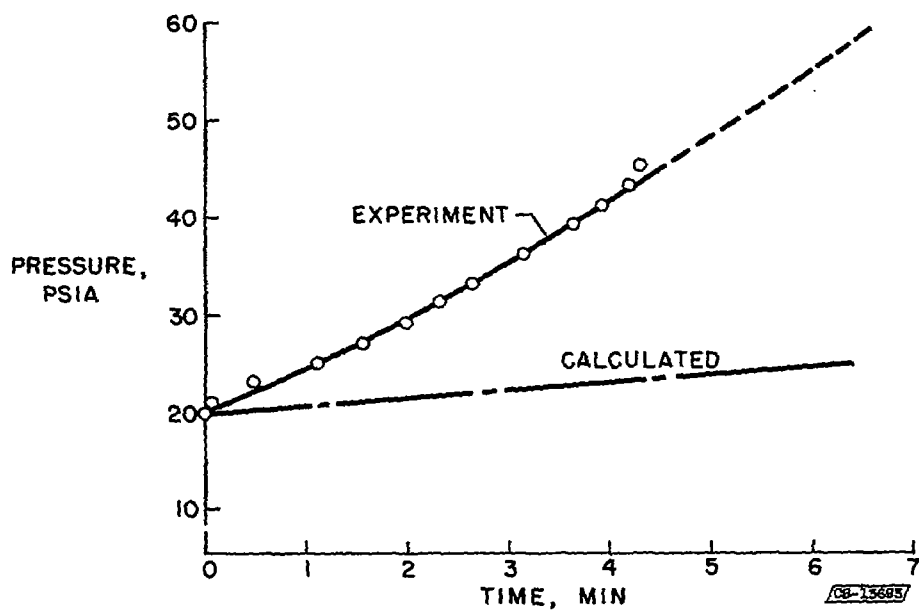


Figure 7. - Pressure-time history for hydrogen in aircraft tank.

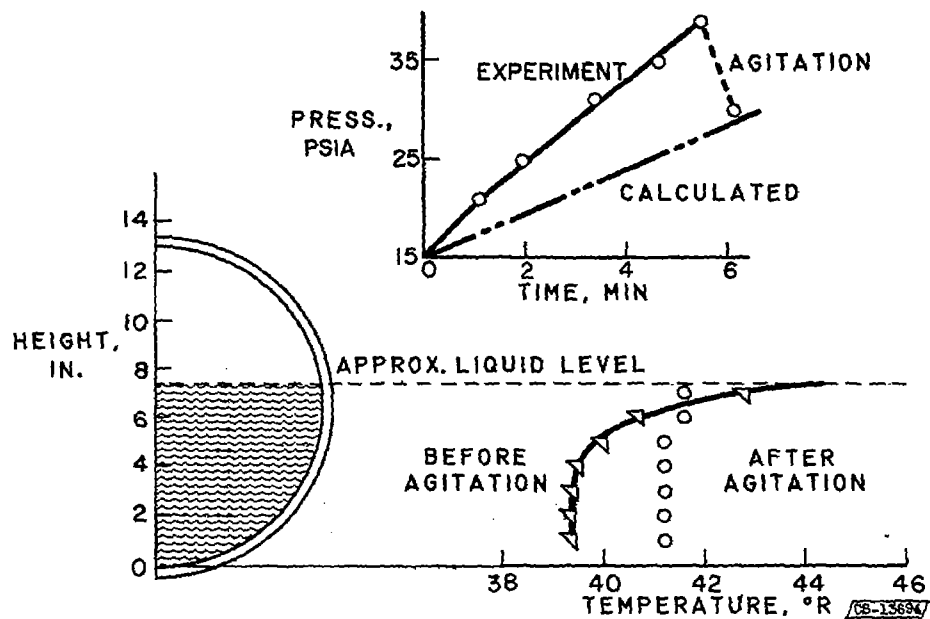


Figure 8. - Temperature profile in liquid hydrogen.

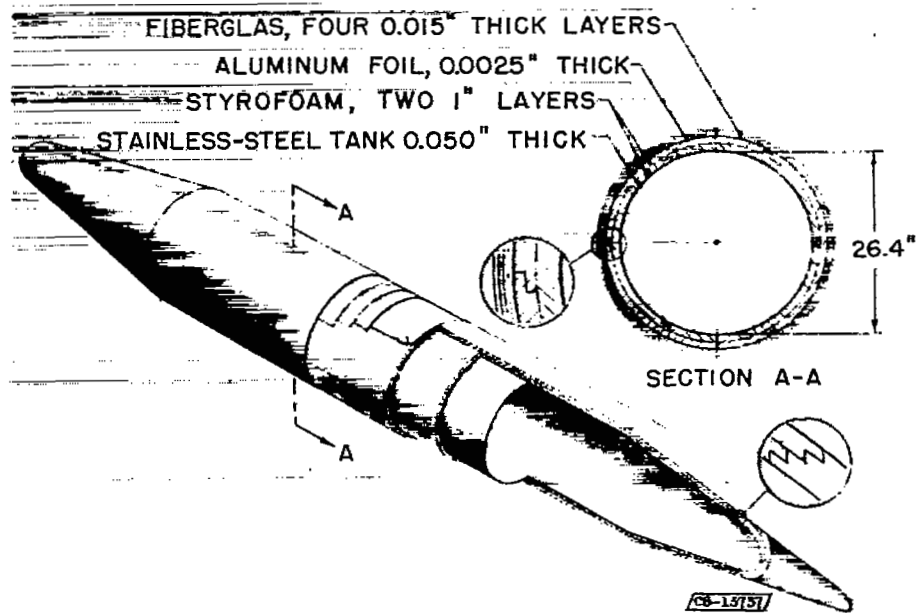


Figure 9. - Wing-tip tank.

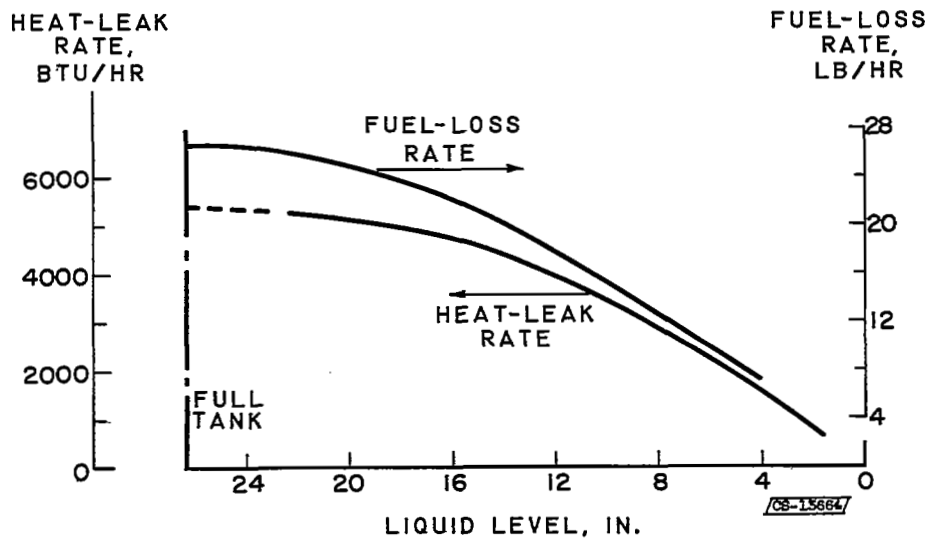
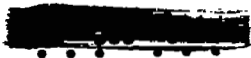


Figure 10. - Heat-leak and fuel-loss rates.

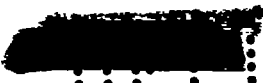


DECLASSIFIED

6 - AIRCRAFT FUEL SYSTEM FOR LIQUID HYDROGEN

Paul M. Ordin  
David B. Fenn  
Edward W. Otto



 **CLASSIFIED** 71

## 6. Aircraft Fuel System For Liquid Hydrogen

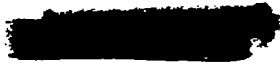
By Paul M. Ordin, David B. Fenn, and Edward W. Otto

The NACA has conducted a special project in order to study the use of liquid-hydrogen fuel for jet bombers, in addition to the work with liquid hydrogen as a high-energy fuel described in the preceding papers. The design of the aircraft fuel system for liquid hydrogen in the B57 bomber began in January, 1956. During the time the NACA has been engaged in this project, studies have been completed on the aircraft system in the altitude facility, on the installation of the system in the B57 aircraft, and on the operation of the aircraft on hydrogen fuel at an altitude of over 49,000 feet and a Mach number of 0.72.

The flight and design problems considered in the project were as follows:

- (1) A dual-fuel system to facilitate the operation of one of the two J65 engines in the B57 aircraft with both JP-4 and hydrogen fuels. This dual-fuel feature permitted takeoff and climb on JP-4 fuel followed by a change to hydrogen fuel at the desired altitude. In addition, the reduced fuel requirements at high altitude permitted maximum flight time on the available hydrogen fuel.
- (2) A simple and accurate fuel control that could be developed in a short time. Such a control was believed possible with an automatic rather than a separate manual control system. In conjunction with the control problem, the existing JP-4 fuel aircraft-control system was to be utilized to regulate the hydrogen flow.
- (3) Safety in handling on the ground and in flight, and in the use of satisfactory lines, fittings, tanks, and related equipment compatible with the space available in the airplane. The aim here was to keep modifications to the present aircraft at a minimum.

A basic flow system which helps to indicate the areas of study and development is shown schematically in figure 1. The hydrogen is stored as a liquid in the aircraft tank. The aircraft tank, discussed in the preceding paper, was designed to hold about 430 gallons of liquid hydrogen. The fuel system was a helium-gas pressure-fed system, because an aircraft pump for liquid hydrogen did not exist. Vacuum-jacketed plumbing was used to contain the liquid hydrogen from the tank to the



heat exchanger. The heat exchanger was designed only to vaporize the hydrogen and was considered because the fuel-control problem would be simpler if a gas rather than a two-phase mixture of liquid and gas was used. In addition, the use of a heat exchanger might permit the application of the cold-sink potentialities of hydrogen. Ram air rather than compressor bleed or exhaust gas was used to vaporize the fuel. The cold hydrogen gas, about 50° R, enters the special fuel regulator. The hydrogen regulator was designed to use the existing JP-4 fuel control loop system in order to regulate the flow of hydrogen; the regulator is a ratio control device which uses the controlled JP-4 fuel to control the flow of hydrogen. The controlled hydrogen flow enters the manifold and then the combustor which was modified for both JP-4 and hydrogen fuel operation. The main areas of study were the liquid fuel tank, ram-air heat exchanger, hydrogen regulator, and combustor modification.

The construction of the hydrogen tank and the results of the heat leak and pressure rise studies are presented in the preceding paper. From the tank pressurized with helium gas, the liquid hydrogen flowed into the bottom of the heat exchanger. The heat exchanger was designed of commercially available core materials and is shown schematically in figure 2. The heat exchanger consisted of 28 integral-finned copper tubes, 5/8-inch diameter, a length of 1 foot, and also had seven 1/2-inch-diameter fins per inch. The integral-fin tubes were selected because separation of the fins from the parent tube can sometimes occur at low temperatures when they are swaged or attached by other means.

The liquid hydrogen then entered the bottom manifold, was vaporized and collected in the upper manifold. The manifolds were constructed of stainless steel, and the copper tubes silver soldered to the manifold plates. This heat exchanger was designed to vaporize 500 pounds of hydrogen per hour; the fuel requirements for one engine at a 50,000-foot altitude and Mach 0.75 with a ram-air flow of 1.75 pounds per second. In addition, the heat exchanger was sized to insure an outlet-air temperature above that of liquefaction in order to prevent the accumulation of liquid air in the exchanger. The experimental results indicated that an airflow of 1.45 pounds per second was required to vaporize the fuel completely, and the resultant exit-air temperature under these conditions was 374° R, about 200° R above liquefaction temperature.

Almost no experimental data exists for heat exchangers designed for the vaporization of liquid hydrogen, therefore, during the investigation over-all heat-transfer coefficients for various fuel flows were obtained. Studies of heat-transfer data through the heat exchanger indicated at least one area of fundamental work which should be investigated. The area for study was cold-hydrogen temperature measurement in a flowing system. Carbon resistors rather than thermocouples were used for measuring these low temperatures. The temperature-millivolt output relation for thermocouples and carbon resistors is indicated on figure 3.

For the copper-constantan thermocouple, a very small output is obtained for a large change in temperature at a low temperature range of 50° to 150° R. For the carbon resistors, where the change in resistance is important, for the same temperature range, a considerably greater signal is available. However, even with the increased output with carbon resistors, there was still some difficulty in obtaining accurate values of the exit-fuel temperatures. The fuel temperatures were used to determine the experimental values of heat-transfer coefficients. The coefficients were calculated from the measured over-all heat balance; that is, from the airflow through the heat exchanger and its temperature drop and from the fuel flow and its temperature rise.

The heat-transfer coefficients were fairly constant through a wide range of fuel flows and indicated a value of about 65 Btu per hour per square foot of tube surface per °F for the designed fuel and airflow. The results of the heat-exchanger studies indicate that hydrogen is a relatively normal boiling liquid, and by using standard engineering practice in design, desired results will occur. As shown by figure 3, the cold gas leaves the heat exchanger and enters the special fuel regulator. The special fuel regulator is actually an addition to the existing JP-4 control system and uses the JP-4 control system to regulate the flow of hydrogen fuel.

The regulated flow of hydrogen fuel is shown in figure 4. The normal JP-4 fuel system pumps the fuel from the tank through the automatic fuel control, which is a hydraulic device, and then into the engine. The existing system is utilized by installing a fuel-ratio meter in the closed loop. This ratio meter is shown on figure 4 and would adjust the hydrogen flow according to the JP-4 flow. In order to use the controlled JP-4 flow to operate a ratio meter, the JP-4 fuel flow was bypassed from the engine through the special fuel meter. When the engine is operating on hydrogen fuel, the JP-4 fuel is bypassed through the ratio meter, and the standard JP-4 control on the engine performs the normal function of maintaining a set speed when hydrogen fuel is burned.

The fuel-ratio meter consists of two separate chambers and is shown schematically in figure 5. The JP-4 fuel flows through one part of the regulator, which contains an orifice for setting up a pressure drop as a function of flow and also a piston which senses the drop. The force developed is then transmitted through a sealed connection lever (with a ratio of 1) to the hydrogen side of the regulator, which contains an orifice, piston, and valve assembly. The hydrogen flow through the regulator acts on the piston to set up a balancing force. Any change in JP-4 flow will change the forces applied to the piston and thus requires a change in hydrogen fuel flow to re-establish equilibrium. With the required increase in fuel flow, a greater force is exerted on the JP-4 piston, and this force is transmitted to the hydrogen fuel side, opening the valve further. In this manner, a unit, which would control the

hydrogen flow in a constant ratio to the flow of JP-4 fuel, was obtained. The ratio used was that of the heating values of the two fuels and was determined by selecting suitable values for the orifice and piston areas. Because the weight flow of hydrogen fuel depends on the density, it was necessary to incorporate a density compensator. As shown on figure 5, the method selected was to adjust the orifice areas with a helium-filled phosphor bronze bellows.

The controlled liquid-hydrogen gas flow continues from the regulator through the manifold into the combustor. A schematic drawing of the original combustor prior to any modifications for burning hydrogen is shown on figure 6. Figure 6 shows a section through the combustor. The combustor is a prevaporizer-type unit in which the JP-4 fuel enters through a 1/4-inch tube into the vaporizer tube. The JP-4 fuel is vaporized, mixed with primary air, and burned. The engine contains 36 vaporizer tubes, and each tube contains a 1/4-inch JP-4 fuel tube. The J65 engine combustor was modified for use with either JP-4 or hydrogen fuel by the addition of a second 1/4-inch tube for each vaporizer tube. The 36 1/4-inch hydrogen-fuel tubes were fed from an external manifold. A photograph looking into the inlet of the modified combustor is shown in figure 7. The JP-4 fuel enters the vaporizer tubes through the straight tubes, and the hydrogen fuel enters through the bent tubes. The only engine modification was the addition of the hydrogen-fuel tubes and manifold.

Prior to the installation of the hydrogen fuel system in the aircraft, the complete engine flow system was investigated in our full-scale altitude facility. A photograph of the engine installation in the test chamber is shown in figure 8. The system contains all our flight equipment and is coupled to the flight engine. The liquid fuel is forced out of the tank by means of helium gas pressure. The liquid-fuel tank and pressurizing systems are located outside the building. With the tank pressurized, the liquid flows through the vacuum jacketed lines to the bottom of the heat exchanger. Dry refrigerated air, simulating the ram-air conditions encountered in flight, is passed over the heat exchanger to vaporize the fuel. The cold-hydrogen gas is then passed through the flow regulator and then into the engine.

During the altitude tests, over 40 transitions from JP-4 to hydrogen fuel were completed. A typical plot of engine speed against time during the transition with the engine initially operating on JP-4 fuel at simulated altitude of 50,000 feet and Mach 0.75 is shown by figure 9. Prior to the introduction of hydrogen, the hydrogen fuel line is purged with helium gas to remove any air, moisture, or foreign matter. The next step involves the operation of the engine on both JP-4 and hydrogen fuel and is accomplished by bypassing some of the JP-4 fuel through the hydrogen regulator and opening the main hydrogen valves. The dual flow into the



combustor begins with an initial drop in speed as is indicated on figure 9. This drop in speed occurs while the JP-4 fuel return line and hydrogen line are being filled. During this time, the hydrogen fuel lines and manifold must be cooled sufficiently to pass sufficient fuel for dual operation. The operation of the engine on hydrogen fuel only occurs when the main JP-4 fuel valve to the engine is closed and all the JP-4 fuel is bypassed through the hydrogen regulator. The engine speed is varied in the normal manner by varying the JP-4 fuel throttle position.

The fuel transition discussed herein is typical of most of the runs made, however, during a few runs, fluctuations in engine speed for a short period during the transition to hydrogen operation were obtained. A plot, showing the change in speed during a fuel transition in which some fluctuations occurred, is shown in figure 10. The speed fluctuations always decreased after 4 to 6 minutes of operation, after which speed could be changed and throttle bursts performed, then the speed would respond in the normal way. Fluctuations in engine speed are probably due to unsteady boiling in the heat exchanger which causes a rapid change in the level of liquid in the heat-exchanger tubes. Further research is required to obtain a better understanding of the unsteady boiling problem.

In previous papers, the importance of temperature profiles were indicated, and the temperature distribution at the turbine inlet for the modified engine was under consideration. A comparison of typical radial temperature profiles measured at the turbine inlet for both JP-4 and hydrogen fuel is shown in figure 11. The engine was operated at an altitude of 50,000 feet and a flight Mach number of 0.75 at the limiting turbine-outlet temperature. The temperature profiles in the radial direction are nearly identical for JP-4 and hydrogen fuels. To obtain a check on the uniformity of the hydrogen-fuel injection, measurements were also obtained of the circumferential temperature distribution. The results of the measurements are shown in figure 12 and no great effect was indicated by changing the fuel. The temperature spread for the JP-4 fuel is normal for the engine operation.

The effect of engine changes on the net thrust developed was studied, and on figure 13 the net thrust as a function of engine speed for operation of both fuels at an altitude of 50,000 feet is shown. As discussed in a previous paper, because of the different gas properties resulting from the combustion of the fuels, the net thrust at a given engine speed and fixed exhaust-nozzle area is lower with hydrogen than JP-4 fuel. With a fixed exhaust-nozzle area sized to give limiting temperature at sea-level rated-speed conditions, the J65 engine burning JP-4 fuel at 50,000 feet reaches limiting turbine-outlet temperatures at about 8100 rpm; at these conditions, the thrust is about 1190 pounds. With hydrogen fuel, at the same altitude conditions, the engine reaches the same

turbine-inlet temperature at an engine speed of 8240 rpm. At this speed, a thrust of 1180 pounds is reached; the limited mechanical rated speed of the engine is 8300 rpm. With the added fuel system, a 10-pound drop in thrust occurred, but some of the gains to be realized with hydrogen fuel, as expected from its heating value, are shown in figure 14. Figure 14 is a plot of specific-fuel consumption against engine speed for the two fuels. A specific-fuel consumption of about 1.2 was measured for JP-4 fuel, and 0.44 pound per hydrogen fuel per pound of thrust for hydrogen fuel was recorded.

In the altitude tank studies, a total of about 30 hours with hydrogen fuel on three different J65 engines was accumulated with a maximum of 20 hours on one engine. Inspection of the combustor and turbine stator indicated no deterioration.

The results of the studies in the altitude facility indicated that there was a workable flight system, and the pilots, who operated the system in the altitude tank, were convinced that the next phase of the program, the flight installation, could be handled.

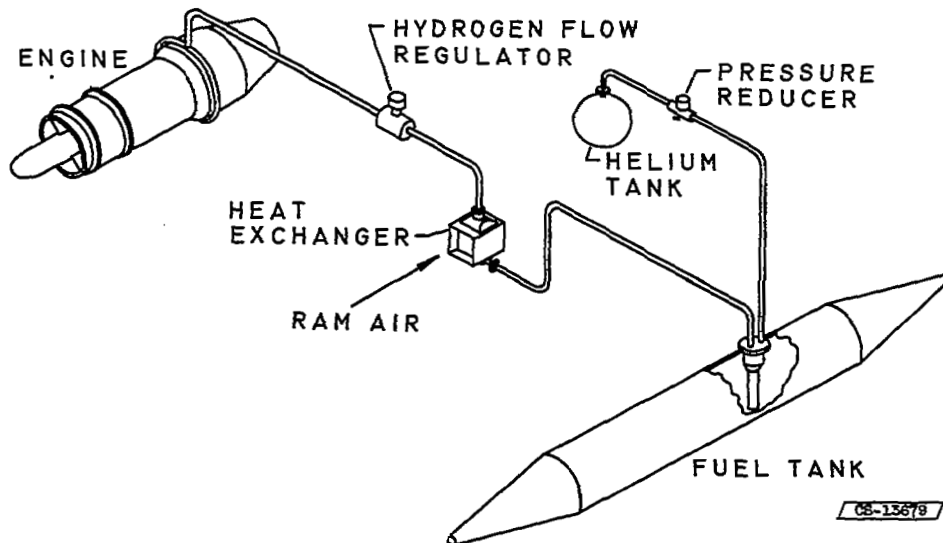


Figure 1. - Hydrogen flow system.

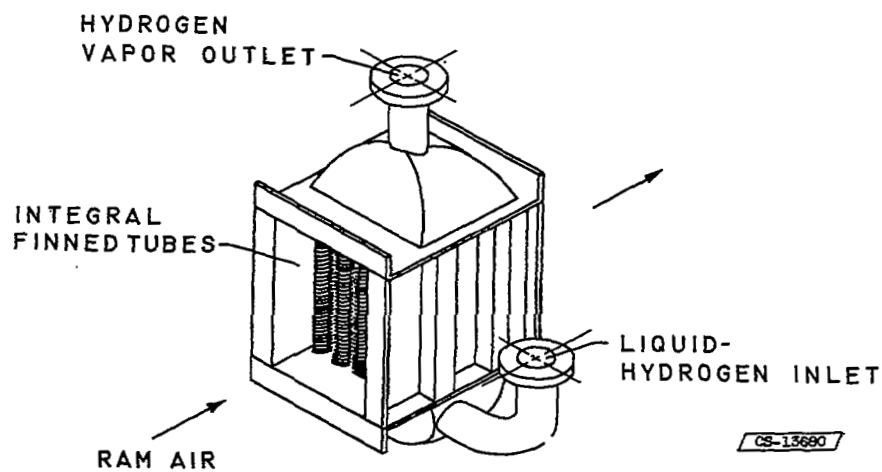


Figure 2. - Diagram of heat exchanger.

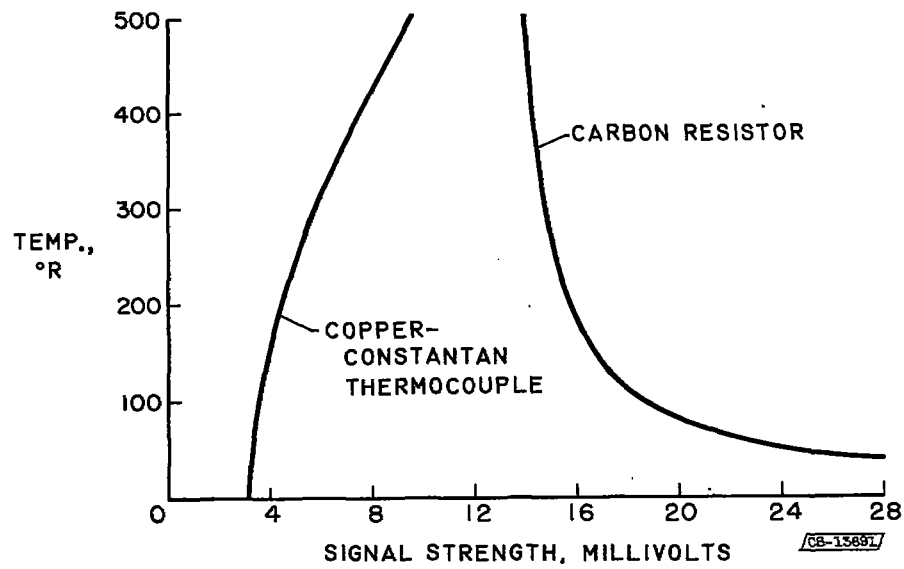


Figure 3. - Comparison of low-temperature measuring devices.

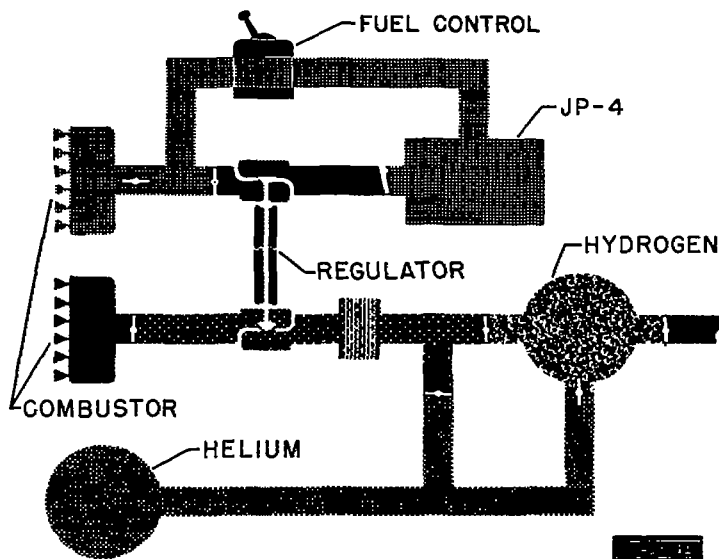


Figure 4. - Engine flow system.

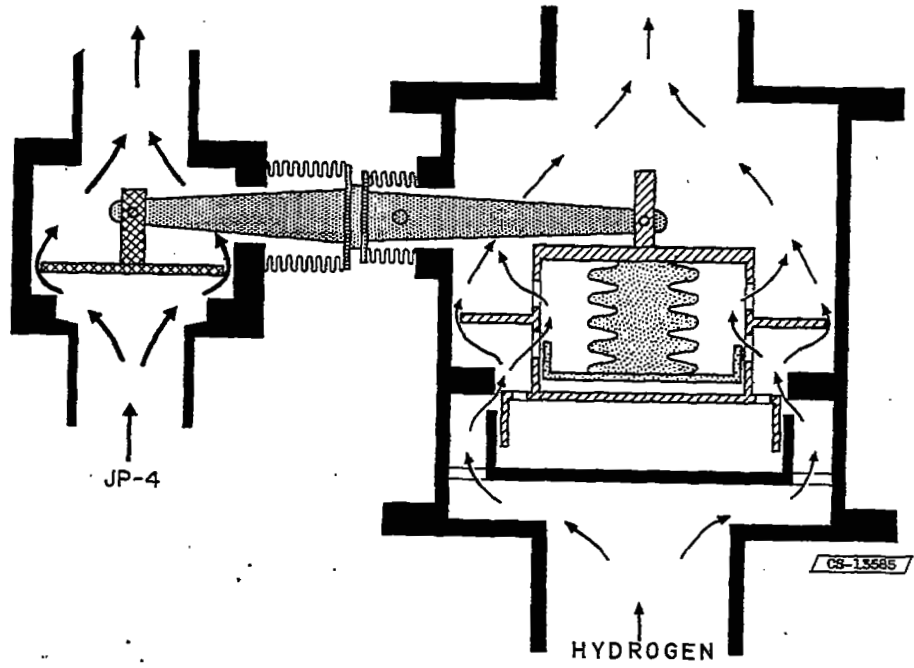


Figure 5. - Hydrogen regulator.

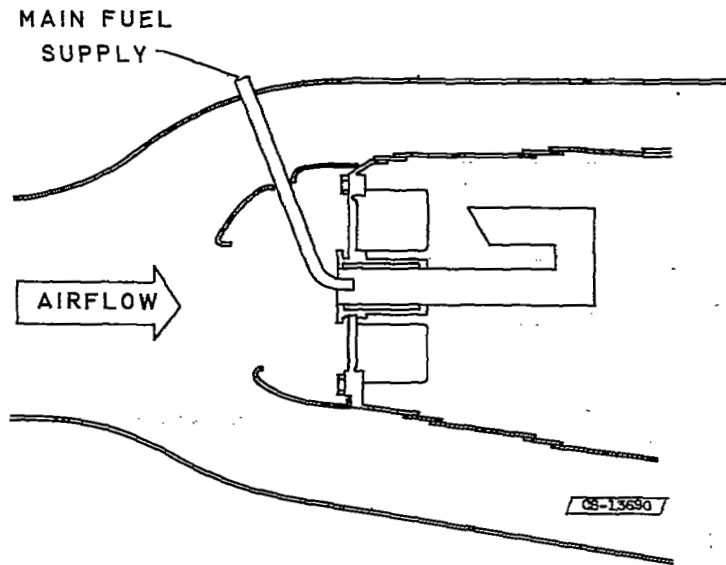


Figure 6. - Standard J65 combustor.

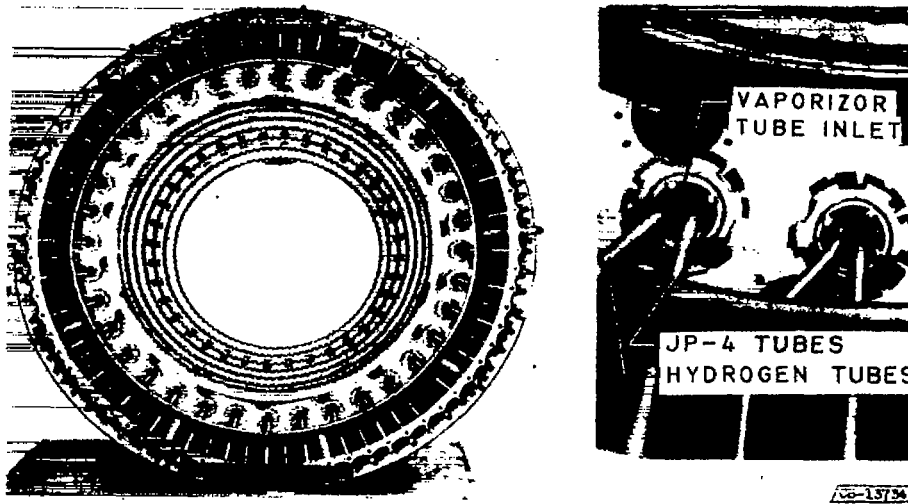


Figure 7. - Combustor modification.

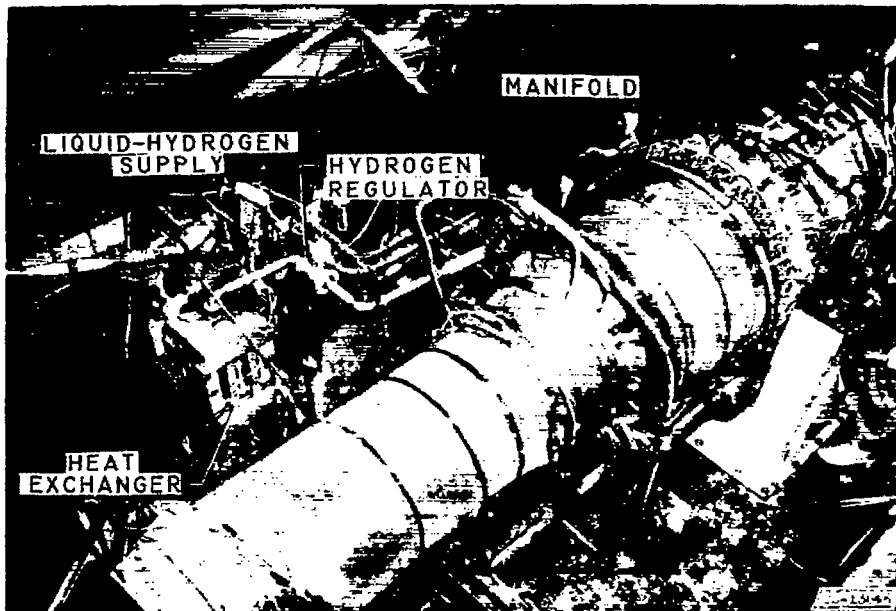


Figure 8. - Engine installation in altitude tank.

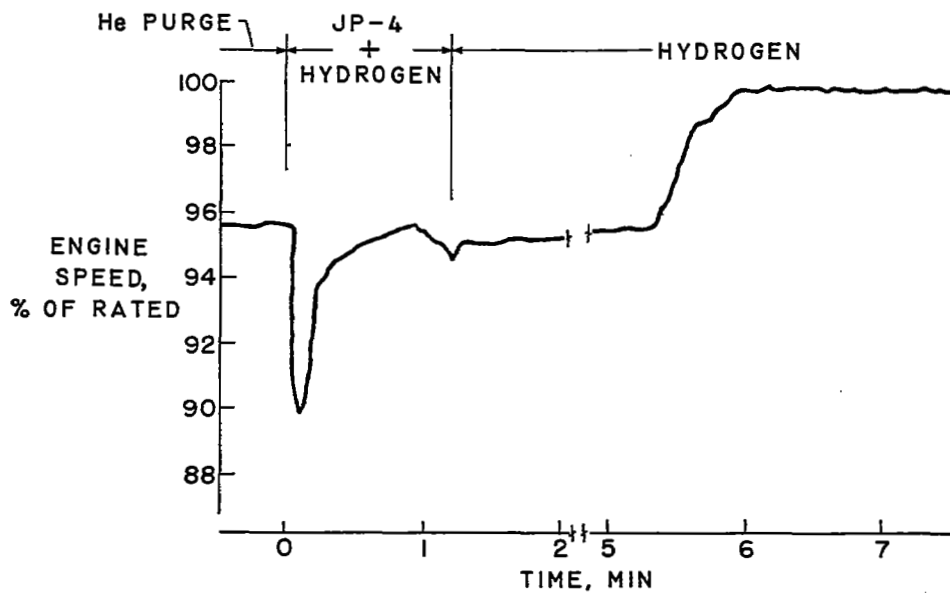


Figure 9. - Engine speed, normal fuel transition.

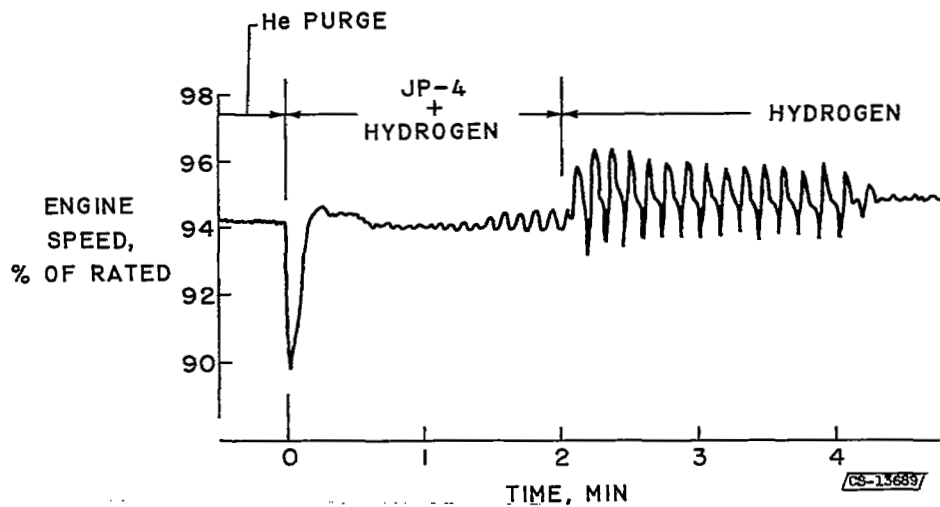


Figure 10. - Engine speed oscillations. Altitude, 50,000 ft; Mach number, 0.75.

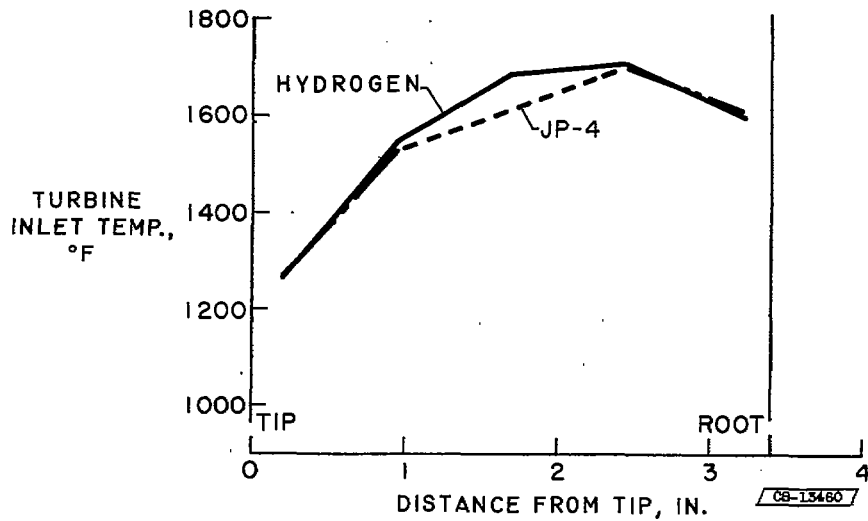


Figure 11. - Turbine inlet radial temperature profiles. Altitude, 50,000 ft; Mach number, 0.75; limiting turbine outlet temperature.

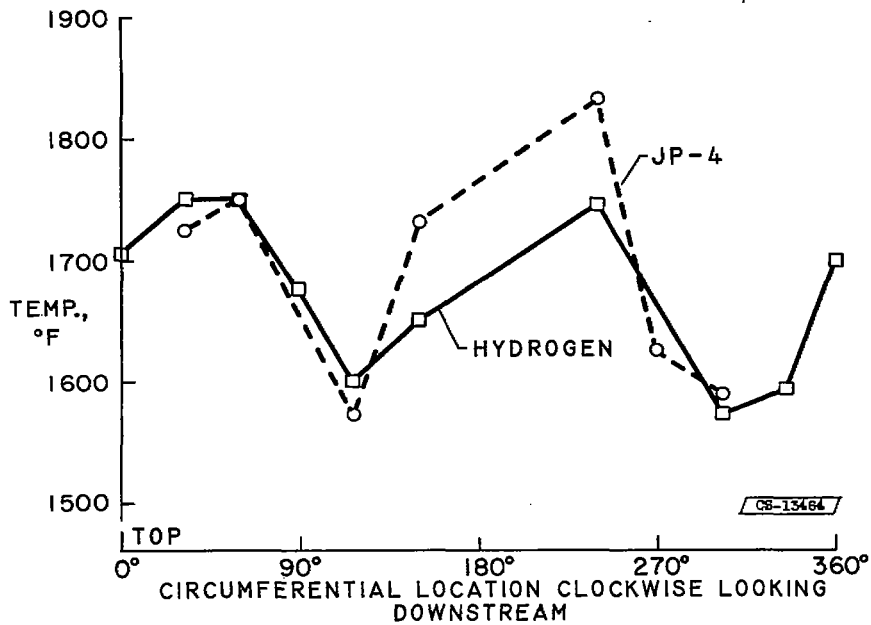


Figure 12. - Turbine inlet circumferential temperature profiles. Mach number, 0.75; altitude, 50,000 ft; limiting turbine outlet temperature.

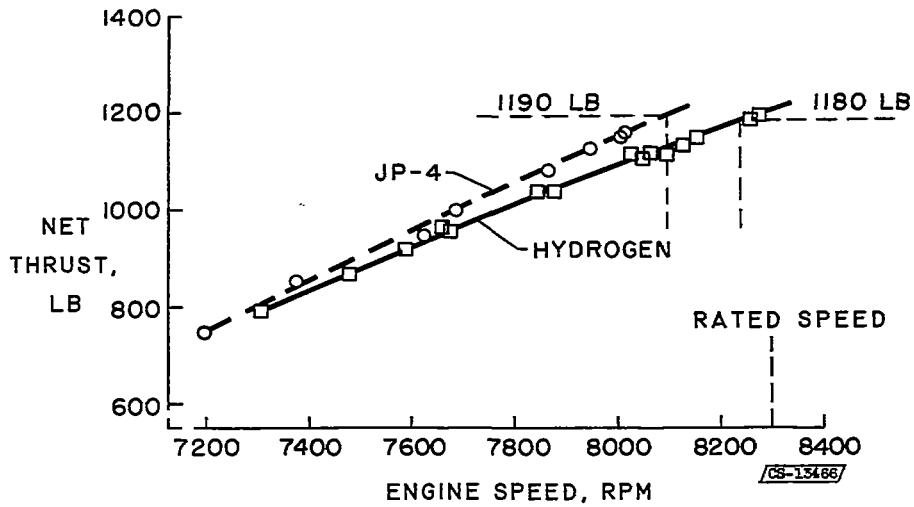


Figure 13. - Net thrust with hydrogen and JP-4. Mach number, 0.75; altitude, 50,000 ft.

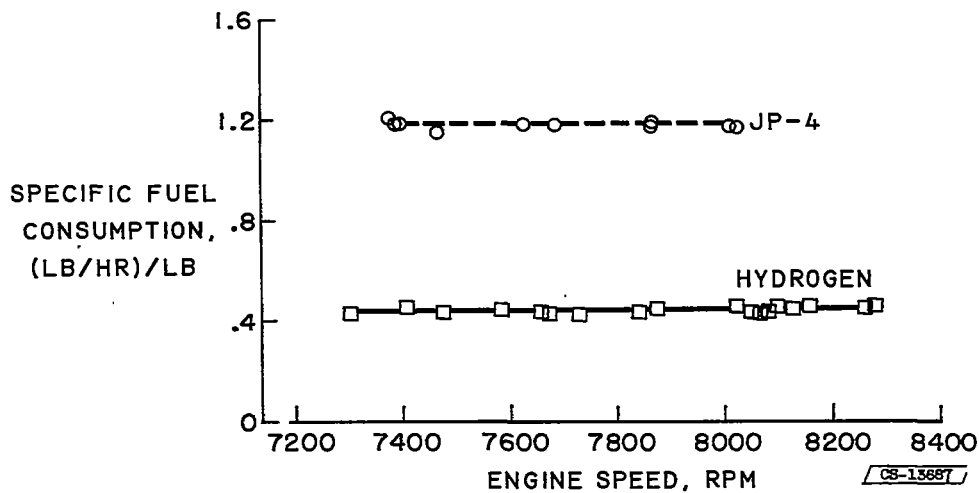


Figure 14. - Specific fuel consumption with JP-4 and hydrogen. Altitude, 50,000 ft; Mach number, 0.75.

7 - FLIGHT EXPERIENCE WITH LIQUID HYDROGEN

Donald R. Mulholland  
Joseph S. Algranti  
William V. Gough, Jr.



## 7. FLIGHT EXPERIENCE WITH LIQUID HYDROGEN

By Donald R. Mulholland, Joseph S. Algranti, and William V. Gough, Jr.

The objectives of the flight-test phase of the NACA liquid-hydrogen research program were, first, to construct a workable fuel system and demonstrate its feasibility during flight; and second, to uncover areas in which laboratory research can best be applied to further the work in this field.

The flight plan for the program was to operate one engine of a B-57 airplane with hydrogen during cruise at approximately 50,000 feet altitude. The climb and descent were to be made on JP fuel. Operation with hydrogen fuel for these flights was to be only long enough to establish complete and satisfactory operation of the engine at altitude. This permitted the use of a reasonably sized fuel tank for the B-57 airplane.

In the laboratory facility, the hydrogen system to supply the J65 engine was tailored to duplicate the installation planned for the B-57 airplane. Therefore, the aircraft fuel system contained almost identical features of the laboratory installation. The fuel-line length was the same, and the fuel tank with the pylon plumbing, the heat exchanger, the special fuel regulator, and the engine were actually transferred to the aircraft installation. These steps were taken in an effort to ensure, as far as possible, a fully tested system for the flight application.

A cutaway view of the special fuel system in the B-57 aircraft is shown in figure 1. The fuel tank is mounted on the left wing tip. The vacuum-jacketed liquid-fuel line extends inboard from the tip just aft of the single main spar to the gunbay compartment, then forward and downward into the bottom of the heat exchanger. The gaseous fuel is conducted from the top of the heat exchanger through an unjacketed line to the special fuel regulator and then through an inboard rib to the special fuel manifold surrounding the engine. The helium supply necessary for pressurizing the fuel tank and purging the fuel system is carried in a tank on the right wing tip. Figure 2 is a photograph of the B-57 airplane with the equipment installed ready for flight. The ram air scoop for the heat exchanger is mounted under the left wing just outboard of the engine nacelle.

The wing-tip location was chosen for the fuel tank for two reasons. First, it was desirable, for this first flight attempt, to provide a fuel tank that could be dropped, and the wing tip was considered the best aerodynamic location for proper separation. Secondly, as a safety measure, the fuel supply and the vent pipe were kept as far from the engine as possible.

The hydrogen fuel tank and the pylon are shown in figure 3. Details of the fuel-tank construction, including type of structural material and insulation, are given in paper 5. The tank is supported on the wing tip by a standard bomb rack installed in the pylon. The vent tube extends along the top of the rear section and exhausts at the aft tip of the tank. This tube is used for venting gas as necessary to stay under the maximum tank pressure and also for dumping the liquid from the tank when necessary. A standard intercostal construction is used inside the shell along the top of the tank for support, and inverted U-bolts hold the tank to the bomb rack.

The tank is approximately 23 feet long and 30 inches in diameter. The standard tank used on the B-57 aircraft is only  $14\frac{1}{2}$  feet long.

Therefore, some aerodynamic flight testing was required to determine the feasibility of using the larger tanks on this aircraft. One of the dummy tanks used for aerodynamic flight tests is shown in figure 4. This is actually an F-84 wing-tip tank modified with additional cylindrical sections to make the length similar to that of the hydrogen fuel tank. Steel pipes are mounted inside the tank to provide for the proper moment of inertia. Several flights with these dummy tanks established that the airplane operation would not be impaired by the use of the larger wing-tip tanks for the flight conditions required for these tests.

Studies were also made to determine the separation characteristics of the fuel tank, should it become necessary to drop the tank. Calculations indicated that the tank should nose upward and translate outward at the time of separation from the wing tip. Drop tests with a scale model of the wing section and the tank were performed in a wind tunnel to verify these results. Moving pictures recorded the model tank drops in the tunnel at simulated low- and high-speed conditions for the B-57 airplane. These pictures were taken in slow motion from three different positions to show the tank separation. The tunnel tests verified the results of the calculations. No tank drops have been made during flight, since the flight operations never required disposing of the fuel tank.

In designing the fuel system, as much of the control plumbing as possible was kept in the outboard area. All the control valves were placed in the pylon along with the bomb rack, except one shutoff valve that was installed near the engine. The pylon containing the special valves and fittings, along with the dip tube, is shown in figure 5. The liquid-control valves shown in the rear part of the pylon are standard

pneumatic valves actuated by helium gas at a pressure of 150 pounds per square inch. This type of pneumatic valve had formerly been used for handling liquid oxygen. The helium-control valves are shown in the front part of the pylon.

Figure 6 is a simplified drawing of the fuel lines in the pylon. The dip tube, which extends into the tank, is a double-walled tube that serves not only as a dip tube but also as a capacitance liquid-level measuring device. Three separate lines extend into the dip-tube opening, one for pressurizing the tank with helium, the second for venting off the gas as the tank pressure builds up, and the third connected to the dip tube for flowing the liquid into or out of the tank. The tank is manually vented as required through operation of the pneumatically operated vent valve. A pressure-relief valve is provided around the vent valve to relieve the tank in case the vent valve should not open. Further, a blowout disk is installed at a second opening in the tank so that the liquid will be forced from the tank through a second dip tube in case other means of pressure relief fail. To date, the vent valve has always functioned satisfactorily and it has been operated many times. To jet-tison the liquid from the tank, a second pneumatic valve is opened so that the liquid will be forced out through the standard dip tube and exhausted through the vent tube at the rear of the tank. To fill the tank, this same line is disconnected at the rear of the pylon and attached to a transfer line from a supply tank. To flow fuel to the engine, a third pneumatic valve is opened to connect the dip tube to the main fuel line.

The main liquid-fuel line is a specially constructed vacuum-jacketed line. Special metal-to-metal flanges with double O-ring metal seals are used to connect sections of the liquid line. A drawing of this type of flanged joint is shown in figure 7. The joint is composed of two flat-faced flanges held together with a V-band clamp. The two hollow metal O-rings provide a double seal. A vent tube is connected to an annulus between the two O-rings to vent any leakage past either O-ring to a safe external low-pressure area. Although this joint is not a low-heat-leak joint, it is particularly applicable to the aircraft installation, since it requires very little space for assembly as compared to the bayonet-type joints normally available on the commercial market.

The heat-exchanger installation on the aircraft is shown in figure 8. The basic heat-exchanger construction is discussed in the preceding paper. The vacuum-jacketed liquid line is connected to the bottom of the heat exchanger, and the unjacketed cold gas line is connected to a similar manifold on the top. The heat exchanger is mounted so that it projects about halfway below the wing skin in order that a ram air scoop can be easily installed over the heat exchanger. The ram-air-scoop installation in figure 9 shows the ram opening on the front of the scoop; a similar exit opening is at the rear.

The fuel regulator and fuel manifold around the engine are identical to those used in the laboratory installation and are fully described in the previous papers.

The helium storage tank mounted on the right wing tip is shown in figure 10. Twenty-four Fiberglas spheres were used to store the helium necessary for purging and pressurization. These spheres were mounted in one of the dummy tanks used earlier for the aerodynamic tests. The spheres were charged to 3000 pounds per square inch. Twenty-two of the spheres were used for the normal helium supply, and two were reserved for emergency use.

All controls for operating the special equipment are mounted in the rear cockpit of the airplane as shown in figure 11. The master control switch and indicating lights for all the valves and the standard indicators for engine exhaust temperature, engine speed, and JP flow are provided. In addition, indicators were installed for hydrogen fuel level, fuel-tank pressure, helium supply pressures, combustible-gas alarm, and other miscellaneous equipment.

Of the many precautionary measures taken for safety, some have been mentioned, such as the location of the fuel tank with respect to the engine, the "droppable" feature of the tank, and the pneumatic helium-operated valves. In addition, microswitches were mounted on the valve stems to provide a positive indication for each valve position. The microswitches were enclosed and purged with low-pressure helium gas to eliminate every source of electrical ignition outboard of the engine. The microswitches were connected to the indicating lights shown on the control panel. It was so arranged that every valve indicating light had to be "on" for each master-switch position to show that all the valves in the system were either in the correct open or closed position. By this means, a valve malfunction could be quickly identified and proper corrective action taken.

Other safety features included a combustible-gas alarm system. The layout of this system is shown in figure 12. For this application, four sampling stations are installed at critical points in the wing: at the wing tip, in the gunbay area near the heat exchanger and the fuel regulator, and in the engine compartment. A sample from each station is continuously passed through a sampling valve located in the bomb bay. Each sample is then cycled through a gas alarm unit located in the cockpit.

Critical areas of the wing are also purged with ram air as a further precaution. The gun-compartment ram-air-purge door is blocked open. Louvres are provided on the wing lower surface and on the pylon skin. Also, the two joints of the liquid line in the wing cavity are hooded and connected to an external low-pressure area to create positive flow away from these regions. Actually, many helium-leak inspections of the entire system were made both before and after flights, and no leaks have yet been found in the hydrogen fuel system.

All the flight tests have been conducted over Lake Erie. To date, five flights have been made. The first two flights were considered only partially successful. Although the change was made to complete operation on hydrogen, insufficient fuel flow was obtained for satisfactory high-speed engine operation. On these flights the hydrogen fuel was jettisoned, the engine was switched back to JP fuel, and the aircraft was returned to the base. The fuel jettison and return to JP fuel was accomplished without incident. Several minor changes were made in the system following these flights, after which three completely satisfactory flights were made.

The flights were all conducted at 48,000 to 49,000 feet altitude, and the hydrogen portion of each of the last three flights lasted approximately 20 minutes by which time the fuel supply was exhausted. Steady-state operation was maintained on the first of the successful flights; and on the last two flights engine speed was varied by use of the standard engine throttle.

The changes in fuel-tank pressure during taxi are presented in figure 13(a). Tank pressure is plotted against time for the wing-tip tank in a stationary position as used in the laboratory and for the aircraft fuel tank during the taxi period prior to takeoff. The curve for the stationary tank shows that the tank pressure increased very rapidly and would reach the maximum tank pressure in about 6 minutes. The pressure rise in the tank during taxi was much less rapid; therefore, venting at maximum tank pressure would be substantially delayed beyond the no-loss time for the stationary tank. This additional no-loss time is realized because temperature stratification of the liquid is prevented during agitation, and thus more of the heat leak into the tank is absorbed into the liquid as the pressure rises. The importance of this comparison of pressure rise was significant in the flight operations, because the results of pressure rise for a stationary tank indicated that venting of the tank at maximum pressure would be necessary during the taxi period. Venting during this time was considered undesirable with regard to safety. Actually, because of the extension of no-loss time due to agitation, venting of the tank was not required until the aircraft reached more than 10,000 feet altitude.

Fuel-tank pressure changes during flight are presented in figure 13(b). In the top curve, altitude is plotted against time beginning with takeoff and extending until the aircraft reached cruise altitude of approximately 50,000 feet. The lower plot shows tank pressure against time after takeoff. As the tank pressure increased and approached the maximum tank pressure, hydrogen gas was vented by use of the manually operated vent valve. As shown by the figure, manual venting of the tank was required eight times during the climb to cruise altitude. The low points of the plot represent the pressure at which the vent valve was arbitrarily closed. The area of importance of the tank pressure plot is

shown immediately after the first venting of the tank, where, as the tank pressure was increasing, the aircraft encountered a moderately turbulent condition and the tank pressure immediately dropped from approximately 42 to 37 pounds per square inch. This indicates again the effect of fuel agitation on tank pressure.

The engine speed and the JP fuel flow during the transition period in flight from JP-4 to hydrogen fuel and back to JP-4 are shown in figure 14(a). The time base begins at the time the tank was pressurized with helium, which was the first step in the process of changing from the JP-4 to hydrogen fuel. A small increase in speed took place when the helium purge was introduced in the hydrogen fuel system. This was caused by the small amount of JP fuel that was forced from the hydrogen manifold into the engine as the helium purge began. Approximately  $1\frac{1}{2}$  minutes later the system was shifted to the split-flow condition where the engine was operated on JP-4 and hydrogen fuel. At this point the speed dropped slightly as the JP fuel was split between the bypass and the normal engine flow system. After approximately another  $1\frac{1}{2}$  minutes the engine was switched completely to hydrogen fuel by turning off the JP fuel flow to the engine. The engine was then operated for 21 minutes on hydrogen without incident, after which the engine was shifted back to JP fuel.

The engine tailpipe temperature for the same flight during the transition period from JP fuel to hydrogen fuel is shown in figure 14(b). At no time during the changeover period did the tailpipe temperature increase beyond acceptable limits. At one point the tailpipe temperature did increase momentarily beyond the normal operating limit of 620° C. This occurred with the small increase in speed at the beginning of the helium purge. This increase of 30° over the normal tailpipe-temperature limit is not of concern, since it lasted such a short time. Actually, the tailpipe temperature can increase to 800° for a momentary period without damage to the engine.

Motion pictures were made of the preflight and inflight activity showing preparation of the aircraft for fuel loading, the actual fuel-loading operations, dismantling of the fuel-transfer equipment before taxi and takeoff, the jettisoning of the liquid hydrogen from the tank at altitude, and condensation trails produced by the test engine. The hydrogen-fueled engine produced a heavy persistent contrail, whereas the engine using JP-4 fuel had no contrail.

In conclusion, operation of the engine on hydrogen fuel during flight has been very satisfactory. The aircraft installation was relatively straightforward, and little modification of the aircraft structure was required. This experience indicates that, for the most part, existing types of equipment can be used for handling hydrogen in an aircraft system. It is important to point out, however, that high standards of workmanship must be used to ensure trouble-free handling of liquid hydrogen.

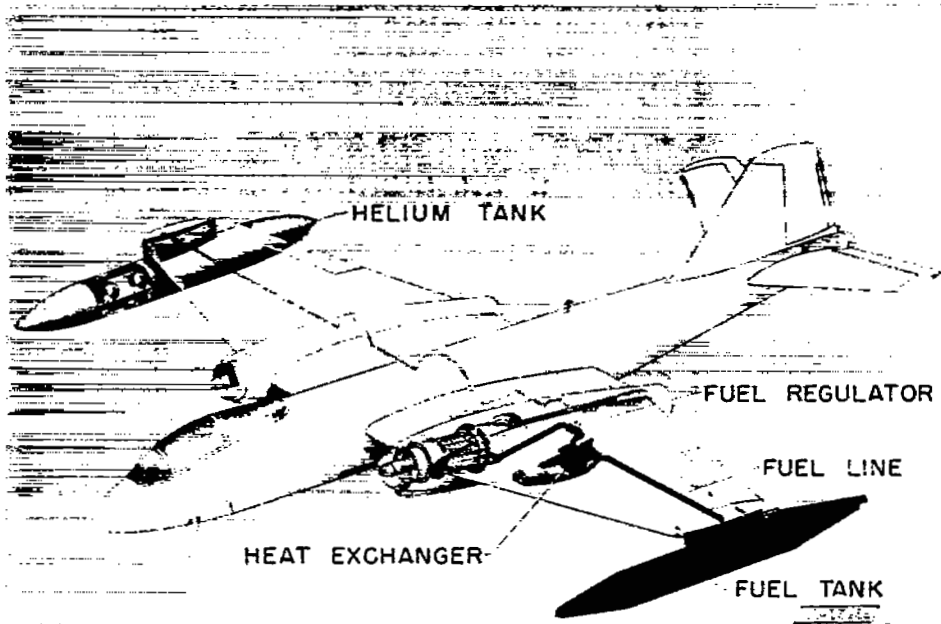


Figure 1. - Hydrogen system for B-57 airplane.



Figure 2. - B-57 airplane used for hydrogen flight tests.

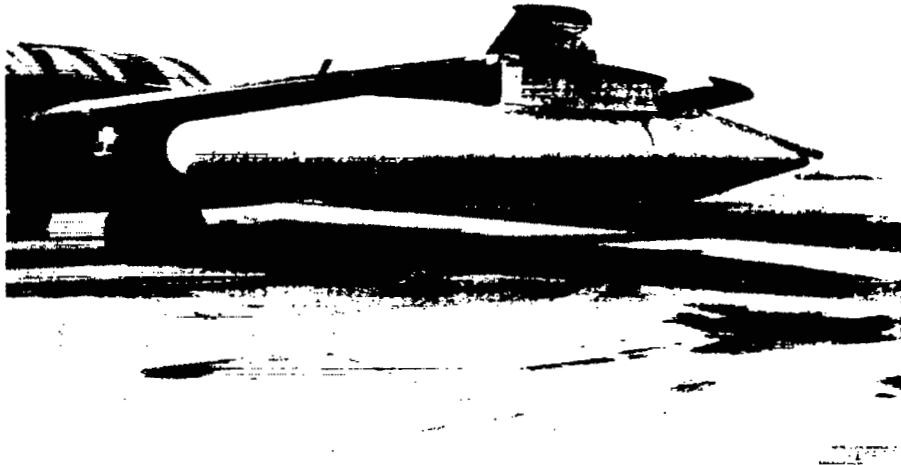


Figure 3. - Hydrogen tank used on B-57 airplane.



Figure 4. - Dummy tank on B-57 airplane for aerodynamic flight tests.

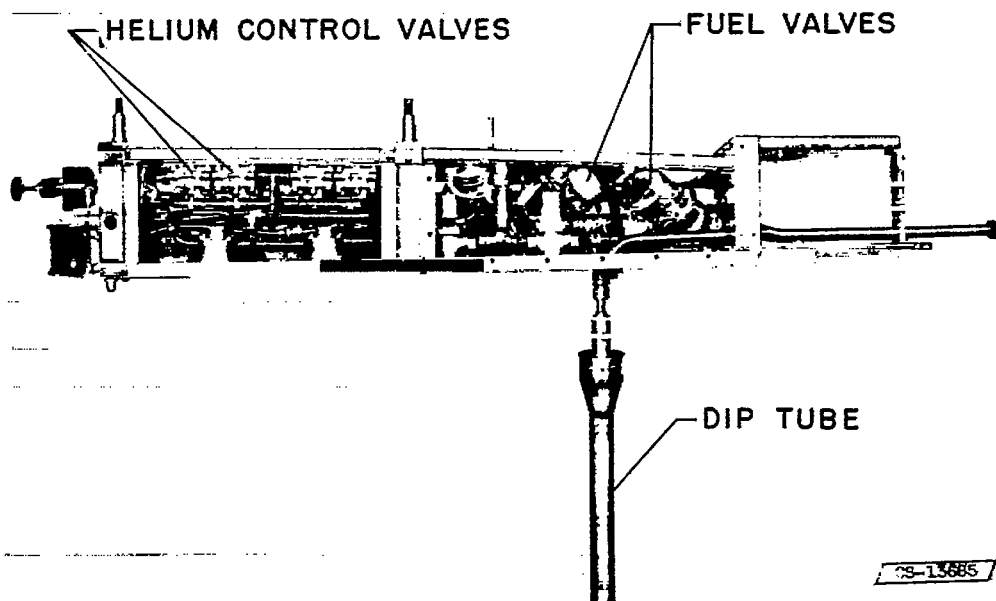


Figure 5. - Pylon for B-57 airplane.

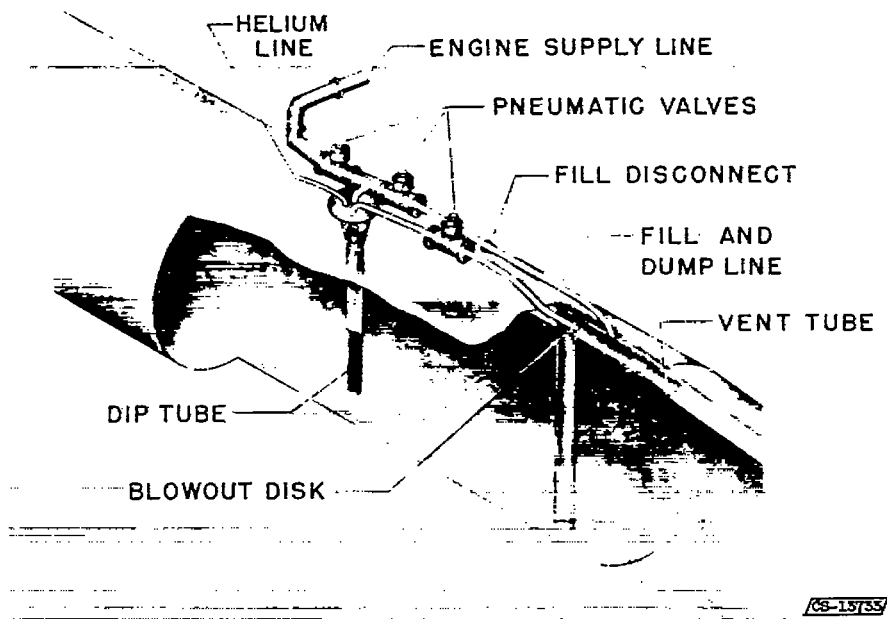


Figure 6. - Fuel system in B-57 pylon.

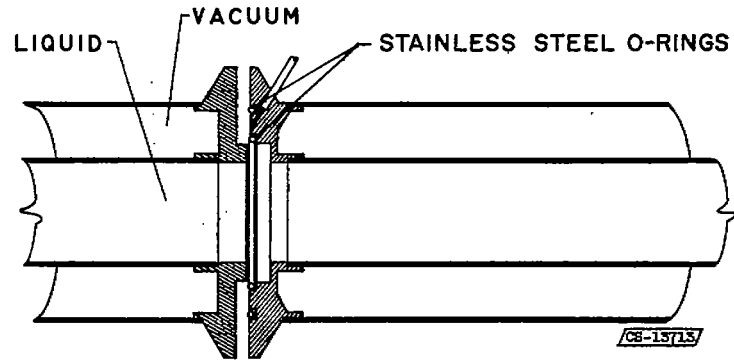


Figure 7. - Flange-type low-temperature joint.

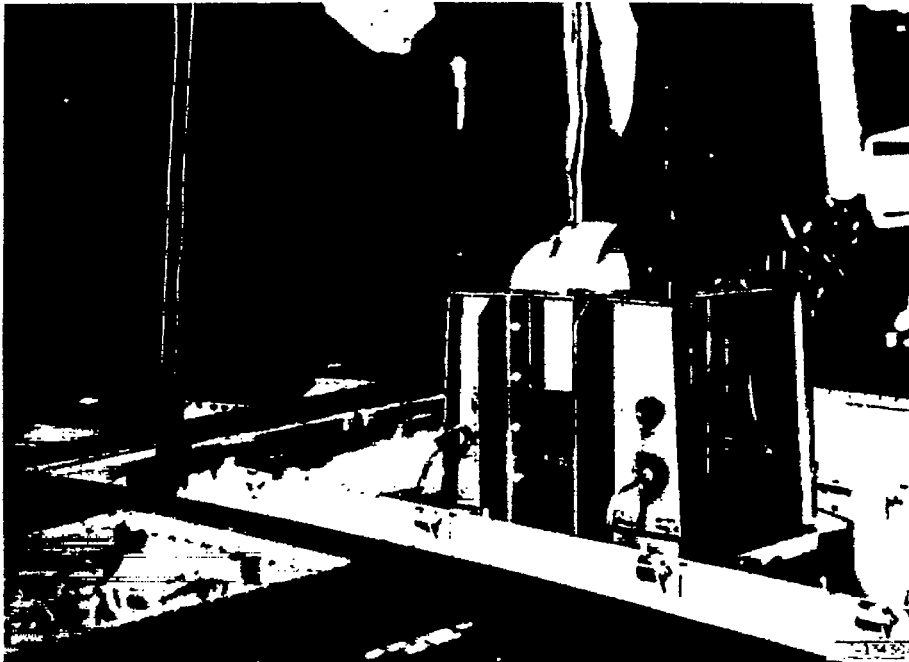


Figure 8. - Heat exchanger mounted on B-57 wing.



Figure 9. - Heat-exchanger air scoop.

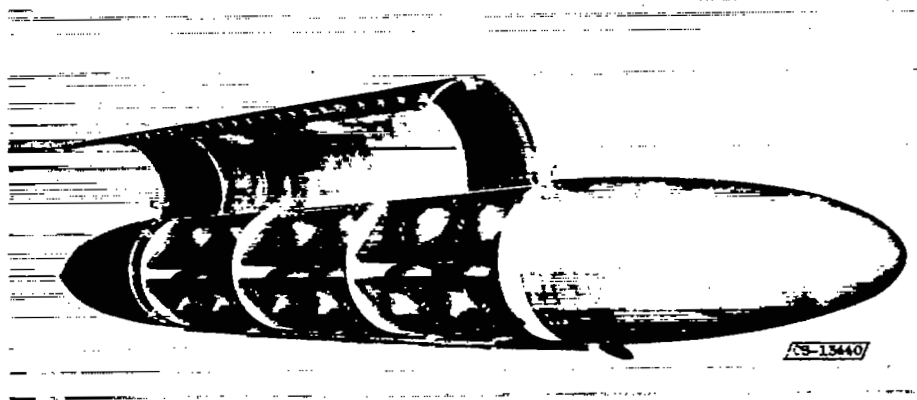


Figure 10. - Helium storage tank for B-57 airplane.

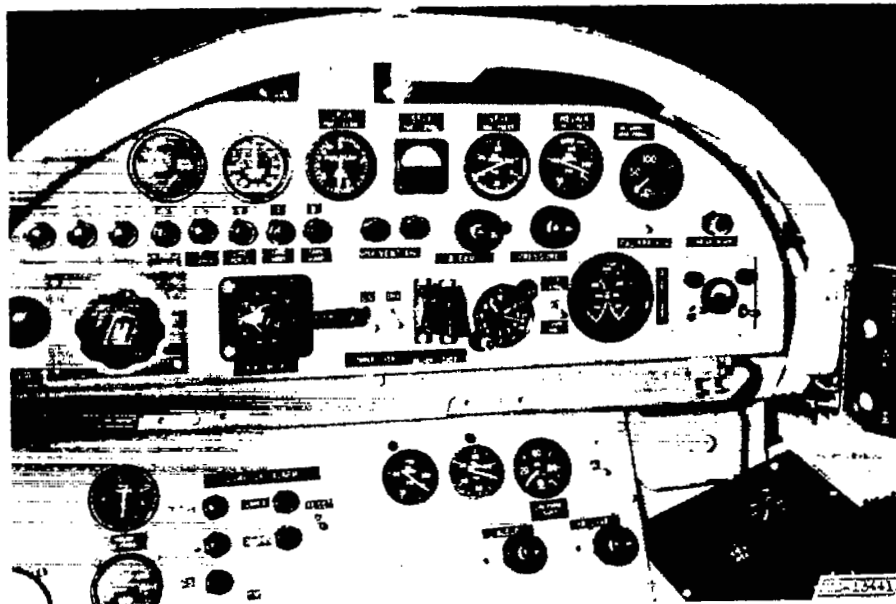


Figure 11. - Flight control panel for hydrogen system in B-57 airplane.

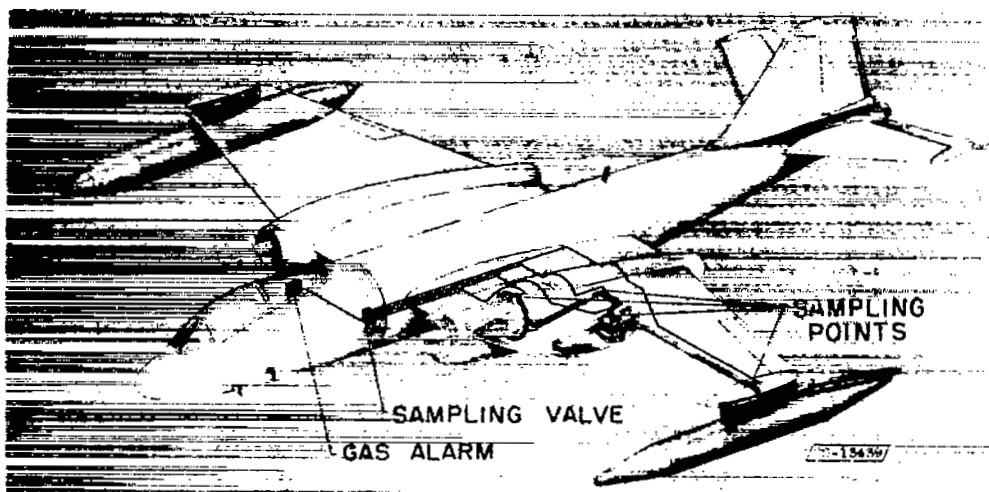
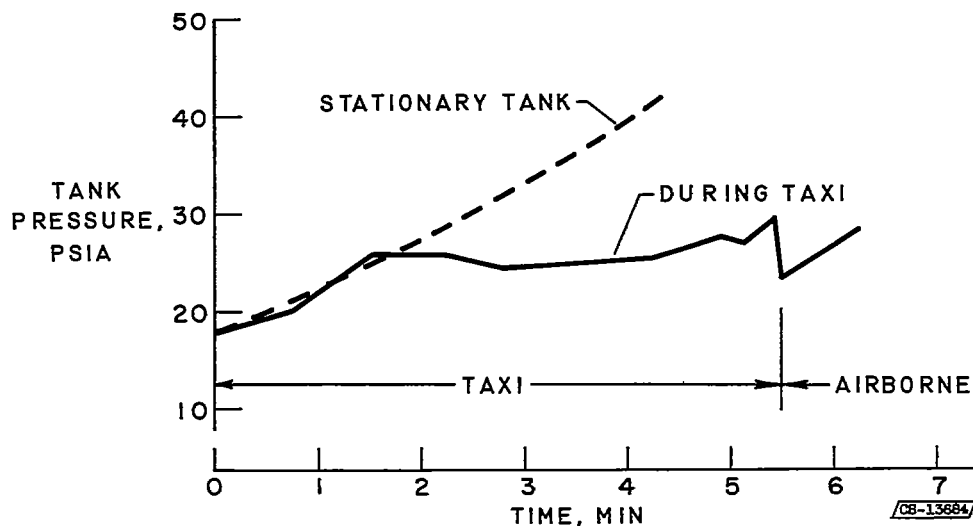
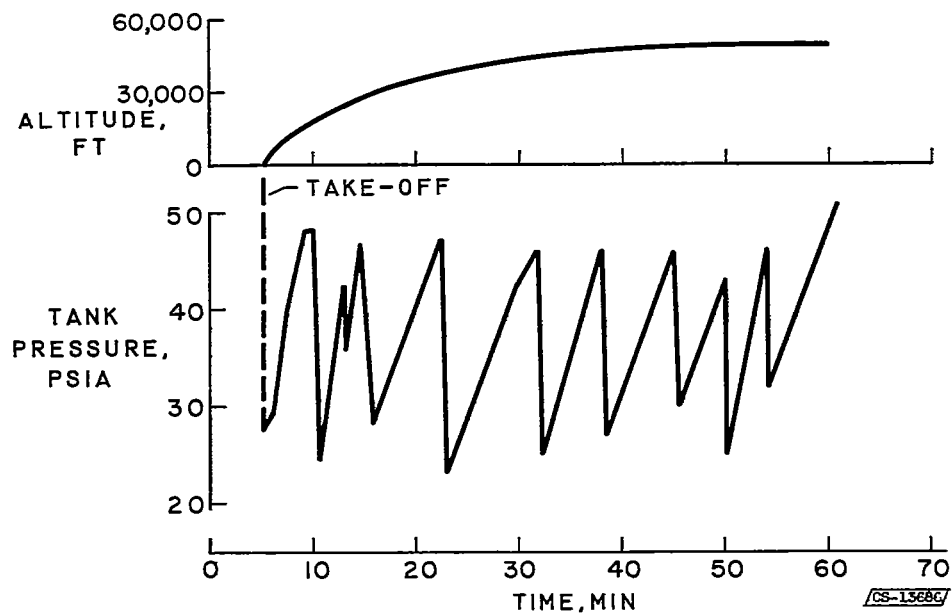


Figure 12. - Combustible-gas alarm system for B-57 airplane.

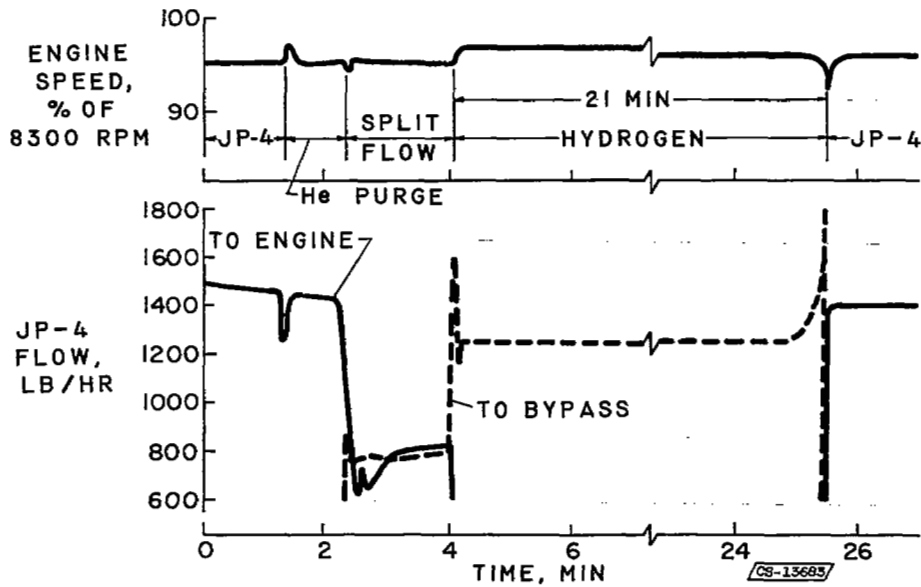


(a) During taxi.

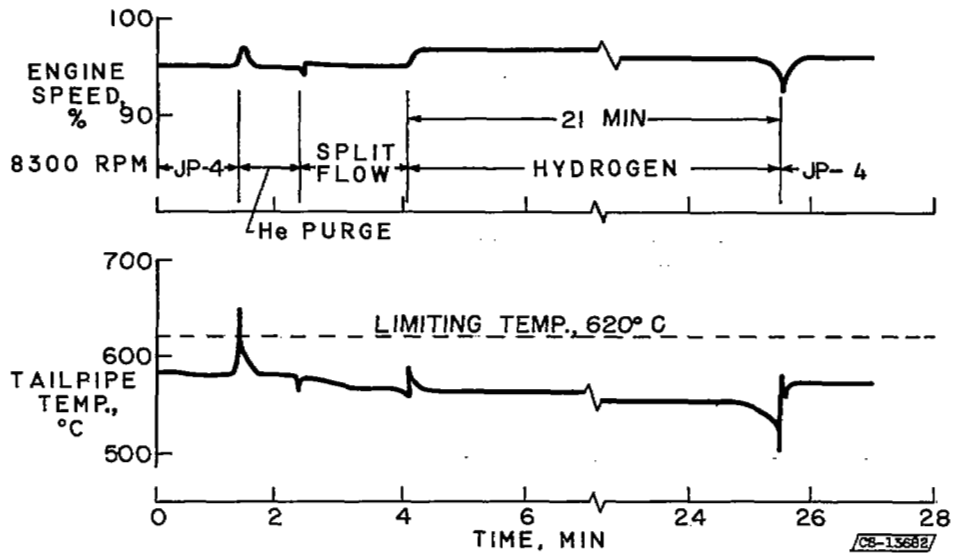


(b) During flight.

Figure 13. - Fuel-tank pressure changes.



(a) Engine speed and JP fuel flow.



(b) Tailpipe temperature.

Figure 14. - Transition to hydrogen fuel during flight.

## BIBLIOGRAPHY

- Cervenka, A. J., and Sheldon, J. W.: Method for Shortening Ram-Jet Engines by Burning Hydrogen Fuel in the Subsonic Diffuser. NACA RM E56G27, 1956.
- Corrington, Lester C., Thornbury, Kenneth L., and Hennings, Glen: Some Design and Operational Considerations of a Liquid-Hydrogen Fuel and Heat-Sink System for Turbojet-Engine Tests. NACA RM E56J18a, 1956.
- Dangle, E. E., and Kerlake, William R.: Experimental Evaluation of Gaseous Hydrogen Fuel in a 16-Inch-Diameter Ram-Jet Engine. NACA RM E55J18, 1956.
- Drell, Isadore L., and Belles, Frank E.: Survey of Hydrogen Combustion Properties. NACA RM E57D24, 1957.
- English, Robert E.: Effect of Combustion Gas Properties on Turbojet Engine Performance with Hydrogen as Fuel. NACA RM E55J17a, 1956.
- English, Robert E., and Hauser, Cavour H.: Thermodynamic Properties of Products of Combustion of Hydrogen with Air for Temperatures of 600° to 4400° R. NACA RM E56G03, 1956.
- Fine, Burton: Further Experiments on the Stability of Laminar and Turbulent Hydrogen-Air Flames at Reduced Pressures. (To be published.)
- Fine, Burton: Stability Limits and Burning Velocities of Laminar Hydrogen-Air Flames at Reduced Pressures. NACA TN 3833, 1956.
- Fleming, W. A., Kaufman, H. R., Harp, J. L., Jr., and Chelko, L. J.: Turbojet Performance and Operation at High Altitudes with Hydrogen and JP-4 Fuels. NACA RM E56E14, 1956.
- Friedman, Robert, Norgren, Carl T., and Jones, Robert E.: Performance of a Short Turbojet Combustor with Hydrogen Fuel in a Quarter-Annulus Duct and Comparison with Performance in a Full-Scale Engine. NACA RM E56D16, 1956.
- Jonash, Edmund R., Smith, Arthur L., and Elavin, Vincent F.: Low-Pressure Performance of a Tubular Combustor with Gaseous Hydrogen. NACA RM E54L30a, 1955.
- Kaufman, Harold R.: High-Altitude Performance Investigation of J65-B-3 Turbojet Engine with Both JP-4 and Gaseous Hydrogen Fuels. NACA RM E57A11, 1957.
- Kerlake, W. R., and Dangle, E. E.: Tests with Hydrogen Fuel in a Simulated Afterburner. NACA RM E56D13a, 1956.

- Krull, H. George, and Burley, Richard R.: Effect of Burner Design Variables on Performance of 16-Inch-Diameter Ram-Jet Combustor Using Gaseous-Hydrogen Fuel. NACA RM E56J08, 1957.
- Morris, James F.: An Analytic Study of Turbojet-Engine Thrust Augmentation with Liquid Hydrogen, Pentaborane, Magnesium Slurry, and JP-4 Afterburner Fuels and a 220-Second Impulse Rocket. NACA RM E56A19a, 1956.
- Rayle, Warren D., Jones, Robert E., and Friedman, Robert: Experimental Evaluation of "Swirl-Can" Elements for Hydrogen-Fuel Combustor. NACA RM E57C18, 1957.
- Reynolds, T. W.: Aircraft-Fuel-Tank Design for Liquid Hydrogen. NACA RM E55F22, 1955.
- Reynolds, Thaine W., and Weiss, Solomon: Experimental Study of Foam-Insulated Liquefied-Gas Tanks. NACA RM E56K08a, 1957.
- Silverstein, Abe, and Hall, Eldon W.: Liquid Hydrogen as a Jet Fuel for High-Altitude Aircraft. NACA RM E55C28a, 1955.
- Sivo, Joseph N., and Fenn, David B.: Performance of a Short Combustor at High Altitudes Using Hydrogen Fuel. NACA RM E56D24, 1956.
- Smith, Ivan D., and Saari, Martin J.: High-Altitude Performance of J71-A-11 Turbojet Engine and Its Components Using JP-4 and Gaseous-Hydrogen Fuels. NACA RM E56L05, 1957.
- Straight, David M., Smith, Arthur L., and Christenson, Harold H.: Brief Studies of Turbojet Combustor and Fuel-System Operation with Hydrogen Fuel at  $-400^{\circ}$  F. NACA RM E56K27a, 1957.
- Wasserbauer, Joseph F., and Wilcox, Fred A.: Combustor Performance of a 16-Inch Ram Jet Using Gaseous Hydrogen as Fuel at Mach Number 3.0. NACA RM E56K28a, 1957.
- Wear, Jerrold D., and Smith, Arthur L.: Performance of a Single Fuel-Vaporizing Combustor with Six Injectors Adapted for Gaseous Hydrogen. NACA RM E55I14, 1955.
- Wilcox, E. Clinton, Weber, Richard J., and Tower, Leonard K.: Analysis of Turbojet and Ram-Jet Engine Cycles Using Various Fuels. NACA RM E56I19a, 1956.

037103

NASA Technical Library



3 1176 01436 5879

